UNIVERSIDAD DE CANTABRIA
-
INSTITUTO DE BIOMEDICINA Y BIOTECNOLOGÍA DE CANTABRIA (IBBTEC)

DEPARTAMENTO DE BIOLOGIA MOLECULAR

"MYC ONCOPROTEIN ROLE IN THE REGULATION OF TRANSCRIPTION, DIFFERENTIATION AND SENESCENCE"

"PAPEL DE LA ONCOPROTEINA MYC EN LA REGULACION DE LA TRANSCRIPCION, DIFERENCIACION Y SENESCENCIA"

Tesis doctoral presentada por
Andrea Quintanilla Cavia para optar al grado de
Doctora por la Universidad de Cantabria

Septiembre de 2013

Javier León Serrano, Catedrático de Bioquímica y Biología Molecular de la Universidad de Cantabria,

CERTIFICA: Que Dña. Andrea Quintanilla Cavia ha realizado bajo mi dirección el trabajo que lleva por título **"Papel de la oncoproteína Myc en la regulación de la transcripción, diferenciación y senescencia" ("Myc oncoprotein role in the regulation of transcription, differentiation and senescence")**

Considero que dicho trabajo se encuentra terminado y reúne los requisitos necesarios para su presentación como memoria de Doctorado y así poder optar al grado de Doctora por la Universidad de Cantabria.

Santander, Septiembre de 2013

Fdo. Javier León Serrano

Esta Tesis ha sido realizada en el Instituto de Biomedicina y Biotecnología de Cantabria (IBBTEC) y en el Departamento de Biología Molecular de la Facultad de Medicina de la Universidad de Cantabria (Santander).

La financiación necesaria para la realización de esta Tesis doctoral ha sido aportada por los proyectos SAF2008-01581 y SAF2011-23796 del Ministerio de Educación y Ciencia y por el proyecto RD06/0020/0017 del Instituto Carlos III. La autora de este trabajo ha disfrutado de una beca predoctoral de Formación de Personal Investigador (BES-2009-021905) asociada al proyecto "Análisis molecular y funcional de la oncoproteína Myc como inhibidora de la diferenciación".

Parte de los experimentos presentados en la Memoria de Doctorado fueron realizados por la Lda. Andrea Quintanilla Cavia en el laboratorio del Dr. Lars-Gunnar Larsson, Department of Microbiology, Tumor and Cell Biology (MTC), Karolinska Institute durante dos estancias (cinco meses en total) financiadas por el Ministerio de Educación y Ciencia con su partida presupuestaria para estancias breves: "Papel de la proteína Sin3B en el bloqueo de la senescencia mediada por Myc en un modelo murino Ras inducible" (EEBB-2011-44278) e "Interacciones funcionales entre Myc y Sin3b en células tumorales" (EEBB-I-2012-05567).

Además, se ha realizado otra estancia breve en el laboratorio del Dr. Juan Carlos Acosta, Institute of Genetics and Molecular Medicine (IGMM), University of Edimburgh, UK, para estudiar el papel de Myc en senescencia en un modelo murino que carece de la proteína Max.

AGRADECIMIENTOS

Me gustaría transmitir mi agradecimiento a todas las personas que han estado implicadas en este trabajo de tesis de una manera u otra, pero especialmente quiero expresar mi sincera gratitud a:

A Javier, por creer en mí y darme la oportunidad de hacer una tesis bajo su supervisión, por transmitir esa fascinación por la ciencia en general y Myc en particular, por esa brillante capacidad para conectar resultados de diferentes temas, por ser siempre positivo con mis resultados dando ideas para nuevos experimentos antes de tirarlo todo a la basura y por mandarme al psiquiatra de vez en cuando. Y sobre todo por ser un buen jefe y mejor persona.

A Dolo, por sus ideas y sus consejos, por su capacidad para enterarse de todo lo que pasa en el labo, por hacer de mediadora en conflictos y por estar siempre disponible para lo que hiciera falta.

A todos los que han colaborado directamente en esta tesis:

A Nacho, Jorge, Mari Cruz y Thaidy por todo el soporte bioinformático, por sus consejos y su paciencia

A Iñigo y Victor por su ayuda con la microscopía.

A Pablo, por su excelente trabajo con Sin3b.

A Nuria, por enseñarme a usar el dChip para analizar los microarrays.

A Flor por su colaboración en el proyecto de ChIP-seq.

A Lorena y a Javi, del grupo del Dr. Crespo, por su intenso trabajo en el proyecto de Erk-Myc-Cdk9.

Al grupo del Dr. Larsson por acogerme en su laboratorio en el Instituto Karolinska y por su colaboración en el proyecto de interacción Myc-Sin3b y en el proyecto de senescencia.

Al grupo del Dr. Acosta (MRC-Edimburgo) por su gran contribución en el proyecto de senescencia en nuestro modelo celular.

A todos los que habéis compartido momentos de laboratorio conmigo, Nacho, Juan, Gabi, Manu, Nuria, Javi, Fonso, Carmen, Lorena, Iago, Marina, Magda, Ana, Carlos, Silvia, Eva y Pilar, por los buenos momentos, risas, consejos, partidos de baloncesto…y por aguantarme estos años; pero sobre todo a Rosa, Lucía, Maña y María porque más que compañeras sois un gran equipo y hacéis que en el labo haya un ambiente de trabajo envidiado por muchos y al alcance de muy pocos. No sé si es porque está muy reciente, pero creo que siempre recordaré con mucho cariño *nuestra gran mudanza*, en la que a pesar del estrés, nos hemos reído muchísimo y podríamos haber escrito un libro con las patadas al diccionario debidas al cansancio y anécdotas varias. *Que para hacer cajas con un día valía…*aunque sólo nos hizo falta un minuto para quitarle la melena al león de la MGM. *Al final, todo salió puturrú! Pregúntaselo a Rosa! (Perdón por el retraso!).*

A Lorena, además de por su colaboración científica, por todas nuestras largas conversaciones en el confocal y por su apoyo moral durante la redacción de esta tesis.

A Juan Carlos por confiar en mí y devolverme la ilusión por continuar una carrera científica, por librarme de una gran experiencia china y por enseñarme que un Rivera de Duero puede ser tan bueno como un Rioja.

A Nuria por nuestros momentos en Edimburgo, y los que quedan…*vaya tela!*

A Rosa por ser mi amiga y mi compañera de batallas estos años y por esa gran *conversación*: "¿Qué quieres que haga? > < ¿Qué quieres que te diga?", y que afortunadamente acabó entre risas y cubos de basura.

A Óscar por sacar tiempo de donde no había para tomar una coca-cola mientras hacíamos webs, blogs, tiendas online y lo que hiciera falta.

A Ángela, Moni, Paula, Laura y demás *gente*, por compartir conmigo los buenos y los malos momentos, tanto cerca como en la distancia, y por tener paciencia con mis horarios y mis circunstancias.

A mi familia por transmitirme valores como la humildad, la sinceridad, la confianza…, que me han ayudado a ser como soy y crecer como persona y por enseñarme a distinguir lo que es importante en la vida.

A mis abuelas que son un ejemplo a seguir y a mis abuelos que me dan fuerza desde donde estén.

A mi madre por su ejemplo de mujer trabajadora incansable.

A mi padre por sus consejos, disciplina y exigencia. Papá, muchas veces durante estos cuatro años de tesis, me he acordado de esos paseos por el Sardinero siendo pequeña, cuando me decías que me fijara en un barco y al rato me hacías buscarlo porque ya no estaba en el mismo sitio. Entonces me explicabas que en la vida hay que ser constante como los barcos, que cuando los ves en el mar parece que están parados pero enseguida se pierden en el horizonte rumbo a su destino. Por su velocidad constante avanzan casi sin darnos cuenta, pero siempre llegan lejos.

A mis hermanos, por apoyarme y defenderme siempre. Sois los mejores!

A Aitor, por luchar conmigo para conseguir siempre todo lo que nos hemos propuesto, por aguantar mis cambios de humor en momentos estrés, por enseñarme a expresar mis sentimientos, por entenderme y apoyarme desde la distancia; y por tantas cosas … estos ojitos verdes siempre ven lo grande que eres!

“No necesito que sea fácil,
sólo necesito que sea posible”

Para mis abuelas.

UNIVERSIDAD DE CANTABRIA
-
INSTITUTO DE BIOMEDICINA Y BIOTECNOLOGÍA DE CANTABRIA (IBBTEC)

DEPARTAMENTO DE BIOLOGIA MOLECULAR

"MYC ONCOPROTEIN ROLE IN THE REGULATION OF TRANSCRIPTION, DIFFERENTIATION AND SENESCENCE"

ANDREA QUINTANILLA CAVIA

Santander 2013

ABBREVIATIONS

Ab	Antibody
ATP	Adenosine Triphosphato
bp	Base pairs
bHLH-LZ	Basic/helix-loop-helix/leucine zipper
BSA	Bovine Serum Albumin
º C	Degree Celsius or centigrade
Cdk	Cyclin dependent kinase
ChIP	Chromatin Immunoprecipitation
CoIP	Coimmunoprecipitation
C-terminal	Carboxi-terminal
D10F	DMEN supplemented with 10% FBS
DAPI	4´,6´-diamino-2 phenylindole dihydrochloride
Dex	Dexamethasone
DK	Deficient Kinase activity
DMEM	Dulbecco's Modified Eagle Media
DMSO	Dimethyl Sulphoxide
DNA	Deoxyribonucleic Acid
dNTP	Deoxyribonucleoside Triphosphate
E-Box	Enhancer Box sequences
EDTA	Ethylenediaminetetraacetic Acid
EGF	Epidermal Growth Factor
ER	Estrogen Receptor
ERK	Extracellular signal Regulated Kinase
e.v.	Empty vector
FBP	FUSE binding protein
FBP-FIR	FBP interacting repressor
FBS	Fetal Bovine Serum
Fbw7	F-box and WD repeat domain-containing 7
FUSE	Far UpStream Element
g	grams
GAP	GTPase-activating protein
GEF	Guanine-nucleotide Exchange Factors
GFP	Green Fluorescent Protein
GO	Gene Ontology
h	Hours
HCl	Hydrochloric acid
HDAC	Histone Deacetylase
hESC	Human Embryonic Stem Cells
HTA	Histone acetyl transferase
hTERT	Human Telomerase Reverse Transcriptase
HVR	Hypervariable Region
IgG	Immunoglobuline
IB	Immunoblot
i.e.	In example
IF	Immunofluorescence
IFN	Interferon
Il	Interleukin
Ink4	Inhibitors of Cdk4
Inr	Initiator element
IP	Immunoprecipitation
iPSC	Induced Pluripotent Stem Cells
IRDye	Infrared dyes
isPLA	*In situ* Proximity Ligation Assay
Kb	Kilobase
kDa	Kilodalton
LiCl	Lithium chloride

Luc	Luciferase
M	Molar
Mb	Megabase
MB	Myc Box
MEF	Mouse Embryonic Fibroblast
mESC	Murine Embryonic Stem Cells
mg	Milligram
min	Minutes
µM	Micromolar
mL	Millilitres
mRNA	Messenger RNA
NaCl	Socium chloride
$NaHCO_3$	Sodium bicarbonate
NGF	Nerve Growth Factor
NLS	Nuclear Localization Sequence
nm	Nanometres
nM	Nanomolar
NP40	Nonidet P-40 (octyl phenoxylpolyethoxylethanol)
N-terminal	Amino-terminal
4OHT	4-O-Hydroxy-Tamoxifen
OIS	Oncogene Induce Senescence
o/n	Over night
PAGE	Polyacrylamide Gel Electrophoresis
PAHD	Paired Amphipatic Helix Domain
PBS	Phosphate Buffer Saline
PCR	Polymerase Chain Reaction
PFA	Paraformaldehyde
PM-MM	Perfect Match-Mismatch
Pol	Polymerase
pTEFb	Positive transcriptional elongation factor b
Rb	Retinoblastome protein
RCA	Rolling Circle Amplification
rDNA	Ribosomic Deoxyribonucleic Acid
RNA	Ribonucleic Acid
RP	Ribosomal Protein
RPKM	Reads per Kb per million of mapped reads
rpm	Revolutions per minute
RPMI	Roswel Park Memorial Institute Media
rRNA	Ribosomic Ribonucleic Acid
RT	Room Temperature
RT-qPCR	Real Time-quantitative Polymerase Chain Reaction
SA-β-gal	Senescence associated β-galactosidase
SAHF	Senescence-Associated Heterochromatin Foci
SASP	Senescence-Associated Secretory Phenotype
SDS	Sodium Dodecyl Sulfate
SDS-PAGE	SDS polyacrylamide gel electrophoresis
Sec	Seconds
SEM	Standard Error of the Mean
Seq	Sequencing
Ser	Serine
SID	Sin3 interaction domain
siRNA	Small interfering RNA
SMS	Senescence-Messaging Secretome
SSC	Saline-Sodium Citrate buffer
T^a	Temperature
TAD	Transactivation domain
TBS-T	Tris-Buffered Saline-Tween20
Thr	Threonine
TPA	12-O-Tetradecanylphorbol 13-Acatate
tRNA	Transfer RNA

TF	Transcription Factor
UCSC	University of California Santa Cruz
UPL	Universal Probe Library
UTR	Untraslated Region
V	Voltios
vs.	versus
Wt	Wild type
ZF	Zinc Finger
$ZnSO_4$	Zinc sulfate

CONTENTS

1. INTRODUCTION

2. AIMS

3. MATERIALS AND METHODS

4. RESULTS

5. DISCUSSION

6. CONCLUSIONS

7. BIBLIOGRAPHY

8. SUMMARY

9. ANNEXS

PUBLICATION

MANUSCRIPT

FIGURE AND TABLE INDEX

1. INTRODUCTION

3. MATERIALS AND METHODS

4. RESULTS

1. INTRODUCTION

1.1. Myc expression and biology

The protooncogene *MYC* was first discovered as a cellular homolog of the oncogene of avian myelocytomatosis virus, v-Myc (Sheiness and Bishop, 1979). The *MYC* gene was originally identified in chicken cells (Vennstrom and Bishop, 1982; Vennstrom, 1982) and, later, the ortholog gene was identified in human, mouse and rat (Crews, 1982; Dalla-Favera, 1982a).

As a transcription factor, c-Myc (Myc henceforth) regulates gene expression. Genome wide chromatin immunoprecipitation studies have revealed that as much as 10-15% of all human genes are under the control of Myc (Fernández, 2003; Li, 2003; Patel, 2004; Zeller, 2006).

A chromosomal translocation was found in Burkitt's lymphoma involving Myc and the Ig loci, where deregulated Myc expression was giving rise to contitutively high levels of Myc (Dalla-Favera, 1982b). In addition to Burkitt's lymphoma, which is a cancer of B lymphoid cells, Myc deregulation has been detected in a wide range of other human cancers and is often associated with aggressive tumors including lung, breast, cervical, ovarian, prostate and colon carcinoma, as well as lymphoma, melanoma and leukemia (Dang, 1999).

Myc belongs to the Myc family, along with N-Myc and L-Myc, encoded by the *MYCN* and *MYCL1* genes (DePinho, 1987; Baudino and Cleveland, 2001). Whereas Myc is ubiquitously expressed, N-Myc is mainly neuronal (Kohl, 1983) and L-Myc is more expressed in lung (Nau, 1985).

All members of Myc family present a nuclear localization, a short half-life and their expression is usually correlated with cell proliferation. Also Myc is highly conserved during evolution.

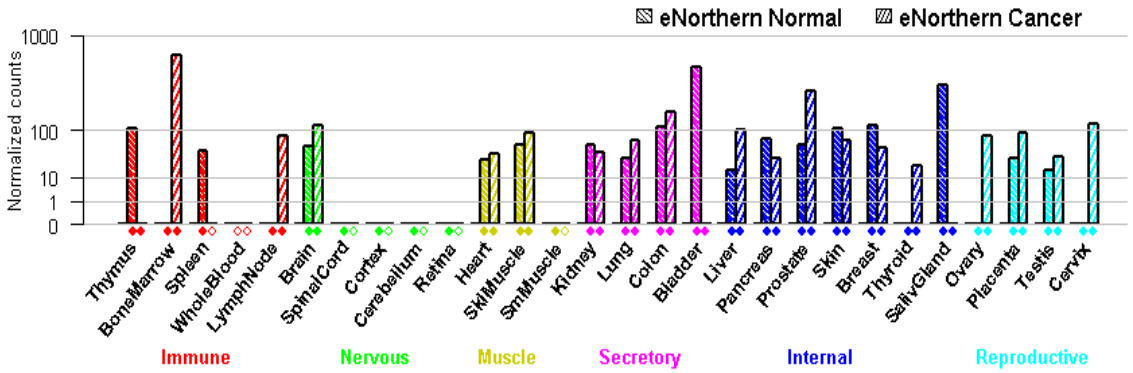

Figure 1.1. Electronic northern for Myc according to data from UniGene. (Updated Ago 2013, http://bioinformatics.mdanderson.org/).

1.1.1. Structure and function of Myc

Human *MYC* is located in the chromosome 8 (8q24.21) and has three exons (Dalla-Favera, 1982a; Dalla-Favera, 1982b). Its expression is regulated through four promoters, called P0, P1, P2 and P3. However, in normal cells, the majority of transcripts initiate at the P1 and P2 promoter (75-90% of Myc transcripts) because of its TATA-Box and the presence of two Inr elements (Wierstra and Alves, 2008).

Two isoforms of Myc can be synthesized depending on the start codon from which translation is initiated. The most prevalent form is generated from AUG start codon located at the 5' end of the second exon. Translation from this codon results in a protein of 439 amino acids and 64 kDa of apparent molecular weight, according to electrophoreticis mobility in denaturing conditions (the theoretical molecular weight of Myc, by amino acidic composition, is 49 kDa) (Persson, 1984).

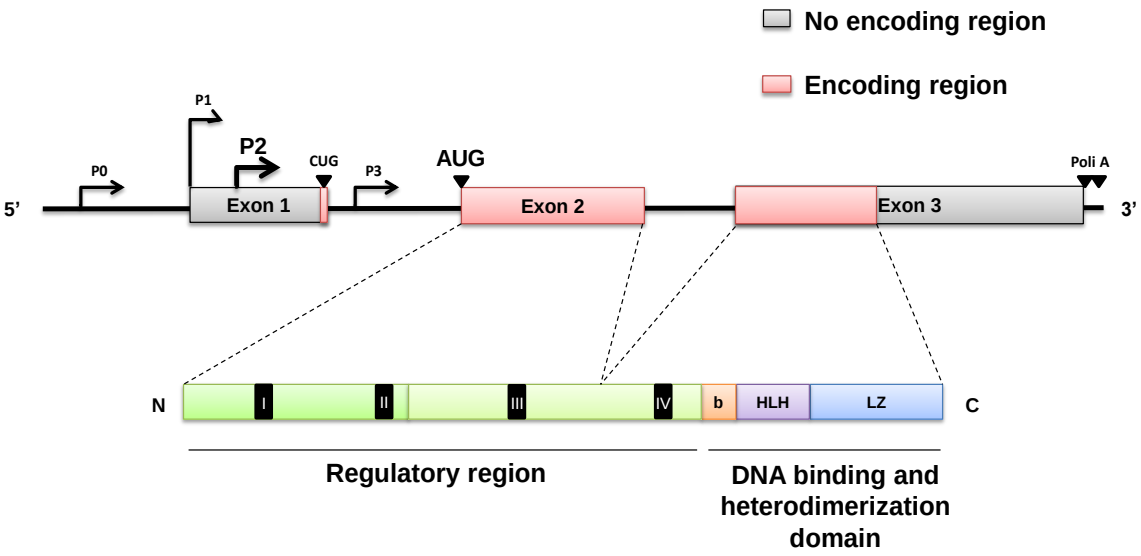

Figure 1.2. *MYC* gene. Four promoters and two start codons and the iosoform generated from AUG start codon are illustrated. In the N-terminal region are located four Myc boxes (MB-I to MB-IV, black boxes), which regulate Myc transactivation and transrepression functions. C-terminal region present a bHLH-LZ domain which allows the dimerization with anothers b-HLH-LZ proteins and the binding to DNA.

There is a longer and minority form of 454 amino acids named Myc-1 (in contrast with the mainly form which is known as Myc-2) which is translated from CUG codon located in the 3' end of first exon (Hann, 1988). Differences in the function between these isoforms are not clear. In some studies, differences between Myc-1 and Myc-2 were not observed (Blackwood, 1994), whereas that in other experiments, differences in transcriptional activity were suggested (Hann, 1994). Other forms can also be found in the cells, particularly Myc-S (from "Myc-Short") which lacks the N-terminal region (Spotts, 1997), or Myc-Nick, which lacks C-terminal region as the

result of the proteolytic cleavage of Myc in the cytoplasm. It has been described that Myc-Nick is functional and has a role in differentiation (Conacci-Sorrell and Eisenman, 2011). In this thesis we will refer to c-Myc-2 as Myc, which is the nuclear prevalent form.

Myc is a transcription factor of the basic/helix-loop-helix/leucine zipper (bHLH-LZ) protein superfamily (Landschulz, 1988; Murre, 1989; Prendergast and Ziff, 1989).

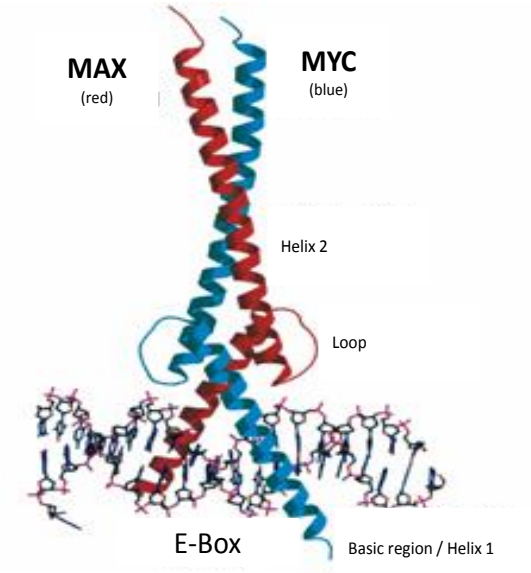

Figure 1.3. 3-D structure of Myc-Max heterodimer bound to DNA. bHLH-LZ domain of the dimer Myc-Max (88 amino acids of Myc and 83 amino acids of Max) was crystalized. (Figure adapted from Nair and Burley, 2003).

Two independent functional regions are observed in Myc protein. One of them is the C-terminal region, which presents a bHLH-LZ domain. Myc is bound to DNA through basic domain, whereas HLH and LZ domain allows the dimerization with other bHLH-LZ proteins, of which the most important is Max (Blackwood and Eisenman, 1991; Grandori, 2000; Nair and Burley, 2006). Thereby, Myc forms a heterodimer with Max and this heterodimer binds to specific DNA sequences termed E-Box (Enhancer Box sequences) with the consensus core sequence 5´-CACGTG-3´ (Blackwell, 1990; Grandori, 2000; Nair and Burley, 2006). The second one is the N-terminal region, which contains four conserved regulatory domains called Myc Boxes (MB-I, MB-II, MB-III and MB-IV) with transactivation and transrepression functions. MB-I and MB-II are located from 1 to 143 amino acids (Kato, 1990). MB-I has two important phosphorylation sites, threonine 58 (Thr58) and serine 62 (Ser62), associated with stability and transforming activity of Myc (Stone, 1987; Sears, 2000). Transcriptional functions of Myc are located in the MB-II. When these regions are mutated, the binding to most transcriptional coactivators is impaired and, as result, the phenotype induced by overexpression of Myc is repressed (Freytag, 1990; McMahon, 1998; Oster, 2003). Finally, MB-III is involved in transcriptional repression (Herbst, 2005;

Kurland and Tansey, 2008), whereas that MB-IV regulates DNA binding, apoptosis, transformation and G2 phase arrest (Cowling, 2006).

1.1.2. Regulation of Myc

Myc monitors many cell functions and therefore *MYC* expression and Myc activity have to be tightly controlled. In fact, its expression is strongly regulated by transcriptional, postranscriptional and postranslational mechanisms, although this regulation is not completly understood. This is because the regulation of the *MYC* promoter is extremely complex with a lot of redundancy, many feedback loops and several cross-regulatory circuits involved (Wierstra and Alves, 2008).

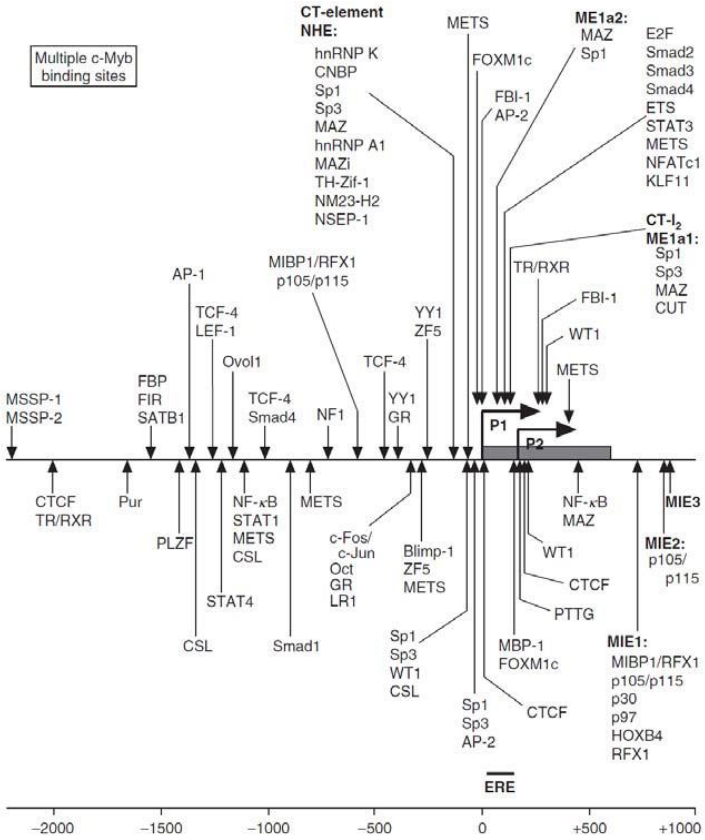

Figure 1.4. Transcription factors binding sites in the *MYC* promoter. The horizontal line represents *MYC* promoter (from -2 Kb to +1 Kb from TSS). Exon 1 is illustred by a grey box. P1 and P2 are the promotors more used in the majority of transcripts. Vertical arrows represent one or more binding sites for a particular transcription factors (Figure adapted from Wierstra and Alves, 2008).

MYC is generally expressed in normal proliferating cells, in which the Myc mRNA has fold from 10 to 40 higher than quiescent cells in which Myc is virtually low expressed and, during growth arrest and differentiation, it drops about 90% (Spencer and Groudine, 1991; Marcu, 1992;

Oster, 2002). In quiescent cells, many complexes of E2F-1, E2F-2, E2F-4, HDAC and pocket family proteins (Rb, p107, p130) are bound to *MYC* promoter and its transcription is inhibited (Albert, 2001).

When cells are proliferating and CDK/Cyclins are active, the aforementioned complexes are disassembled and other transcription factors, such as TCF3, Sp1 or YY1, bind to *MYC* promoter inducing Myc overexpression. However, this increase is transitory and must be tightly regulated (Hann, 1985; Rabbitts, 1985; Thompson, 1985), thus there is an important sequence localized in Myc regulatory region named FUSE (Far Up-Stream Element). Firstly, this region is recognized by FBP (FUSE Binding Protein) which actives transcription and, later, FBP-FIR (FBP Interacting Repressor) is recruited, resulting in the inhibition of *MYC* transcription (Chung and Levens, 2005; Liu, 2006). This way, cells get a quick pulse of Myc and are lead to cycle progression.

The joining of FBP to FUSE sequence allows continuous Myc expression while its capacity of negative autoregulation keeps expression by negative feedback loop (Facchini, 1997; Luo, 2004; Wierstra and Alves, 2008).

Myc levels drop rapidly at the beginning of cell differentiation until disappearance in terminally differentiated cells. Repression of Myc during differentiation is usually regulated, directly or indirectly, by factors of transcriptional control depending on each cell type. Some of these factors have direct role in the repression of *MYC* during the differentiation like Blimp1, C/EBPα, C/EBPβ, METS, Ovol1, GATA1 and Mxi1. Moreover, the complexes formed by E2F and the pocket proteins collaborate in the Myc silencing during the differentiation, cooperating with some of the above transcription factors (Klappacher, 2002; Ogawa, 2002; Iakova, 2003).

Myc mRNA stability is also regulated. It has a short half-life of less 30 min because its sequence is rich in A and U, above all in 3' end, which lead to low stability (Jones and Cole, 1987). Another regulation mechanism of mRNA stability consists in the binding to C-terminal domain of several proteins with RNase activity (Bernstein, 1992; Prokipcak, 1994; Lee, 1998). Upon mitogenic stimuli Myc mRNA levels reach their maximum within two hours, then remains at a lower level throughout the cell cycle as does the protein (Hann, 1985; Thompson, 1985). Also, antiproliferative signals lead to a rapid reduction of Myc mRNA levels (Dean, 1986).

At the post translational level Myc can be modified in multiple ways. Acetylation by CBP/p300, Gcn5 and Tip60 at different lysine residues leads to increased transcriptional activity and stabilizes Myc protein (Vervoorts, 2003; Patel, 2004; Faiola, 2005; Menssen, 2012). Myc protein has many phosphorylation sites of which two are well studied, Ser62 and Thr58, localized in the MB-I. Modifications of these residues regulate Myc activity and stability (Henriksson, 1993; Lutterbach and Hann, 1994). Thr58 in Myc may also be modified by O-linked glycosylation in a reciprocal manner to phosphorylation, but the biological function of this modification is still unknown (Chou, 1995a; Chou, 1995b). Recently the Pim-kinases have been shown to phosphorylate Myc in the C-terminal domain leading to its stabilization (Zhang, 2008).

Suggested kinases for Ser62 are ERK, CDK1 and JNK, whose phosphorylation has been reported to result in increased Myc stability (Sears, 2000; Hann, 2006). Ser62 phosphorilation is also priming for Thr58 phosphorilation by GSK3 (Lutterbach and Hann, 1994; Sears, 2000), which mediates ubiquitylation of Myc by the E3-ligase Fbw7 and the subsequent degradation by the proteasome (Welcker, 2004; Yada, 2004; Sears, 2004).

1.1.3. Myc-Max-Mxd network: Transactivation

The Myc-Max-Mxd network consists of several transcription factors of the bHLH-LZ family. To be active and to bind to specific target sequences in the DNA, called E-Boxes (5'-CACGTG-3'), these factors act as dimers.

Myc needs to dimerize with Max protein through the bHLH-LZ domain to be able to activate transcription (Blackwood and Eisenman, 1991; Wenzel, 1991; Blackwood, 1992; Prendergast and Ziff, 1992). Also, Myc function in transactivation, transformation and apoptosis is dependent of Max interaction (Amati, 1992; Amati, 1993), because Myc is unable to homodimerize.

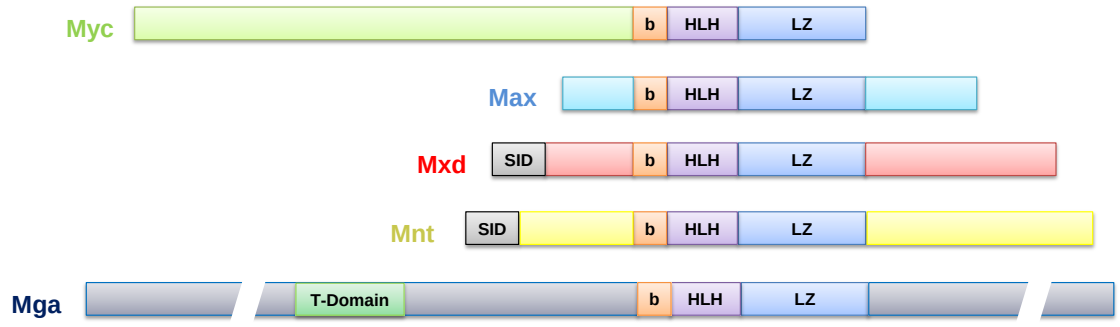

Figure 1.5. Structure of bHLH-LZ proteins: Myc, Max, Mxd, Mnt and Mga.

The central player in this network is Max, a small ubiquitously expressed protein that is very stable (Berberich, 1992). Max has two isoforms due to alternative splicing: Max (21 kDa) and Max9 (22 kDa) (Blackwood and Eisenman, 1991; Prendergast, 1991; Arsura, 1995).

Max can form heterodimers with all others proteins of the network as well as homodimers (Littlewood, 1992), which can bind to E-Boxes *in vitro*, but no function of this binding has been shown *in vivo* (Berberich, 1992; Kretzner, 1992; Yin, 1998). Phosphorylation of Max by Casein Kinase II has been shown to inhibit the DNA-binding of the Max homodimers but not any Max heterodimer (Berberich and Cole, 1992).

Max interacts with two families of bHLH-LZ proteins: the Myc family and the Mxd family. These two families are functional antagonists; the Myc family activates transcription (Blackwood and Eisenman, 1991; Marchetti, 1995; Luscher and Larsson, 1999; Grandori, 2000; Nair and Burley,

2006), while the Mxd family represses transcription of overlapping but not fully identical target genes (Hurlin and Huang, 2006).

Myc-Max heterodimers act by facilitating the recruitment of others proteins of transcriptional machinery. It was described that Myc-Max dimer interacts with proteins as TBP, TFII-I, TFII-F and TRRAP (Henriksson and Luscher, 1996; Facchini and Penn, 1998; Sakamuro and Prendergast, 1999; Eisenman, 2001; Levens, 2003).

The Mxd family consists of Mxd1-4 (Mad1, Mxi1, Mad3 and Mad4), Mnt and Mga. All these proteins, except Mga, contain a Sin3 interaction domain (SID) by which they recruit the corepressor complexes N-Cor and Sin3 containing HDAC activity (Ayer, 1995; Heinzel, 1997; Laherty, 1997).

The Mxd proteins antagonize Myc and Mxd-Max complex forming a strong repressor of transcription. Mxd-Max heterodimers repress transcription, at least partially, by recruiting a co-repressor complex Sin3 protein that interacts with a number of proteins, including histone deacetylases (HDACs), that deacelylates histones in order to produce a more tightly packed chromatin structure, thus preventing the transcriptional activation that occurs through E-Boxes (Ayer, 1993; Ayer, 1995; Alland, 1997).

Myc is expressed at very low levels in resting cells and its expression is induced when with the entry into cell cycle to growth, whereas Max is expressed at similar in both states. Hence, the expression of Myc target genes will be blunted by Mxd-Max in resting cells, where Mxd is expressed at high levels (Latchman, 1998). Myc-Max, Max-Max and Mxd-Max dimers are in an equilibrium determined by their availability in each cell, resulting in activation conditions (Myc-Max), no activation (Max-Max) or repression (Mxd-Max) of their target genes (Grandori, 2000; Baudino and Cleveland, 2001). The functional antagonism of Mxd and Myc proteins is explained at the molecular level by changes in chromatin remodeling (Luscher, 2001).

Mga on the other hand contains a T-domain, which is a DNA-interacting domain. Mga's biological function remains unclear, but it has been identified as a part of an E2F6 repression complex (Ogawa, 2002).

Mnt is perhaps the Mxd member with the clearest Myc antagonistic function. It is ubiquitously expressed and binds to similar promoters as Myc (Toyo-oka, 2006). Further, cells lacking Mnt show a phenotype resembling Myc upregulation and deletion of Mnt in cells lacking Myc partly rescues the slow growth phenotype of these cells (Hurlin, 2003; Nilsson, 2004). These results and the fact that Mnt is functionally regulated during the cell cycle (Popov, 2005) has lead to the hypothesis that Mnt-mediated repression is the default setting at the target genes, and Myc has to overcome this to activate transcription.

Myc regulates transcription through several mechanisms, including recruitment of histone acetylases, chromatin modulating proteins, basal transcriptional factors and DNA methyltransferases (McMahon, 1998; Cheng, 1999; Eberhardy and Farnham, 2002; Fernández, 2003; Kanazawa, 2003; O'Connell, 2003; Brenner, 2005).

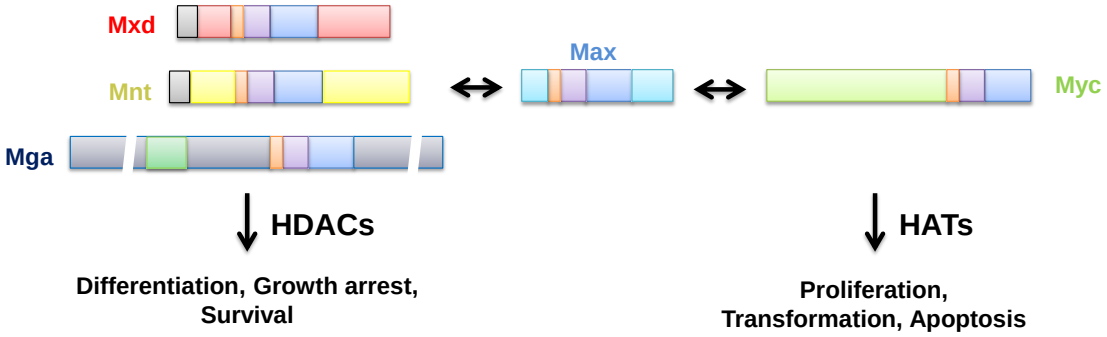

Figure 1.6. The Max network. Max is the central player capable of interacting with members of two families of bHLH-LZ proteins, the Myc and the Mxd family. Mxd proteins repress transcription from a specific set of target genes inducing cellular processes like differentiation and growth arrest. Myc family members activate transcription of those target genes and stimulate proliferation, transformation and apoptosis.

1.1.3.1. Mechanisms

Transactivation by Myc appears to require interactions of Myc´s MB-II domain with a member of PI3K-related kinase protein family called TRRAP (McMahon, 1998), which binds the histone acetylase GCN5 that leads an increase of transcription (McMahon, 2000). Moreover, Myc´s MBII domain can also recognize to Tip48 and Tip49 proteins or ATPasa/helicase proteins, whose activity is essential for the control of cellular growth and proliferation mediated by Myc (Wood, 2000; Bellosta, 2005).

In addition, Myc´s MBI domain is able to recruit Cyclin T1 and CDK9, both components of pTEFb, which induces an increase of transcription through C-terminal domain phosphorylation of the RNA Pol-II (Eberhardy and Farnham, 2001; Eberhardy and Farnham, 2002; Rahl, 2010). This interaction has been shown to be sufficient for activation of a synthetic promoter construct suggesting that Myc stimulates elongation of transcription (Eberhardy and Farnham, 2002).

Additionally, Myc has also been reported to interact with other protein complexes involved in transcriptional regulation. For instance, Myc binds INI1, which is a homologue of yeast SNF5 protein and a subunit of SWI/SNF complex involved in chromatin remodeling in an ATP dependent manner. Dominant negative mutants of INI1 inhibit Myc-induced transcription (Cheng, 1999; Amati, 2001; Luscher, 2001).

1.1.3.2. Myc and RNA-Pol initiation complex

Transcription factors bind to specific DNA sequences and regulate gene expression by recruiting the transcription initiation apparatus to promoters (Ptashne and Gann, 1997; Hochheimer and Tjian, 2003). Recent studies have shown that an additional level of regulation

must occur subsequent to initiation at certain genes and it have been proposed that certain transcription factors regulate this step (Peterlin and Price, 2006; Core and Lis, 2008; Margaritis and Holstege, 2008). The evidence described here indicates that promoter-proximal pausing is a more general feature of transcription by RNA polymerase II (Pol II) in vertebrate cells.

Multiple lines of evidence support the contention that Myc-Max generally plays a role in Pol II pause release at its target genes and does so through recruitment of pTEFb. Loss of Myc reduces the levels of elongating Pol II but does not affect the levels of promoter proximal Pol II. Inhibition of Myc-Max function leads to a substantial reduction in the levels of Ser2-phosphorylated Pol II in cells, which is the form associated with elongation, but does not affect the levels of Ser5-phosphorylated Pol II, associated with initiation (Gargano, 2007; Rhal, 2010; Larochelle, 2012; Ghamari, 2013).

Myc recruits pTEFb (forms by CDK9 and CyclinT1), where CDK9 is responsible for Ser5-phosphorylated Pol II (Larochelle 2012; Ghamari, 2013). Consistent with a role in pause release, Myc is associated almost exclusively with genes that are actively transcribed. Furthermore, it has been reported that Myc occupies promoter-proximal sites, which are heavily enriched for the E-Box core motif that it binds, where Myc would be optimally positioned to recruit pTEFb.

Some researchs suggest that tumor cells that overexpress Myc have enhanced expression of proliferation genes due to the role of Myc in recruiting pTEFb to efect Pol II pause release at these genes (Rahl, 2010). It is therefore possible that combinations of drugs that reduce the activity of both, Myc and pTEFb, could be especially effective therapeutic agents in tumor cells that overexpress Myc.

1.1.3.3. Myc target genes and their functions

A lot of studies have attempted to describe how many and which are the genes regulated by Myc. The development of new techniques of massive screening and sequencing (such as microarrays, ChIP-on-ChIP, ChIP-PET or ChIP-seq) has generated a large amount of information about the genes regulated by Myc. It is estimated that 10%-15% of all human genes are recognized bound by Myc, and at least 1000-4000 genes are regulated directly by Myc (Coller, 2000; Guo, 2000; O'Hagan, 2000b; Schuhmacher, 2001; Fernández, 2003; O'Connell, 2003; Patel, 2004; Ceballos, 2005; Lawlor, 2006; Dang, 2006; Zeller, 2006).

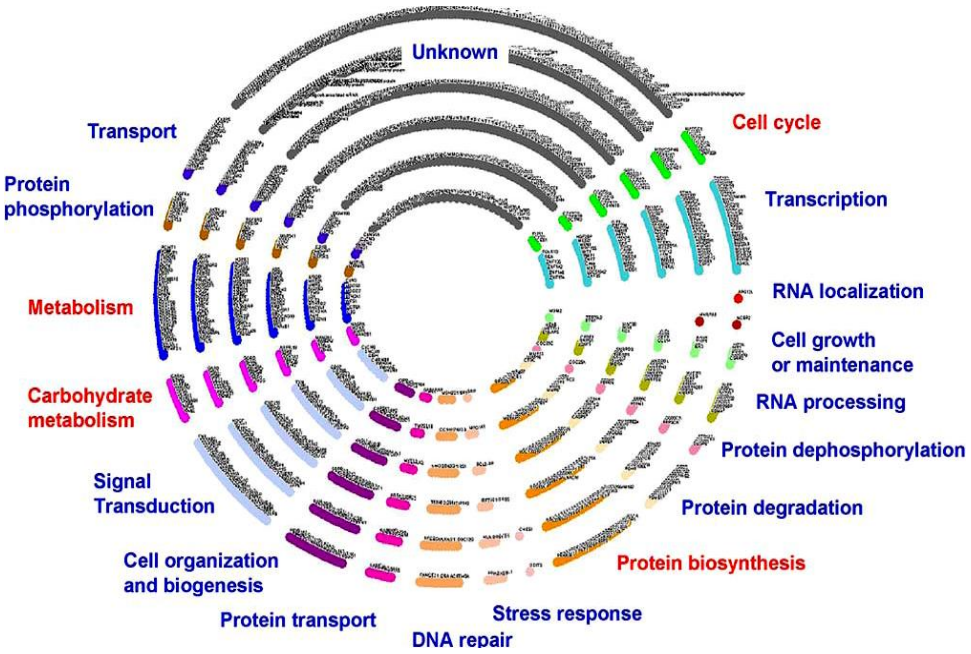

Figure 1.7. Distribution of Myc targets by gene ontology (GO). At least one thousand five hundred Myc targets (small circles) are displayed in concentric rings with functional groups colored and labeled. GO groups highlighted in red are statistically over-represented. (Figure adapted from Dang, 2006)

However, only a fraction of genes appears to be universally regulated by Myc independently of cell type or species (Zeller, 2003), whereas other target genes differ among cell type, species or origin. Some of the variations could be attributed to cell type specific to activate specific sets of genes in response to Myc (Barr, 1998; Frye, 2003; Yang, 1991). Recently, new reports have gone further and they have proposed that Myc acts as a general amplifier of transcription at promoters already engaged with the transcriptional machinery though mechanism related to the promotion of transcription elongation (Lin, 2012; Nie, 2012).

Biologic functions of Myc proteins depend on its transcriptional activity (activation or repression), which promotes a variety of biological responses related to cell cycle control, genomic instability, immortalization, metabolism, ribosome biogenesis, apoptosis, intercellular communication and control of terminal differentiation (Grandori, 2000). All these functions are important in cancer because deregulation of these functions may lead to tumoral phenotype.

1.1.4. Transrepression

The mechanism by which Myc represses transcriptionally certain genes have been traditionally less studied than the mechanisms of transactivation. However, the evidence that Myc-mediated transcriptional repression is key to their ability transforming (Facchini and Penn, 1998; Claassen and Hann, 1999).

Myc is able to repress transcription of many of their target genes through two different mechanisms. One is dependent on the Myc-Max binding to some sequences located near transcription start site, called Inr elements (Amundson 1998; Li, 1994) whose consensus sequence is YYCAYYYYY (where Y is a pyrimidine). Subsequently, it was found that Myc can interact with transcription factors which are capable of bind to Inrs, as Miz1, YY1 or TFII-I, inhibiting its activity (Roy, 1993; Shrivastava, 1993; Staller, 2001; Seoane, 2001; Seoane, 2002; Wanzel, 2003; Wu, 2003).

A key role in the Myc-mediated transcriptional repression mechanism is played by the transcription factor Miz1. Myc-Max dimers interact with Miz1 through Myc C-terminal domain avoiding Miz1-p300 dimer formation, which leads to their inhibition (Seoane, 2001; Staller, 2001). Therefore Myc has been related with the inhibition of the expression of many genes through mechanisms dependent on Inr sequences (Li, 1994; Ma and Martensson, 1995; Wang, 1999; Park, 2001; Yang, 2001). Among the genes repressed by Myc through Inr regions are Gas1, c/EBPα, CyclinD1, p21 p27, p15 or Myc itself (Dang, 1999; O'Hagan 2000; Staller, 2001; Wanzel, 2003; Gartel ans Shchors, 2003).

Moreover, in the p21 promoter, Myc forms a complex with Miz-1 and Dnmt3a, which would also contribute to inhibit the transcription through DNA methylation (Brenner, 2005).

There is other mechanism of transrepression Inr independent. Among these genes are involved Gadd45 or PdgfβR (Marhin, 1997; Izumi, 2001). The repression of these two genes happens by binding to the transcription factor NFY. And another mechanism depends on direct binding of Myc to transcription factor Sp1-Sp3, in which Myc interact with Sp1-Sp3 through its central region inhibiting their transcriptional activity (Feng, 2002; Vaqué, 2005).

1.1.5. Biological functions of Myc

1.1.5.1. Myc in apoptosis

In the absence of growth factors, Myc overexpression may induce apoptosis. In fact, it was suggested like a build-in safety mechanism to defend the cell against inappropriate proliferation (Askew, 1991; Evan, 1992; Shi, 1992). Curiously, Myc-induced apoptosis requires the same regions of Myc for transactivation and transformation (Evan, 1992).

Furthermore, Bcl2 is an oncoprotein that inhibits apoptosis and proved to cooperate with Myc (Vaux, 1988). The Eμ-Bcl2-Myc mice, overexpressing Myc and Bcl2, show hyperproliferation of B cells and develop tumors much faster than Eμ-Myc mice that solely overexpress Myc due to Bcl2 that antagonizes the pro-apoptotic effect of Myc (Strasser, 1990). In cell cultures Bcl2 showed to abrogate Myc-driven apoptosis in a manner that does not affect Myc's proliferative activities (Fanidi, 1992; Wagner, 1993). In fact, cells lacking Myc are more resistant to apoptosis

than control cells with Myc (de Alboran, 2004). Moreover, Myc needs to dimerizate with Max to induce apoptosis (Amati, 1993).

Myc has been shown to induce apoptosis in both a p53-dependent and a p53-independent manner. The p53-dependent pathway is well established and involves Myc activating ARF that inhibits Mdm2 (a inhibitor of p53) (Zindy, 1998) and thereby stabilizing p53 which leads to either growth arrest or apoptosis (Sakamuro, 1995; Meyer, 2006). However, in human leukaemia cells Myc can antagonize the apoptosis induced by active p53 (Ceballos, 2000; Ceballos, 2005)

The pro-apoptotic protein Bax has been shown to functionally cooperate with Myc (Eischen, 2001; Soucie, 2001; Juin, 2002; Maclean, 2003; Finch, 2006). Bax also mediates apoptosis triggered by Myc and inhibits Myc-induced lymphomagenesis (Eischen, 2001). Since apoptosis can be triggered by an activated oncogene it has to be overcome in a cancerous cell. Loss of proapoptotic regulators and mutations in p53 has been proposed as strategiesy to overcome cell death.

1.1.5.2. Myc in cell cycle regulation and proliferation

As indicated above, Myc is not expressed in quiescent cells, but it can be induced quickly in proliferate cells through addition of growth factors (Spencer and Groudine, 1991; Marcu, 1992; Oster, 2002).

G1 phase is shortened and transition from G1 to S phase is enhanced by the presence of Myc (Facchini and Penn, 1998; Karn, 1989; Roussel, 1991; Steiner, 1995). Consistent with this, reduction in the levels of Myc through deletion or antisense oligonucleotides induces cell cycle inhibition and, in some cases, differentiation (Heikkila, 1987; Holt, 1988; Mateyak, 1997). In this context, fibroblasts and B-lymphocytes from Myc conditional knock-out mice present a proliferation rate reduced regarding wild type mice (de Alboran, 2001). Myc induces cell cycle proliferation through different mechanisms, while Myc represses the transcription of genes as Gadd45 or Gadd153 (growth arrest and DNA damaging-inducible 45 and 153, respectively) inducing cell cycle inhibition by different factors (Chen, 1996; Marhin, 1997).

CDKs and Cyclins are induced by Myc, as Cyclin D1, Cyclin D2, Cyclin E1, Cyclin A2, Cyclin B1 and CDK4 (Hermeking, 2000; Bouchard, 2001; Menssen and Hermeking, 2002; Fernández, 2003). Also other proteins of great importance for cell cycle progression as Cdc25A, E2F1 and E2F2 are also induced by Myc (Jansen-Durr, 1993; Galaktionov, 1996; Gartel and Shchors, 2003).

Finally, Myc also is implicated in the control of degradation of a lot of cell cycle regulators proteins. Recently, it has been observed that Myc induces the expression of Skp2 (Bretones, 2011), a ubiquitin ligase belongs to SCF complex, whose function is the regulation of the proteolysis of many proteins, between them several proteins implicated in the cell cycle

inhibition. Therefore, Myc has a global role in the regulation of the cell cycle, highlighting its role in G1-S transition.

1.1.5.3. Myc in differentiation

Myc is expressed in almost all normal proliferating cells and requires its suppression to occur terminal differentiation process of many cell types (Freytag, 1988; Hoffman and Liebermann, 1991; Hoffman, 1996). Members of Myc family have a significant impact on cellular differentiation programs. This is mainly reflected in three facts:

I) Each member of Myc family has a different pattern expression during development suggesting functions not redundant (DePinho, 1991; Lemaitre 1996; Morgenbesser and DePinho, 1994; Douglas, 2001; Bull, 2001).

II) The decrease in Myc expression is a recurrent observation in cells that are differentiating (Gonda and Metcalf, 1984; Larsson, 1994; Henriksson and Luscher, 1996; Chang 2000).

III) Ectopic expression of Myc blocks differentiation into a variety of cell types *in vitro* and *in vivo* (Iritani and Eisenman, 1999; León, 2009).

Differentiation program is very sensitive to the levels of expression of Myc and it is enough to induce differentiation in many cellular systems (Bacon and Wickstrom, 1991; Facchini and Penn, 1998). Often the removal of Myc expression is an essential step to complete the differentiation program (Chang, 2000). In fact, Myc is able to inhibit master genes of differentiation. For example, C/EBP-α drives the differentiation of murine cells to adipocytes and has been shown that Myc antagonized C/EBP-α-mediated transactivation of Gadd45 (Tao and Umek, 1999; Johansen, 2001). Also, Myc inhibits GATA1 to block differentiation of human myeloid cells (Acosta, 2008) and Erg1 to block differentiation of macrophages (Shafarenko, 2005). Therefore, the suppression of Myc is one of the earliest events related with antimitogenic regulatory signals allowing the differentiation process (Gonda and Metcalf, 1984; Larsson, 1994; Henriksson and Luscher, 1996; Facchini and Penn, 1998; León, 2009).

However, examples have also been described in which the overexpression of Myc does not inhibit differentiation. In those cases where Myc does not inhibit differentiation, this process is usually compatible with proliferation, for example in human epidermal stem cells (Gandarillas and Watt, 1997; Flores, 2004) or hematopoietic stem cells and B lymphocytes (Wilson, 2004; Habib, 2007; Delgado and León, 2010), where Myc increases the population of precursors cells of a particular cell lineage. In case of stem cell is required a step of proliferation, where Myc is active before the cells differentiate (Larsson, 1988; Gandarillas and Watt, 1997; Flores 2004).

Proliferation and differentiation are mutually exclusive functions in many models. Thereby, it has been argued that Myc impairs differentiation by preventing the exit from cell cycle and maintaining the cell in a proliferative state (León, 2009). Consistently with these assumptions,

Mxd expression, which is antagonist of Myc functions, is increased in a lot of models of differentiation (Luscher, 2001; Zhou and Hurlin, 2001).

Differentiation is a complex process where cells dramatically change their size, morphology, metabolic activity and responsiveness to signals. These changes are largely due to highly controlled modifications in gene expression. However, each cell type expresses a different subset of genes.

1.1.5.4. Myc in protein synthesis and cell size

Myc overexpression is related with new protein synthesis and an increase of cell size (Mateyak, 1997; Iritani and Eisenman, 1999). Many of the Myc target genes are involved in protein synthesis including several ribosomal proteins as L3, L15, S2 and S6 and translation factors as eIF4E and eIF2α (Rosenwald, 1993; Coller, 2000; Kim, 2000). Myc induces the transcription of genes related with rRNA, ribosomal biosynthesis (Kim, 2000; Schlosser, 2003) and the RNA polymerase I (Pol I) transcription (Grewal, 2005; Arabi, 2005; Grandori, 2005). Moreover, Myc is able to activate the promoter of the RNA polymerase III (Pol III), which synthesizes tRNA and ribosomal 5s RNA (Felton-Edkins, 2003).

Myc has also been shown to directly stimulate rDNA transcription in response to mitogenic signals and thereby plays a key role in regulating ribosome biogenesis and cell growth (Grandori, 2005).

Taken together with the fact that Myc is able to induce both Pol I and Pol III transcription, Myc emerges as a master regulator of protein synthesis, as prerequisite for cell growth and proliferation. Also, Myc has been reported to induce cell growth independent of cell division (Iritani and Eisenman, 1999; Johnston, 1999).

1.1.5.5. Myc in metabolism

Myc upregulates components of the nucleotide and polyamine synthesis machinery like ODC and CAD (Bello-Fernández, 1993; Miltenberger, 1995). Myc also regulates genes involved in energy metabolism for example by stimulating expression of the GLUT1 glucose transporter, as well as almost all glycolytic enzymes, particularly lactate dehydrogenase (Ldh), hexokinase 2 (Hk2), and enolase 1 (Eno1), several genes encoding glycolytic enzymes and many other genes of the glycolytic pathway, as well as a group of nuclear genes involved in mitochondrial function (Morrish and Hockenbery, 2003; Dang, 2013). It is believed that Myc is a pivotal contributor to the Warburg effect in tumors, as the preference of cancer cells to generate energy through aerobic glycolysis rather than oxidative phosphorylation (Dang, 2009; Li and Simon, 2013). In adition, a large number of genes related to metabolism are regulated by Myc, such as, biosynthesis of nucleosides, amino acids and iron (Bello-Fernández, 1993; Wu, 1999; Osthus, 2000).

Myc has been shown to increase mitochondrial biogenesis and function via regulation of nuclearly encoded mitochondrial proteins and the mitochondrial transcription factor (TFAM). These data support the hypothesis that Myc also drives proliferation by maintaining mitochondrial functions not strictly related to oxidative phosphorylation. Myc has also been related with increased both the transport of glutamine and the glutaminolysis in mitochondria, which is important energy source in tumor cells (Dang, 2009; Dang, 2010).

1.1.5.6. Myc and stemness

Recently, two new sets of data have fuelled the interest on Myc in relation to cell differentiation and cancer: the role of Myc in the reprogramming of adult differentiated cells into pluripotent stem cells and the finding that Myc is required for *in vivo* tumorogenesis induced by other oncogenes. Although it was known that Myc can block the differentiation of murine embryonic stem cells (mESC) (Cartwright, 2005).

The field has boomed since the discovery of Myc as one of the four transcription factors of the "magic brew" able to reprogram murine and human differentiated cells into the induced pluripotent stem cells (iPSC) (the other three factors being Oct4, Sox2 and Klf4) (Takahashi, 2007; Okita, 2007; Wernig, 2007; Lowry, 2008; Park, 2008). Although Myc is not strictly required for reprogramming, it increases the efficiency of iPSC generation at least 10-fold (Welstead, 2008).

ChIP-on chip and ChIP-sequencing experiments have revealed that Myc binds to a large number of genes also in embryonic stem cells (Kim, 2008) including the promoters of reprogramming factors as Oct4 and Sox2 (Coller, 2000). Therefore, *MYC* is an important gene for the maintenance of the stemness.

1.1.5.7. Myc in tumorogenesis

Considering that Myc enables a rapid cell growth and proliferation, stimulates cell cycle progression independent of mitogenic stimuli, induces immortalization, blocks differentiation (Lachman and Skoultchi, 1984; Coppola and Cole, 1986; Freytag, 1988), induces genomic instability (Felsher and Bishop, 1999; Vafa, 2002) and promotes angiogenesis by stimulating VEGF mRNA translation (Baudino, 2002; Mezquita, 2005) and by inhibiting TSP1 (Watnick, 2003), it is no wonder that a majority of human tumors have deregulated Myc (Vita and Henriksson, 2006).

Deregulated expression of *MYC* is found in a wide array of human cancers, in many cases associated to disease progression (Nesbit, 1999; Oster, 2002) like melanoma, breast cancer, lung cancer and some types of human lymphoma and leukemia among others. Moreover, N-Myc is involved in neuroblastome and L-Myc in lung and ovary cancer.

Myc-cancer relationship is related with Myc protein accumulation in tumoral cells. The first mechanism identified for Myc overexpression in cancer was the retroviral infection in chicken cells (Sheiness and Bishop, 1979), but in human cells four mechanism have been so far identified:

a) *MYC* translocations.

   Myc was the first example of oncogenic activation by chromosomal translocation in human cancer. In Burkitt's lymphoma, *MYC* is translocated from chromosome 8 to the heavy or light chain of immunoglobulin loci to the chromosomes 14 and, more rarely, 2 or 22 (Dalla-Favera, 1982a; Taub, 1982).

b) Transcriptional amplification.

   It has been reported that in tumor cells expressing high levels of Myc the transcription factors accumulates in the promoter regions of active genes and causes transcriptional amplification, producing increased levels of transcripts within the cell's expression program. The increasing levels of Myc results in increased binding to the set of existing active genes, with negligible binding to new sets of genes (Lin, 2012). Numerous gene expression studies have identified sets of genes whose expression levels are altered by changes in Myc levels (Schuhmacher, 2001; Zeller, 2003; Schlosser, 2005; Dang, 2006; Ji, 2011).

c) Activation of *MYC* promoter.

   Nowadays, promoter activation through hormones or growth factors, activation of their receptors, different signaling pathways or transcriptional effectors activity may also trigger Myc deregulation and protein accumulation without chromosomal aberrations or physical defects in the gene (Wierstra and Alves, 2008).

   In addition, common single nucleotide polymorphisms (SNP) on human chromosome 8q24, which predispose to colon, breast, prostate, and bladder tumors, have been implicated in deregulated *MYC* expression. This region containing 8q24 SNP rs6983267 confers increased cancer risk (Dang, 2009).

d) Stabilization of Myc protein.

   In many cases this stabilization is due to mutations in critical Ser and Thr in the N-terminal regions (Wilda, 2004). Furthermore, it has been described mutations in the sequence of *MYC* related to cancer and which cause increased stability of Myc (Gavine, 1999; Salghetti, 1999). Also, mutations affecting Myc phosphorylation in Thr-58 or Ser-62 increasing the stability of the protein and it have been associated with cancer (Gupta, 1993). These mutations are especially abundant in Burkitt's lymphoma (Bhatia, 1993; Albert, 1994; Axelson, 1995). In other cases, Myc is overexpressed by other factors whose activity triggers an enhancer in the mRNA or protein stability, inducing Myc overexpression (Welcker, 2004).

Conditional transgenic Myc models have demonstrated that many tumors are dependent on Myc for their maintenance as turning off Myc expression leads to tumor regression (Arvanitis

and Felsher, 2006). In these models, Myc inactivation leads to proliferative arrest and re-differentiation, senescence or apoptosis, predominating one of these response depending one the particular tumor model. In agreement, many tumors reappear when *MYC* is reactivated, as observed in liver, breast and pancreatic islet cell tumors (Boxer, 2004; Pelengaris, 2004; Shachaf, 2004). Sustained regression after brief *MYC* inactivation was demonstrated for osteosarcomas (Jain, 2002) and lymphomas (Giuriato, 2006). For osteosarcomas *MYC* inactivation differentiates the tumor cells to normal cells. This appears to be the case for hepatic tumor cells as well, but among the differentiated cells are dormant tumor cells, regaining their neoplastic phenotype on *MYC* reactivation. Inactivation of *MYC* in liver tumors, osteosarcomas and lymphomas induced a rapid senescence response with cells positive for SA-β-gal staining detected after only two days from Myc inactivation. Generally, this response depends on up-regulation of p53, p16 and p15 but not the DNA-damage or p38 kinase pathways often activated in OIS (Oncogene-Induced Senescence, see below) (Wu, 2007).

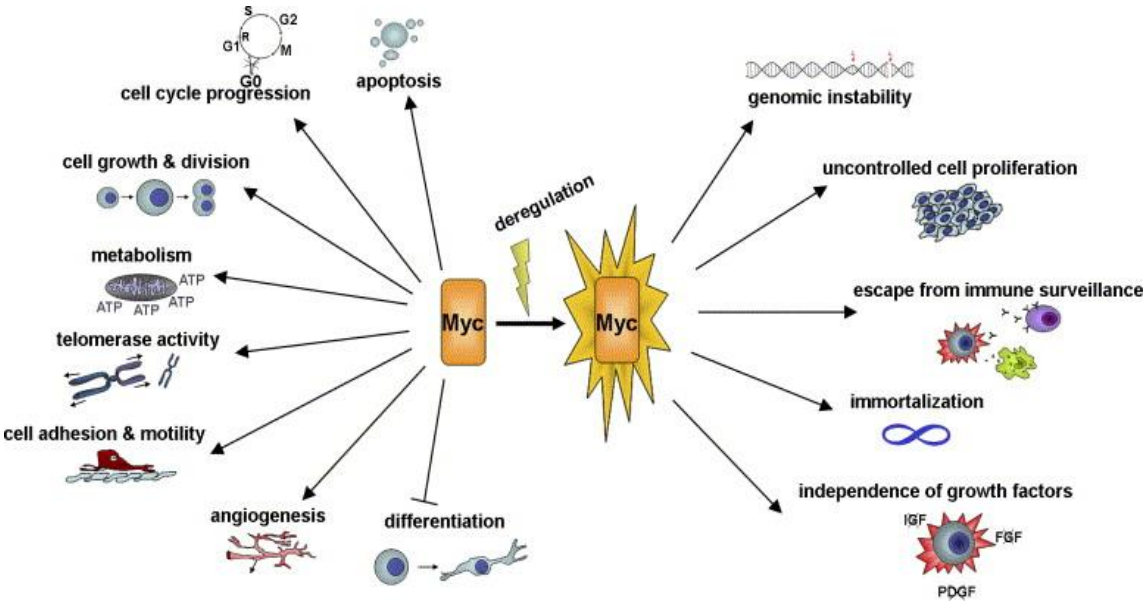

Figure 1.8. Cellular processes controlled by Myc during normal conditions and during tumorogenesis. Myc is a key regulator of many biological activities including cell growth and division (regulation of chromatin modification and components of the biosynthetic machinery); cell-cycle progression (modulation of cyclins, CDKs, CDKs inhibitors and phosphatases); apoptosis (p53 dependent or independent mechanisms); cell differentiation (down-regulation of growth arrest genes); cell metabolism (glycolysis, amino acid biosynthesis and transport, synthesis of macromolecules and DNA metabolism); angiogenesis (up-regulation of *VEGF*); cell adhesion and motility (control of expression of integrins). (Figure adapted from Vita and Henriksson, 2006).

1.2. Sin3 proteins

Sin3 proteins were originally identified in yeast where it have important role in transcription regulation of many genes (Vidal, 1991). These proteins have high levels of conservation from yeast to human.

In vertebrates, there are two Sin3 proteins, Sin3a and Sin3b. Main differences between themselves have been found in the N-terminal region.

1.2.1. Structure of Sin3 proteins

Sin3 proteins have high molecular weight (in human, Sin3a has 1273 amino acids, whereas that Sin3b has 1162). Its N-terminal region include three PAH domains (Paired Amphipatic Helix) each one, which has four amphipatic helix two by two and separated by flexible region (Wang, 1990; van Ingen, 2006).

Structurally, the main difference between Sin3b and Sin3a is located in N-terminal region immediately before the two first PAH domain, which is considerably shorter in Sin3b (Silverstein and Elkwall, 2005).

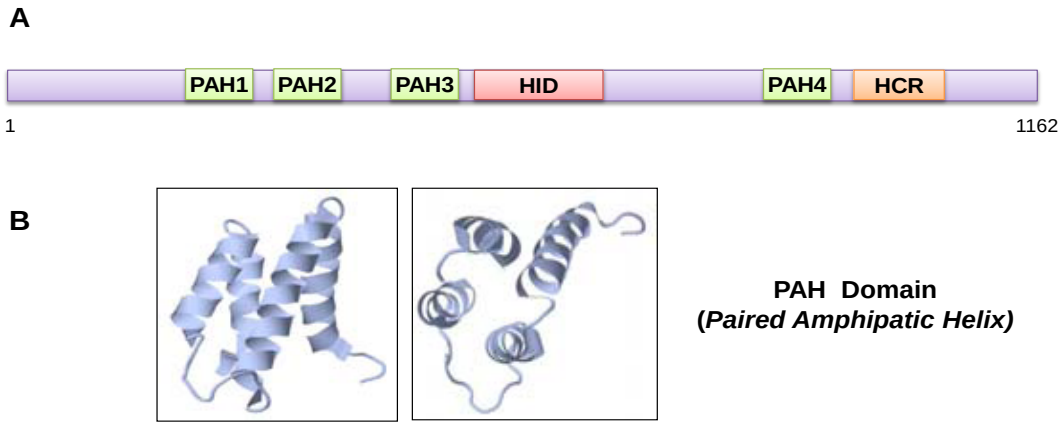

Figure 1.9. Sin3b structure. (A) PAH, HID and HCR domains of Sin3b are illustrated. **(B)** PAH domains cristalysized are shown.

PAH domains are able to interact with many proteins, mainly with transcription factors, among them are found Mnt and members of Mxd proteins family (Ayer, 1995; Schreiber-Agus, 1995; Rao, 1996; Eilers, 1999; van Ingen, 2004). Sin3 proteins also have HDACs Interaction Domain (HID) (Laherty, 1997; Hassig, 1997) and HCR domain, which is located in the C-terminal region and it is highly conservative from yeast to human.

1.2.2. Functions of Sin3 proteins

Sin3 proteins are involved in regulation of transcription, mainly acting as negative regulator, although it has also been studied their ability to activate transcription (Silverstein and Ekwall, 2005).

The function most widely studied of the Sin3 proteins is its role on the deacetylation of histones. The histones have, in the N-terminal region, a tail of lysines which can be acetylated. The state of histone acetylation is closely associated with transcriptional activity. A high degree of acetylation involves a transcriptionally active state, while deacetylation correlates with inactivation of transcription (Kuo and Allis, 1998; Li, 2004; Gibbons, 2005).

Proteins responsible of histone acetylation are called histone acetyltransferases (HAT), while histone deacetylases (HDAC) catalyze the deacetylation. The relation between HDACs and Sin3 initially was observed in yeast, where Sin3 and Rpd3, the histone deacetylase of *S. cerevisiae*, physically interact and cooperate in repression of transcription (Vannier, 1996; Kasten, 1997). In mammals, it has been described that the deacetylase activity is necessary to Sin3-mediated gene repression (Hassig, 1997). Furthermore, Sin3b and Sin3a, are part of protein complexes with HDACs and other proteins like RBBP4, RBBP7, SAP30, SAP18 and SDS3 (Laherty, 1997; Zhang, 1997; Zhang, 1998; Zhang, 1999; Dorland, 2000).

However, it is important to note that most of the studies on the Sin3 interaction with other proteins in mammals have been performed with Sin3a, and there is much less information on Sin3b interactions.

There is another alternative mechanism of histone deacetylation where Sin3 is involved in the repression of transcription, which involves the addition of monosacharides to proteins. PAH4 of Sin3 domain allows the interaction with the enzyme OGT, a transferase enzyme with N-acetylglucosamines to Ser or Thr residues, which has been related to the repression of transcription on certain promoters (Yang, 2002). For example, the addition of these sugars to the C-terminal region of Pol II produces inhibition of transcription elongation (Kelly, 1993).

Sin3a also has an important role in the maintenance of heterochromatin. The Sin3a and complexes formed by HDAC1 and HDAC2 have been associated with silencing of expression due to the presence of CpG islands. MeCP2 protein interacts with high affinity for methylated CpG islands, and, through its transrepression domain, inactivates the transcription. MeCP2 interacts directly with the complex formed by Sin3a and histone deacetylases (but not Sin3b), being directed into these areas of the genome and thereby contributing to permanent inactivation of transcription (Nan, 1998). Furthermore, Sin3 also was involved in rDNA silencing in mammals by interaction with nucleolar chromatin remodeling complex (NORC) (Zhou, 2002).

Another function associated with Sin3 proteins is DNA repair. In yeasts, Lys16 deacetylation of the histone H4 by Sin3-Rpd3 complexes promotes the repair of double-stranded DNA breaks (Jazayeri, 2004). It seems that the chromatin deacetylation allows to adopt an open conformation, which facilitates access of repair machinery to damaged area.

Although, in general, the role of histone deacetylases and Sin3 is repression of transcription, it has also been described examples in which the effect is the activation. This occurs, among others, in the case of gene regulation in response to osmotic stress in *S. cerevisiae*, whose expression is necessary for the recruitment of Sin3 and Rpd3 histone deacetylase to yeast promoters (de Nadal, 2004).

Sin3 proteins do not have DNA-binding domain, so their recruitment to specific regions of the genome depends on its association with transcription factors and proteins that interact with the DNA (Grzenda, 2009). The first interaction described between Sin3 and a transcription factor, and the best characterized, was between Sin3a and Mxd1. This interaction occurs through the PAH2 domain of Sin3a and the SID domain of Mxd1 (Eilers, 1999). Mxd1 recruits, by Sin3a, deacetylase activity to promoters that contain E-Boxes in their sequence. Mxd1 can interact with Sin3a and Sin3b, however there is evidence to say that the interaction with one way or another does not occur arbitrarily, but that could be dependent on cell type or pathway involved.

Despite of their high homology between their sequences and overlapping in many of its functions, there are evidences that indicate that Sin3a and Sin3b also perform independent and different functions. Not only mammals possess several Sin3 proteins, already in the yeasts there are different members of this family with features not interchangeables (Dang VD, 1999).

Sin3a deficient mice die at very early embryonic stages, and its cells are unable to grow in culture. These cells express Sin3b, which indicates that it is unable to substitute Sin3a for all its functions. Meanwhile, Sin3b deficient mice die in late stages of embryo development (David, 2008). Also, there are proteins that interact exclusively with one of the two forms of Sin3 (Nagy, 1997; Rayman, 2002; Xu, 2006).

1.3. Ras proteins

In mammals, three *RAS* genes, designated *H-RAS*, *K-RAS* and *N-RAS*, encoding for four proteins of 21 kDa, H-Ras, N-Ras, K-Ras4A and K-Ras4B (Barbacid, 1987). These proteins belong to the Ras superfamily that in humans is composed for approximately 150 members (Wennerberg, 2005).

The Ras GTPases operate as molecular switches that link extracellular stimuli with a diverse range of biological outcomes. Although many studies have concentrated on the protein-protein interactions within the complex signaling cascades regulated by Ras, it is becoming clear that the spatial orientation of different Ras isoforms within the plasma membrane is also critical for their functions. H-Ras, N-Ras and K-Ras use different membrane anchors to attach to the plasma membrane (Prior and Hancock, 2001).

1.3.1. Structure of Ras proteins

The only region of the Ras isoforms that exhibits significant sequence divergence is the last 24 residues of the protein, which conform the hypervariable region (HVR), which exhibits approximately 10-15% conservation compared with > 90% identity over the N-terminal 165 residues (Lowy and Willumsen, 1993).

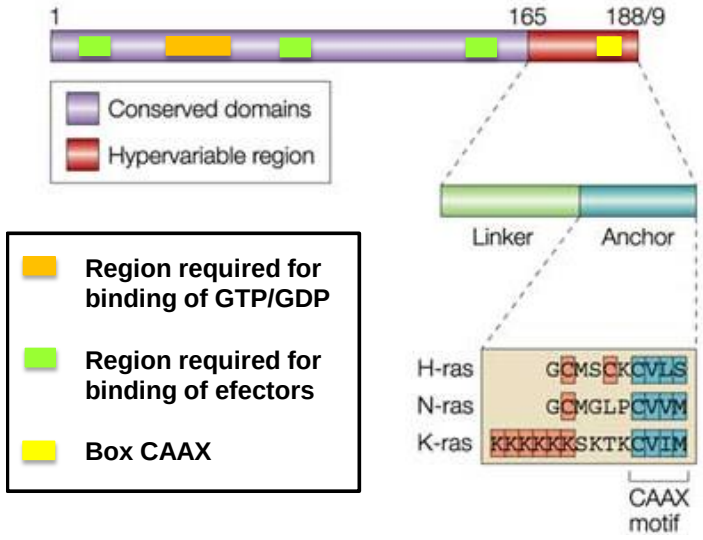

Figure 1.10. Ras structure. The amino-terminal catalytic domains (amino acids 1–165) of H-RAS, N-RAS and K-RAS are highly conserved (90–100% identical). The carboxy-terminal sequences diverge significantly and are referred to collectively as the hypervariable domain (HVR). Region required for binding of GTP/GDP, region required for binding of efectors and Box CAAX are illustrated. (Figure adapted from Hancock, 2003).

The HVR was shown to contain two signal sequences that cooperate in targeting Ras to the plasma membrane. The first signal sequence is the CAAX Box (C=cysteine, A=aliphatic amino acid, X=serine or methionine) present at the extreme C-terminal (Willumsen, 1984). The CAAX Box is sequentially post-translationally modified to render it more hydrophobic: the cysteine is farnesylated, the AAX sequence is removed by proteolysis, and then the C-terminal cysteine is carboxylmethylated. The second signal sequence consists of a polybasic stretch of six lysine residues (amino acids 175-180) in K-Ras, palmitoylation of cysteine 181 in N-Ras or of cysteines 181 and 184 in H-Ras (Hancock, 1990; Hancock, 1991) allowing the location of the various forms Ras in different regions of the plasma membrane (Prior and Hancock, 2001).

The common part contains binding domains to guanine nucleotides, one interaction region to exchanger factors of GTP/GDP and one interaction region to effector proteins (see below).

1.3.2. Biochemical activity of Ras

Ras proteins are GTPases (Gibbs, 1984; McGrath, 1984; Sweet, 1984). GTP-binding activates Ras causing a conformational change that allows interactions with their effectors while GDP-binding involves inactivation of Ras.

Ras activation and inactivation proccess is tightly regulated in the cell. There are factors that favor the exchange of GDP for GTP, called factors of exchange of guanine nucleotide or GEFs (Wolfman and Macara, 1990; Bonfini, 1992; Ebinu, 1998; Pham, 2000). Ras activated interacts with several effector proteins and thus it activates several cellular signaling pathways. Some Ras effectors identified are Raf, PI3K, Ral-GDS, Nore-1, MEKK, PKCζ, PLCε, AF6, Rin1 and Tiam (Zhang, 1993; Hofer, 1994; Rodriguez-Viciana, 1997; Vavvas, 1998).

Due to its low GTPase activity, Ras needs association with stimulating proteins of GTPase activity or GAPs for inactivation (Martin, 1990; Downward, 1992; Eccleston, 1993). GAP proteins increased Ras GTPase activity, promoting its inactivation, whereas those GEF proteins involve exchange of GDP for GTP, promoting Ras activation.

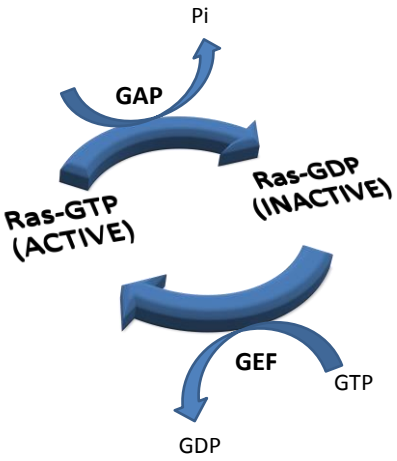

Figure 1.11. As GTPases, Ras-family proteins cycle between GTP-bound and GDP-bound forms. The kinetics of GTP hydrolysis and GDP dissociation are catalysed by two classes of auxiliary protein: GAPs (GTPase-activating proteins) and GEFs (guanine-nucleotide exchange factors), respectively. GEFs promote the release of bound GDP and the capture of a new GTP molecule, which activates Ras-family proteins, whereas GAPs stimulate the low intrinsic GTPase activity of Ras GTPases, resulting in inactivation.

1.3.3. Biological activity of Ras

The diversity of signaling pathways activated by Ras involves a variety of biological effects, depending on the analyzed system: proliferation, senescence, stop growth, differentiation, motility and apoptosis. Also Ras can develop different phenotypes and biological process depending on the cell line (Shields, 2000).

Often Ras is mutated in human tumors (Malumbres, 2003; Pylayeva-Gupta, 2011). The most common mutations are punctual mutations that cause constitutive activation of Ras, preventing the hydrolysis of GTP. The most relevant Ras activating mutations are those affecting codons 12 and 61 (Tabin, 1982; Bos, 1984).

At the beginning, Ras was described as oncogene, and in fact, its transforming ability has been studied extensively (Barbacid, 1987). However, the majority effect of overexpression of constitutively active forms of Ras on cell lines is the differentiation, above transformation (Crespo and León, 2000). For its relationship with the work carried out this Thesis we will focus on the roles of Ras on senescence.

1.3.3.1. Replicative senescence

Moorhead and Hayflick, more than 50 years ago, discovered that normal cells stop dividing after 60-80 population doubling in culture. This phenomenon was studied in human primary fibroblasts, which were shown to have a limited lifespan in culture. This was called replicative senescence, and was described as an irreversible growth arrest of cells that had lost their ability to divide after a certain number of divisions (Hayflick and Moorhead, 1961). Also, they proved that this growth arrest was not due to anything present in the culture media as they took early passage cells and transferred them into the conditioned media without any change but it was due to some intrinsic factors, termed “Hayflick factors” (Hayflick and Moorhead, 1961), which would accumulate inside the cells until their senescence.

Today this proliferative limit is considered to be triggered largely by erosion of the telomeres but also by various intrinsic and extrinsic factors such as agents causing DNA damage, oxidative stress, structure alteration, chemotherapeutic drugs, activation of certain oncogenes and physiological stress, or even the process of reprogramming to induced pluripotent stem cells can trigger premature senescence or stress-induced senescence (Kuilman, 2010). However, different stress stimuli are thus capable of inducing a senescent phenotype without affecting the telomeres.

1.3.3.2. Markers of senescence

Senescence is a stable and irreversible cell cycle arrest induced at the end of the cellular lifespan or in response to different stresses and associated with specific morphological changes.

Senescent cells are viable almost indefinitely, at least *in vitro*, even if they have stopped dividing and synthesizing DNA. They typically undergo dramatic morphological and functional changes and acquire a very distinct gene and protein expression profile. For instance, these cells acquire increased adhesion to the extracellular matrix and a flattened and much enlarged phenotype with increased granularity and formation of intracellular vacuoles (Dimri, 1995; Campisi, 2001;

Serrano and Blasco, 2001; Narita, 2003).

Hall-marks of senescence are upregulation of several different mediators of growth arrest, p53, pRb, p21, members of the Ink4 family like p16 or p15 (Lowe and Sherr, 2003; Campisi, 2005; Gil and Peters, 2006), induction of Senescence-Associated β-galactosidase activity (SA-β-gal) (Dimri, 1995) and formation of Senescence-Associated Heterochromatin Foci (SAHF) (Narita, 2003). In addition, senescence cells secrete a complex mixture of extracellular matrix and soluble factors, referred to as the senescence-associated secretory phenotype (SASP) or senescence messaging secretome (SMS) (Kuilman and Pepper, 2009; Coppe, 2010; Acosta, 2013).

Senescence has been most widely studied in fibroblasts *in vitro* but is also well defined in melanocytes and epithelial cells as well as cancer cells (Serrano, 1997; Jones, 2000; Lin and Lowe, 2001; Olsen, 2002; Shay and Roninson, 2004; Michaloglou, 2005). Other cell types suggested to undergo senescence include haematopoetic and neural progenitors (Geiger and van Zant, 2002; Palmer, 2001). Morover, senescent fibroblasts secrete proteins that can influence the tissue microenvironment (Shelton, 1999; Chang, 2002; Zhang, 2003; Mason, 2004; Trougakos, 2006) as well as proinflammatory cytokines such as IL-1, IL-6 and IL-8 (Kuilman, 2008; Orjalo, 2009; Acosta, 2013). Interestingly, paracrine factors produced by senescent cells have major effects on the growth and survival of tumor cells (Krtolica, 2001) and also of primary cells (Acosta, 2013).

1.3.3.3. Oncogene-Induced Senescence

Oncogene-induced senescence (OIS) is a protective mechanism to avoid tumor formation as a barrier for tumor progression.

Ras was the first human oncogene identified and found to be able to transform immortalized rodent cells and collaborate with immortalizing genes in oncogenically transforming primary cells, inducing cell cycle arrest when it is introduced alone into primary cell (Parada, 1982; Serrano, 1997). Unlike replicative senescence, this OIS can not be bypassed by expression of hTERT, confirming its independence from telomere attrition (Wei and Sedivy, 1999).

Ras accumulation into wild type cells was proved to trigger proliferation followed by an irreversible growth arrest accompanied by the accumulation of p53 and Ink4 proteins (Serrano, 1997). The oncogene (Ras, Raf, NF1-loss, PTEN-loss,…)-induced senescence was also found to be bypassed by the inactivation *in vitro* of pRb and p53 pathways, suggesting similarities to tumor suppressor mechanisms (Courtois-Cox, 2008).

In adition, mutations that disrupt p53 or p16, which are sustaining cellular senescence, cooperate with tumor progression (Braig, 2005; Chen, 2005; Collado, 2005; Lazzerini, 2005; Michaloglou, 2005).

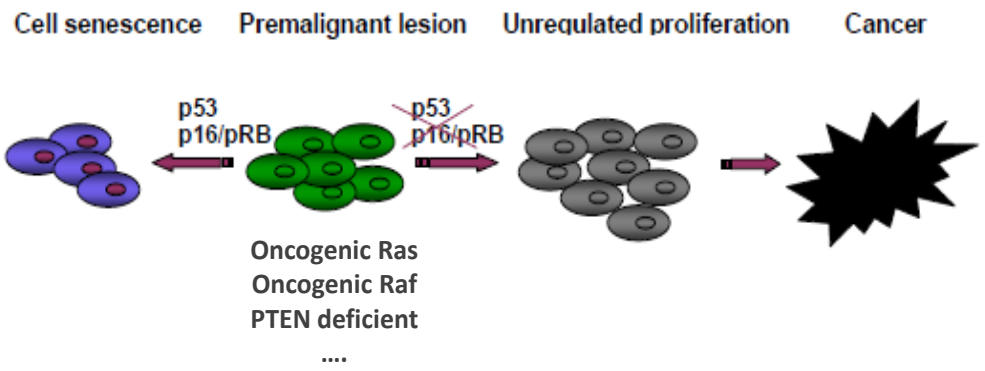

Figure 1.12. Oncogene-induced senescence as an anti-cancer fail-safe mechanism.

1.3.3.4. Cancer and senescence

Cellular senescence can compromise tissue repair and regeneration and contribute to depletion of stem/progenitor cell compartments. The OIS could also lead to removal of defective and potentially cancerous cells from the proliferating pool thereby limiting tumor development (Campisi and d'Adda di Fagagna, 2007; Collado, 2007). In contrast to normal somatic cells, cancer cells have the potential to proliferate indefinitely and this acquisition of an infinite proliferative potential was proposed to be one of the key events required for malignant transformation (Hanahan and Weinberg, 2000). The mechanisms that control cellular senescence, the signalling transduction pathways involved in cellular senescence and how the diverse signals that result in senescence are all integrated remain poorly defined. There are several common key regulation checkpoints and very subtle differences between tumorogenesis and senescence pathways and the balance between one another is a fine line.

Senescence cells are present in a wide range of premalignant lesions (Collado, 2005; Braig, 2005; Sun, 2007; Sarkisian, 2007; Bennecke, 2010; Carragher, 2010). Senescence markers have been demonstrated in several contexts *in vivo*, in which oncogenes or tumor suppressor genes were perturbed (Kuilman, 2010).

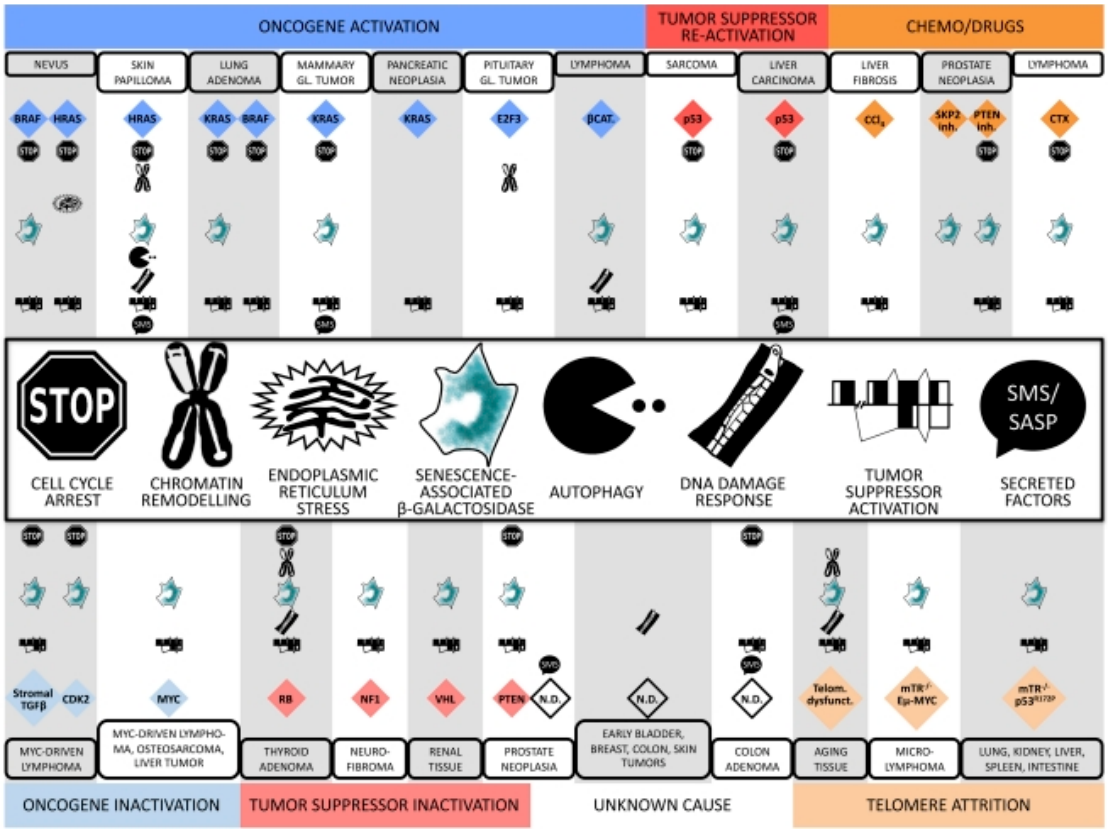

Figure 1.13. Several markers of cellular senescence have been identified in early neoplastic lesions in both mice and humans. Representative examples are shown in the various columns, with the type of genetic lesions or other types of stress (stress categories, color-coded) that instigate senescence at the very top and very bottom, and from thereon inward: the tissue types, specific stress signals, biomarkers, and symbols legends, respectively. For instance, in B-Raf mutant nevi, the stress category is oncogene activation (blue), the tissue type is nevus, the specific stress signal is B-Raf, and the biomarkers reported are cell cycle arrest, increase in SA-β-gal activity, and tumor suppressor activation. (CTX) Cyclophosphamide; (βCAT) β-catenin; (GL) gland; (N.D.) not determined. (Figure adapted from Kuilman, 2010).

1.3.3.5. Secretome and Inflammasome

Senescent cells secrete a complex mixture of extracellular and secreted factors usually referred to as the SASP (Senescence-Asociated Secretory Phenotype). It has been also called senescence messaging secretome (SMS). The production by senescent cells of secreted factors has been describe much years ago and nowadays gene expression profiles have confirmed that senescent cells secrete factors related to wound healing, inflammatory response or cytokine and chemokine signalling (Collado, 2005; Mason, 2009; Kuilman, 2008). The senescent secretome includes extracellular proteases, growth factors, proinflamatory cytokines (as IL-1α, IL-1β, IL-6) or chemokines (as IL-8).

IL-1α and IL-1β are minor SASP components (Coppe, 2008). Both proteins are secreted at low levels, compared to IL-6 and IL-8. IL-1 (both α and β forms) is a multifunctional cytokine that regulates inflammatory and immune responses primarily by initiating a signal transduction cascade that ultimately induces IL-6 and IL-8 expression. Recombinant IL-1α and IL-1β bind the same receptor (IL-1R) and exert similar biological effects. However, IL-1β is active solely as a mature secreted form, whereas IL-1α is rarely secreted at high levels and acts either intracellularly or as a cell surface-bound protein (Apte, 2006). Moreover, IL-1α, in contrast to IL-1β, can function as an uncleaved precursor protein (pIL-1α) as well as a processed (cleaved) protein.

Upon binding its receptor, IL-1R, IL-1 induces the formation of a complex containing IL-1R and its coreceptor (IL-1RAcP). This complex triggers a series of cytoplasmic events that ultimately activate the transcription factor NFKB, which then transactivates numerous genes, including those encoding IL-6 and IL-8 (Chien, 2011). In addition, C/EBPβ was recently shown to be important for IL-6 and IL-8 expression in senescent cells (Acosta, 2012; Kuilman, 2008).

Inflammasomes are molecular platforms activated upon cellular stress that trigger the maduration of proinflamatory cytokines such as IL-1β to engage innate immune defenses. Several inflammasomes have been described, among them the ones containing NLRP1, NLRP3, IPAF and AIM2 (Schroder and Tschopp, 2010). There are different types of inflammasomes, but all they have in common is that they have a site of interaction with caspase-1 that once activated will drive to the activation of IL-1 (Lamkanfi, 2012). Generation of IL-1β via cleavage of its proform requires the activity of caspase-1, although the mechanism involved in the activation of the proinflammatory caspases remains elusive (Martinon, 2002).

1.4. Protein kinases

Action of kinases and phosphatases determinate phosphorylation balance and the phosphorylation level of each substrate protein. Phosphorylation usually results in a functional change of the target protein by changing enzyme activity, cellular location, stability or association with other proteins.

The human genome contains about 500 protein kinase genes and they constitute about 5% of all human genes (Johnson, 2002; Manning, 2002). Up to 30% of all human proteins may be modified by kinase activity, and kinases are known to regulate the majority of cellular pathways, especially those involved in signal transduction (Lee, 1995; Manning, 2002).

1.4.1. MAPK family

Mitogen-activated protein kinases (MAPK) are a family of Ser/Thr protein kinases widely conserved among eukaryotes and are involved in many cellular programs such as cell proliferation, cell differentiation, cell movement and cell death. MAPK signalling cascades are

organized hierarchically into three-tiered modules. MAPKs are phosphorylated and activated by MAPK-kinases (MAPKKs), which in turn are phosphorylated and activated by MAPKK-kinases (MAPKKKs). The MAPKKKs are in turn activated by interaction with the family of small GTPases and/or other protein kinases, connecting the MAPK module to cell surface receptors or external stimuli.

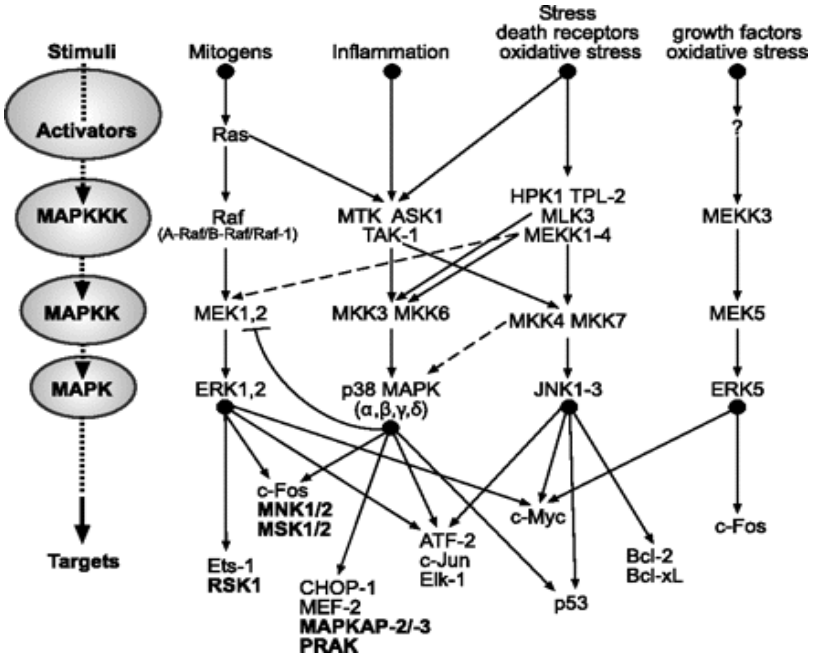

Figure 1.14. MAPK-signaling pathways. MAPK-signaling pathways are organized in modular cascades in which activation of upstream kinases by cell surface receptors lead to sequential activation of a MAPK module (MAPKKK → MAPKK → MAPK). Shown are the major MAPK pathway components and examples of the MAPK pathway target proteins. Target kinases are in bold. Dotted lines indicate context-dependent signaling connections between MAPK modules. (Figure adapted from Junttila, 2008).

Four MAPK have been described until now: ERK1/2 (Boulton, 1990; Boulton, 1991), p38 (Zervos, 1995; Sudo, 2002), JNK (Gupta, 1995) and ERK5 (Kamamura, 1999; Buschbeck and Ulrich, 2005).

1.4.1.1. ERK2 and Elk1

The ERK pathway belongs to the family of mitogen-activated protein kinase (MAPK) cascades. The activation of the ERK2-MAPK pathway by growth factors activates a Ras-like GTPase, which subsequently induces a three-step kinase cascade involving phosphorylation of family members as B-Raf, MEK and ERK.

Activated ERK translocates to the nucleus, where it phosphorylates to its interaction partners and induces changes in gene expression (Khokhlatchev, 1998; Bonni, 1999; Hu, 2009). ERK

signalling has been shown to be involved in cell-cycle progression (Yamamoto, 2006), differentiation (Lai, 2001) and proliferation (Zhang and Liu, 2002). Moreover, deregulation of ERK can lead to severe diseases and cancer (Keld, 2011; Suojun, 2012).

In addition, it has been reported that ERK2 binds at active promoters of genes involved in metabolic pathways and cell-cycle progression, many of which are essential for survival, proliferation or pluripotency of hESCs. It is very likely that sequence specific DNA-binding activity of ERK2 is independent of its kinase activity (Hu, 2009). Moreover, DNA-binding of ERK2 correlates with the occurrence of specific DNA sequence motifs identified as C/G-AAA-C/G (Hu, 2009), as well as binding sites for the transcription factor Elk1 (Zhang, 2008; Goke, 2013).

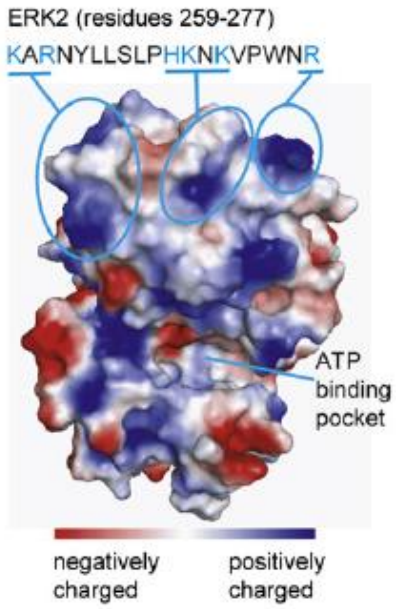

Figure 1.15. Structural analysis for DNA-binding domain in ERK2. Calculated using PyMol, the electrostatics surface potential of ERK2 is color-coded. A surface patch (residues 259–277) comprised of three positively charged clusters are indicated with the amino acid sequence showing above. The ATP-binding pocket is also shown. (Figure adapted from Hu, 2009).

Elk1 is a transcriptional activator downstream of ERK2. However, genome-wide geneexpression data shows that knockdown of Elk1 leads to both reduced and elevated gene expression, indicating that Elk1 might act as a repressor as well. Surprisingly, and in stark contrast to ERK2, Elk1 binding is highly enriched near genes involved in proliferation, further suggesting that Elk1 has a partially distinct function from ERK2. It has been studied differences between ERK2 and Elk1 DNA-binding and their genome-wide localization showed ERK2 colocalization with Elk1 at promoters defining three distinct sets of genomic loci (Goke, 2013).

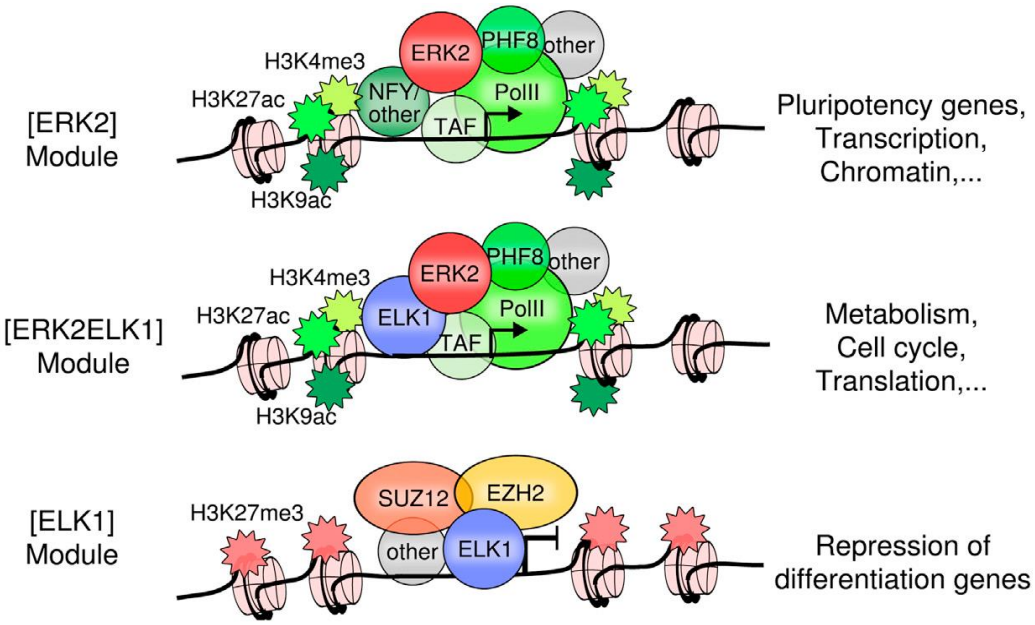

Figure 1.16. Model of the transcriptional regulatory network Elk1-ERK2. ERK2 and Elk1 colocalization defines three distinct modules that target different sets of genes. Combinatorial binding of ERK2 and Elk1 with transcription factors, chromatin regulators, and the basal transcriptional machinery integrates external signalling into the cell-type-specific regulatory network. (Figure adapted from Goke, 2013).

1.5. UR61 as differentiation model

PC12 cells are derived from rat feochromocitoma, a neoplasia of neuroendocrine system generated in the suprarenal glands.

After nerve growth factor (NGF) addition, PC12 cells show proliferative arrest and neuronal differentiation with formation of neurites and overexpression of neuronal markers (Greene and Tischler, 1976; Muñoz, 1993; Dragunow, 2000). U7 cell line derives of PC12, but has easier growing and worse respond to NGF, however it differentiates likewise (Greene and Rukenstein, 1981; Burstein and Greene, 1982; Guerrero, 1986; Guerrero, 1988). The UR61 cell line is a stable U7 subline that contains a mouse N-Ras oncogene (Q61E). This Ras induction results in a neuronal-like differentiation, which is associated with neuritogenesis, expression of a set of neuron-specific genes and nuclear expression of c-Jun (Guerrero, 1986; Guerrero, 1988; Thomson, 1990) which is blocked by Myc (Vaqué, 2008).

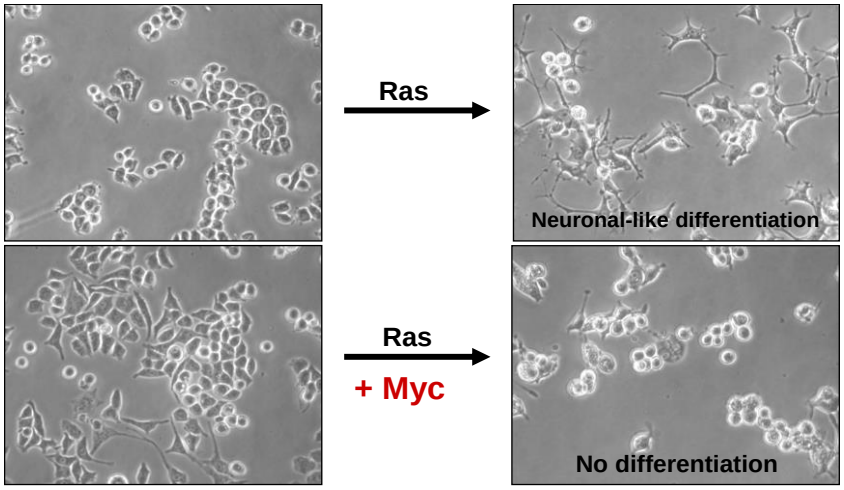

Figure 1.17. Myc blocks Ras-mediated differentiation in UR61 cells. (Figure adapted from Vaqué, 2008).

Activated Ras (K-Ras, N-Ras or H-Ras) induces neuronal differentiation in PC12 and its derived cells (Crespo and León, 2000). The differentiation induced by low concentrations of dexamethasone (as low as 20 nM) in UR61 is analogous to differentiation induced by NGF in PC12, thus in both cases almost 100% of cells has extension of neurites.

NGF actives Ras-MAPK pathways inducing differentiation in these cells (Cowley, 1994; Johnson and Vaillancourt, 1994). This process requires the c-Jun upregulation, which increases the transcription of typical neuronal genes through ERK and JNK activity (Leppa, 1998; Xiao, 2006).

In PC12, cells shifting ERK activation from transient to sustained inducing neuronal differentiation (Marshall, 1995). The ERK activation in response to NGF depends on Ras, B-Raf and Rap-1 activation, which allows its prolongued phosphorylation over time (von Kriegsheim, 2009). The NGF-dependent sustained ERK activation depends on the Rap-1 activation mediated by the NGF receptor (TrkA) rather than the Ras activation (Brightman and Fell, 2000). In fact, the activation of the NGF-induced ERK in a mutant PC12 lacking this receptor was transient, not sustained (Yaka, 1998).

Importantly PC12, U7 and UR61 cells lack of wild-type Max and express a Max, termed Max^{PC12}, whose dimerization domain is delectioned (Hopewell and Ziff, 1995). These are the single cell line known lacking Max and it has been described in this cellular model that Myc does not require Max for transcriptional activity (Ribon, 1994).

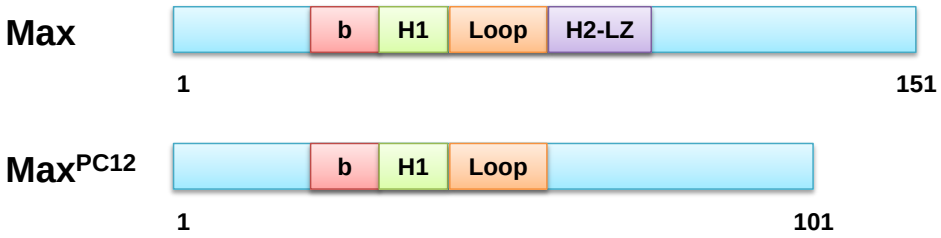

Figure 1.18. Max^{PC12} structure. PC12 and their derived cell lines express Max^{PC12}, truncated Max protein and unable to dimerize with Myc because lacks of H2-LZ domain.

2. AIMS

Myc is an oncogenic transcription factor of the bHLH-LZ family. *MYC* is one of the most frequently activated oncogenes in human cancer. Whereas the mechanisms by which Myc stimulates proliferation have been studied in some detail, the mechanisms by which Myc blocks differentiation are much less known. Previous work supports the hypothesis that, at least in some systems, Myc blocks differentiation by repressing genes that drive cell differentiation.

However, despite of nearly half of Myc target genes are repressed, little is known on the mechanisms responsible for Myc-dependent repression. In order to identify potential new Myc interaction proteins it was performed in our laboratory a screening yeast two-hybrid assay, using as bait complete Myc protein, in which Sin3b transcriptional co-repressor was detected.

PC12 is a rat pheochromocytoma cell line that differentiates in response to the activation of the Ras-MEK-ERK pathway. An unique feature of this cell line is that it is deficient in Max so far has been described as an “obligate” partner of Myc in transcriptional activation. UR61 is a PC12-derived cell line with dexamethasone-inducible expression of activated N-Ras oncogene. Ras induction results in neuronal-like differentiation of UR61. It has been described that Myc blocks this Ras-mediated differentiation of UR61 cells and that this effect is mediated by inhibition of c-Jun upregulation.

Moreover, there are several cellular models in which Ras induces senescence. Therefore, it would be interesting to explore Ras-mediated senescence in our model Max-deficient.

The general aims of the present study were to gain further insight into Myc function in regulation of transcription and differentiation, and also in Ras-induced senescence. For these purposes we established the following aims:

1. To identify Myc target genes that could explain the Myc-dependent inhibition of neuronal-like differentiation of pheochromocytoma cells using genome-wide approaches.
2. To explore the mechanisms for Myc-independent transcriptional activity of Max.
3. To investigate endogenous interaction between Myc and Sin3b.
4. To elucidate weather Ras induces senescence and the effect of Myc on the Ras-ERK dependent senescence of pheochromocytoma cells.
5. To investigate the ERK-binding to *MYC* promoter and its effect on *MYC* transcription.

3. MATERIALS AND METHODS

3.1. Cell culture

3.1.1. Cell lines and culture

K562 cell line derived from human chronic myeloid leukemia and was originally purchased to American Type Culture Collection. The cell line K562/S is a K562 subline that can grow attached to the surface of culture plates. This line was selected after multiple passes K562 cells in cell culture dishes, removing non-adherent. This cell line was grown in RPMI culture media (Gibco-Life Technologies) supplemented with 10% FBS (Fetal Bovine Serum) (Gibco-Life Technologies), 80 µg/ml of gentamicin and 2 µg/ml of ciprofloxacin, at 37º C in a 5% CO_2 atmosphere.

UR61 cell line derives from the rat pheochromocytoma PC12 cell line and contains a mouse N-Ras oncogene driven by a dexamethasone-inducible promoter (Guerrero, 1988). Cells were grown attached to the plates in DMEN culture media (Gibco-Life Technologies) supplemented with 10% FBS, 80 µg/ml of gentamicin, 2 µg/ml of ciprofloxacin and 250 µg/ml of neomycin (Gibco-Life Technologies), at 37º C in a 5% CO_2 atmosphere.

URMYC (constitutive expression of Myc), URMYCMAX3 (constitutive expression of both Myc and Max) are UR61 stable sublines generated in our lab by retroviral transfections. Both sublines were grown in the same conditions than UR61 cells and their specific resistance selections (50 µg/ml of hygromycin B for pBabe-Myc vector and 1 µg/ml of puromycin for pBabe-Max vector). The plasmid and viral constructions used are shown in Table 3.1 and Table 3.2., respectively.

UR61-MT-Max2324 (zinc-inducible expression of Max) was generated from UR61 by stable transfection and selected with 100 µg/ml hygromycin B (Invitrogen). This stable subline was grown in the same culture media than UR61.

IMR90-MycER and IMR90-RasER stable sublines were generated by retroviral infection of IMR90 and selected, respectively with 0.5 µg/ml of puromycin and 400 µg/ml of neomycin. IMR90, are human diploid fibroblast and also were growing in DMEN supplemented with 10% FBS and antibiotic-antimycotic (Gibco-Life Technologies), which contains penicillin, streptomycin and amphotericin B, at 37º C in a 5% CO_2 atmosphere.

Others cell lines used in this Thesis, as HeLa, 293T, NIH3T3 and MEFs, were grown in DMEM supplemented with 10% FBS, 80 µg/ml of gentamicin and 2 µg/ml of ciprofloxacin, at 37º C in a 5% CO_2 atmosphere.

3.1.2. Transient transfections

Cells were electroporated by Amaxa Nucleofector device using 100 µl of Ingenio Electroporation Solution (Mirusbio) per transfection with efficiencies ranging 50-70% of transfected cells as

scored by the expression of GFP when cotransfected with GFPmax vector. Number of cells, concentration of plasmid and nucleofection program was chosen according to cell-transfection database of Amaxa-Lonza. In all cases, were transfected 3 µg of DNA per million of cells, while the Amaxa transfection program depends on cell line: U-030 to NIH3T3, I-013 to HeLa and Q-001 to 293T.

For the generation of sublines with zinc inducible expression of Max, UR61 cells were transfected with pHebo-MT-Max vector in which the full-length human Max cDNA was cloned in the sense orientation. Exponentially growing UR61 (10^7 cells) were centrifuged 5 min at 1500 rpm and the pellet was suspended in 0.8 ml of DMEN containing 30 µg of the pHebo-MT-Max vector. The same was performed with pHebo-MT, the corresponding empty vector. Cells were electroporated at 260 V and 1 mF with BioRad Electroporator device. Following electroporation cells were cultured in DMEN with 10% FBS. 48 h after electroporation, hygromycin B (100 µg/ml) was added to the cell culture for selection of resistant cells. This selection was remained for several weeks until a pool of resistant cells was obtained. Individual cell clones were isolated by limiting dilution method in T96 well plates. Several sublines were expanded and analyzed for Max expression. We performed a pool of clon 23 and 24 and called UR61-MT-Max2324, whose Max-induction is showed in Results 3.1.6..

Table 3.1. Plasmid used as expression vectors. Respectively empty vectors are shown as e.v..

Expression vector	Insert	sp.	Origin	Reference
pHebo-MT (e.v.)	-		Dr. Grignani Laboratory	Grignani. 1990
pHebo-MT-Max	Max	Human	Dra. Delgado Laboratory	
pCEFL (e.v.)	-		Dr. León Laboratory	Vaqué, 2005
pCEFL-ERK-NLS	ERK-NLS (constitutively active)	Human	Dr. Crespo Laboratory	Rodríguez, 2010
pCEFL-ERK-DK	ERK-DK (not kinase activity)	Human	Dr. Crespo Laboratory	Rodríguez, 2010

Table 3.2. Viral constructions used.

Viral construction	Insert	sp.	Origin	Reference
pBabe (e.v.)	-		Dr. Amati Laboratory	Vlach, 1996
pBabe-Myc	Myc	Human	Dr. Amati Laboratory	Vlach, 1996
pBabe-Max	Max	Human	Dr. Amati Laboratory	Vlach, 1996
MSCV (e.v.)	-		Dr. Acosta Laboratory	
MSCV-Ras	RasV12	Human	Dr. Acosta Laboratory	

3.1.3. Infection with retrovirus

20 µg of the retroviral vectors, 2.5 µg of the plasmid encoding the VSVG envelope protein and 7.5 µg of a vector expressing the gag-pol retroviral proteins were transfected in 293T cells

(reach 60-80% confluence) with 75 µl of PEI reagent (at a concentration 1 mg/ml) per transfection.

48 h post-transfection, the media enriched in retroviral particles from the transfected 293T cells is collected and filtered using 0.2 mm pore size filters. Then filtered media containing retroviral particles was complemented with polybrene to a final concentration of 4 mg/ml and added to IMR90 cells (60-80% confluence). After 3 h, repeat the infection adding the viral supernatant without aspiration, and twice more, three infection rounds in total. 3 h after last infection media was replaced with fresh media to decrease VSVG-induced toxicity.

48 h post-infection, IMR90 infected cells were splitted (1:4) and selected with the corresponding resistance antibiotic.

3.1.4. Induction of cell differentiation and senescence in UR61 cells

The addition of 100 nM Dexamethasone (Dex) (Sigma) for 24-48 h induces Ras overexpression and differentiation in UR61 cells for 24 h (Vaqué, 2008). Moreover, Ras induces senescence after treatment over five days in these cells.

To grow this cell line over 48 h is necessary to establish a previous layer of matrigel 1:3000 (Gibco-Life Technologies) diluted in DMEN.

3.2. Assessment of Senescence and Proliferation

3.2.1. SA-β-Galactosidase staining

Cells were washed in cold PBS, fixed for 15 min at RT in PBS-0.5% Glutaraldehyde (Sigma), washed twice in PBS-1 mM $MgCl_2$ pH6 and incubated at 37 °C o/n (no CO_2) with fresh senescence staining solution: 0.5 mg of 5-bromo-4-chloro-3-indolyl P3-D-galactoside (X-Gal), 3.2 mg of Potassium ferricyanide ($K_3Fe(CN)_6$) and 1.05 mg of Potassium ferrocyanide ($K_4Fe(CN)_6$ $x3H_2O$) per ml. Then, samples was washed twice in PBS and observed at microscopy.

3.2.2. Caspase-1 activity assay

Caspase-1/ICE Fluorometric Assay Kit (R&D Systems) was used to measure caspase-1 activity. Essentially, cells were treated with Dex for eight days, collected and lysed (Lysis Buffer from Kit) Cell lysates were tested for protease activity by the addition of a caspase-specific peptide that is conjugated to the fluorescent reporter molecule 7-amino-4-trifluoromethyl coumarin (AFC). This cleavage of the peptide by the caspase releases the fluorochrome that, when excited by 400 nm wavelength light, emits fluorescence at 505 nm, detected with a microplate fluorescence reader (Thermo ScientificTM Varioskan). Caspase-1 activity were quantified each 30 min for 8 h.

3.2.3. Crystal violet assay

Cells were washed once in cold PBS, fixed for 1 h at RT in PBS-1% Glutaraldehyde and, after twice washes with PBS, which were removed and the samples were air-dried at RT. Then, cells were stained with 0.15% crystal violet (Sigma), scanned and quantified at 595 nm after dissolution in 1% Acetic acid.

3.3. RNA analysis

3.3.1. RNA isolation

Total RNA was prepared either with the Trizol reagent (Invitrogen) or with the RNA Easy Extraction Kit (Quiagen).

By the first method, cells were harvested by centrifugation, at 1,500 rpm for 5 min, and washed with cold PBS. After a spin at 1,500 rpm for 5 min, pellets were lysed with Trizol by pipetting up and down (1 ml per 5-10x10^6 cells). Homogenized samples were incubated for 5 min at RT to let the complete dissociation of nucleoprotein complexes. 0.2 ml of chloroform per ml of Trizol was added and samples, which were vortexed vigorously for 15 sec and incubated at RT for 3 min. Then samples were centrifuged at 12,000 rpm for 15 min at 4 ºC to separate the mixture into three phases: a phenol-chloroform phase, an interphase and a colourless upper aqueous phase (the volume of the aqueous phase is about 60% of the volume of Trizol used for homogenization). RNA remains exclusively in the upper aqueous phase, which is transferred carefully into fresh tube and RNAs were precipitated with 0.5 ml of Isopropyl alcohol per ml of Trizol used. After 10 min at RT, samples were centrifuged at 12,000 rpm for 10 min at 4 ºC. Supernatant was removed and RNAs were washed once with 1 ml of 75% Ethanol-DEP per ml of Trizol and centrifuged at 7,500 rpm for 5 min at 4 ºC. Then ethanol was removed and samples were air-dried for 5-10 min. Finally, RNAs were dissolved in nuclease free-water through a pipette tip and store at -80 ºC.

To prepare RNA used for RNA-sequencing and for microarray hybridization, we used columns following the RNA Easy Extraction Kit (Qiagen), following the manufacturer´s instructions.

3.3.2. Reverse transcription and quantitative polymerase chain reaction

RT was performed with iScript cDNA Synthesis Kit (BioRad). Supermix reaction was added to 1 µg getting 40 µl total volume and then it was incubated in a Thermal Robocycler using the following protocol (Priming: 5 min at 25 ºC; reverse transcription: 30 min at 42 ºC; inactivation: 5 min at 85 ºC; and cold store at 4 ºC). The cDNA samples can be stored at -20 ºC until used.

qPCR was performed with the IQ SYBR Green Supermix Kit (BioRad) in a BioRad MyiQ device and IQ5 Optical System software. To the samples were added some components (specific oligonucleotides at 100 nM and IQ SYBR Green Supermix).

The PCR conditions were determined depending on the nature and complexity of the primers and the cDNA template. In general, was used the the following PCR protocol:

I. Enzyme activation and initial denaturation: 3 min at 95 ºC.

II. PCR protocol (40 cycles):

A. Denaturing: 15 sec at 95 ºC.

B. Annealing: 15 sec at 56 ºC (or specific Tª depending on primers)

C. Extension: 20 sec at 72 ºC.

III. Final extension: 5 min at 72 ºC.

IV. Melt curve: 5 sec at 55-95 ºC (in 0.5 ºC increments)

To quantification, the Ct values of samples were normalized respect to the internal control RP-S14, S18 or β-actin, which have been used as housekeeping gene. Primers sequences used in RT-qPCR assays are shown in Table 3.3.

The PCR products were checked on 1.5% agarose gels.

Table 3.3. Primers used in the RT-qPCR assays to measure mRNA expression levels.

Gene	Sp.	Primer sequence (5'-3')	Annelling Tª
β-actin	Rat	CTAAGGCCAACCGTGAAAAG ACCCTCATAGATGGGCACAG	56
RP-S14	Rat	CAAGGGGAAGGAAAAGAAGG GAGGACTCATCTCGGTCAGC	56
Cdkn1a (p21)	Rat	CTTGTCGCTGTCTTGCACTC GCTTTCTCTTGCAGAAGACCA	58
c-Jun	Rat	CGCACGCTCCTAAACAAACT CGTTTCCATCTTTGCAGTCA	57
Neuromodulina (GAP43)	Rat	GTCAAACCGGAGGATAAGG CTTCTCCACACCATCAGCAA	57
SNAP25	Rat	AGAATCGCCAGATTGACAGG CCATGAGAGAAGCATGAAGGA	57
Aqp3	Rat	AGGAGTTGATGAACCGTTGC AAGCCAAGTTGATGGTGAGG	56
Bmi1	Rat	TGATAAAAGGTACTTGCGATGC ATGTAGGCAATGTCCATGAGC	56
Ink4a (p16)	Rat	AAGGCGAACTCGAGGAGAG GCACCATAGGAGAGCAGGAG	56
Klf5	Rat	GTCGTCTCATTTAAAAGCTCACC CACACCACGCACTGGAAC	56
LdhB	Rat	TCTGGATTCTGCTCGGTTTC GACTCCTGCCACATTCACC	56
Max	Rat	CACCATAATGCACTGGAACG CTGGTGCGTATGGTTTTTCC	56
Msn	Rat	GTGAAGGAGGGCATTCTCAA	56

		ATACCTGGATCCGCTCTTCC	
Ndrg1	Rat	GTCTCCTGCAAGAGTTCGATG TGTCGTGATACGTGAGGATGA	56
Ngfr	Rat	GTGTGTGAAGAGTGCCCAGA GTAGACCTTGGGATCCATCG	56
Pak1	Rat	TCCAAACCCAGAGGAGAAGA AACTCCCCTGTGACAGCATC	56
Ptn	Rat	GAAAATTTGCAGCTGCCTTC CACACACTCCATTGCCATTC	56
Ret	Rat	TTGGTCCAGTCCAACAACAA GCACAGACACGTTGAAATGG	56
Rgs2	Rat	AGGAGAAGCGGGAGAAAATG GCTTTTCTTGCCAGTTTTGG	56
Rgs4	Rat	TGAATCGCTGGAAAACCTG CTTCTTGGCCTTGGGACTTA	56
Scg2	Rat	GGTTGACGAGGAACAGAAGC CACCTCTTCCTGGGTTTGAG	56
Syp	Rat	GAGGGACCCTGTGACTTCAG CAGGTGCTGGTTGCTTTTC	56
Th	Rat	GGAGGCTGTGGTATTTGAGG CCGGGTCTCTAAGTGGTGAA	56
Vgf	Rat	GCCCTCGACCATCTTTCATA TCAGAGAACGCTCGCAATC	56
Chga	Rat	GAGGGTCCTCTCCATCCTTC AAGCTGCTGTGTTGCTGTTG	56
Fgfr1	Rat	AACGTGGAGTTCATGTGCAA GCAGAGTGATGGGAGAGTCC	56
Tspan2	Rat	TGGACTATGGTTTCGATTTGG CACTGTGACTCACGCATGG	56
Tspan5	Rat	TTGGGAATAACGTTTCTTGGA CTGCAAACCCCAGAATGAA	56
Mdm2	Rat	GAACTACCTGGGGAACGACA AGGCAATCAGCAGAATGGTC	56
Il1-α	Rat	GGCTCACTTCATGAGAACTGC CTGATCTGGGTTGGATGGTC	56
Il6	Rat	CCGGAGAGGAGACTTCACAG ACAGTGCATCATCGCTGTTC	56
Il1-β	Rat	CAGGAAGGCAGTGTCACTCA GTCGTCATCATCCCACGAG	56
Myc	Rat	GAGGTGGAAAACCCGACAG CAGCAGCTCGAATTTCTTCC	56
Ppp1r14c	Rat	CACCAGCAGGGAAAAGTGAC CATACAGCTGACCCAGTTGC	56
Myc	Mouse	CTGTGGAGAAGAGGCAAACC GCAGCTGGATAGTCCTTCCTT	56
RP-S18	Mouse	CGCCGCTAGAGGTGAAATT TTGGCAAATGCTTTCGCTC	56
Max	Human	TGTTGTTGTCGGTGACTTCC CATTATGATGAGCCCGTTTG	56
Myc (amplicon lenght 124bp)	Human	TCCTTGCAGCTGCTTAGACG TGCACCGAGTCGTAGTCGAG	56
Myc (amplicon lenght 527bp)	Human	AAGACTCCAGCGCCTTCTCT GTTTTCCAACTCCGGGATCT	56
RP-S14	Human	TATCACCGCCCTACACATCA GGGGTGACATCCTCAATCC	56
Actin beta	Human	AAAATCTGGCACCACACCTTC TAGCACAGCCTGGATAGCAA	56
Ink4a (p16)	Human	CGGTCGGAGGCCGATCCAG GCGCCGTGGAGCAGCAGC	56

Ink4b (p15)	Human	GAATGCGCGAGGAGAACAAG CCATCATCATGACCTGGAT	56
Cdkn1a (p21)	Human	CCTGTCACTGTGTCTTGTACCCT GCGTTTGGAGTGGTAGAAATCTG	56
Il-6	Human	CCAGGAGCCCAGCTATGAAC CCCAGGGAGAAGGCAACTGG	56
Il-8	Human	GAGTGGACCACACTGCGCC TCCACAACCCTCTGCACCCA	56

3.4. Protein analysis

3.4.1. Immunoblot

Cells were harvested by centrifugation, at 1,500 rpm for 5 min, washed in cold PBS and suspended in lysis buffer (150 mM NaCl, 50 mM TrisHCl pH8, 1 mM EDTA, 1% NP40, 0.2% SDS, 20 mM NaF) supplemented with protease/phosphatase inhibitor cocktail (Millipore). Lysates were sonicated 10 min in Bioruptor sonicator (5 pulses of 30 sec each one) to shear DNA and then it was incubated on ice for 30 min with occasional mixing to extract the proteins. Then, lysates were centrifuged at 12,000 rpm for 20 min at 4 ºC. Supernatants were collected and stored at -20 ºC.

Protein concentration was measured in duplicate by Bradford protocol (Bradford, 1976) using BSA standard curve. It was added loading buffer 1x (63 mM TrisHCl pH6.8, 10% Glycerol, 2% SDS, 0.01% Bromophenol blue and 5% β-mercaptoethanol). Samples were heated at 95 ºC for 5 min and run on SDS-PAGE minigel (BioRad) at 150 V in running buffer (0.25 M TrisHCl pH8.3, 1.92 M Glycine and 1% SDS) until the blue front was at the bottom of the gel.

Percentage of the gel was 8% to 15% according to the size of the protein(s) to be detected (<25 kDa, 15%; 25-50 kDa, 12%; 50-90 kDa, 10%; 90-200 kDa, 8%). Proteins were transfered into nitrocellulose membrane. A Mini-Gel Box Electrotransfer apparatus (BioRad) was used at 400 mA for 1 h to transfer in transfer buffer (0.25 M of TrisHCl pH8.3, 1.92 M glycine and 10% Methanol).

Membrane was blocked for 1 h in TBS-T (20 mM Tris pH7.5, 137 mM NaCl and 0.05% Tween20) with 5% non-fat dry milk under agitation. Following, the membrane was incubated with primary antibody diluted in TBS-T with 1% BSA for 1-3 h at RT under agitation or o/n at 4 ºC. After three washed in TBS-T for 10 min each one at RT, the membrane was incubated with secondary antibodies (1:10,000) conjugated with IRDye680 or IRDye800 fluorochromes (LiCor Biosciences) and visualized on Odyssey scanner (LiCor Biosciences).

Table 3.4. Primary and secondary antibodies used. It is indicated their use in immunoblot blot (IB), immunofluorescence (IF), immunoprecipitation (IP) and chromatin immunoprecipitation (ChIP).

Antigen	Type	Origin	Reference	Use and dilution
Actin	Goat polyclonal	Santa Cruz Biotechnology	I-19, sc-1616	IB (1:2000)
HDAC1	Rabbit polyclonal	Santa Cruz Biotechnology	H-51, sc-7872	IB (1:1000)
Max	Rabbit polyclonal	Santa Cruz Biotechnology	C-124, sc-765	isPLA (1:100)
	Rabbit polyclonal	Santa Cruz Biotechnology	C-17, sc-197	IF (1:100) isPLA (1:100) ChIP
Mxd1	Rabbit polyclonal	Santa Cruz Biotechnology	C-19, sc-222	isPLA (1:100)
Myc	Mouse monoclonal	Santa Cruz Biotechnology	C-33, sc-42	isPLA (1:25) IB (1:500)
	Mouse Monoclonal	Thermo Scientific	Ab5, MS-1054	IB (1:500)
	Rabbit polyclonal	Santa Cruz Biotechnology	N-262, sc-764	IB (1:1000) IP ChIP IF (1:100) isPLA (1:50)
Sin3b	Rabbit polyclonal	Santa Cruz Biotechnology	A-20, sc-996	IB (1:1000) IP ChIP IF (1:100) isPLA (1:50)
	Mouse monoclonal	Santa Cruz Biotechnology	H-4, sc-13145	IB (1:1000) isPLA (1:50)
CDK9	Rabbit polyclonal	Santa Cruz Biotechnology	C-20, sc-484	ChIP
	Rabbit polyclonal	Santa Cruz Biotechnology	H-169, sc-8338	IF (1:100) isPLA (1:100)
	Mouse monoclonal	Santa Cruz Biotechnology	D-7, sc-13130	IF (1:100) isPLA (1:100)
CDK2	Rabbit polyclonal	Santa Cruz Biotechnology	M2, sc-163	IF (1:100) isPLA (1:100)
RNA-Pol II P-Ser2	Rabbit polyclonal	Bethyl Labs	A300-654A	ChIP
RNA-Pol II P-Ser5	Rabbit polyclonal	Bethyl Labs	A300-655A	ChIP
ERK2	Rabbit polyclonal	Santa Cruz Biotechnology	K-23, sc-153	IB (1:1000) IF (1:100) isPLA (1:100)
	Mouse monoclonal	Santa Cruz Biotechnology	D-2, sc-1647	IF (1:100) isPLA (1:100)
Secondary antibodies	Donkey anti-rabbit	Alexa Fluor 488	A-21206	IF (1:500)
	Goat anti-mouse	Alexa Fluor 594	A-11037	IF (1:500)
	Goat anti-rabbit	Alexa Fluor 555	A-21428	IF (1:500)

3.4.2. Immunoprecipitation

3-5x10^6 cells was harvested and washed once in cold PBS. Then cells were centrifuged for 5 min at 1,500 rpm and pellet was suspended in non-denaturing lysis buffer (50 mM Tris pH7.5, 150 mM NaCl, 1% NP40 and 1 mM EDTA) supplemented with protease/phosphatase inhibitor cocktail (Millipore).

Lysates were sonicated 5 min in Bioruptor sonicator (5 pulses of 30 sec each one) to shear DNA and then it was incubated on ice for 30 min with occasional mixing. After, lysates were centrifuged at 12,000 rpm for 20 min at 4 ºC.

Supernatant was collected and distributed in different eppendorfs. 3 µg of primary antibodies and IgGs (as control of immunoprecipitation) were added and incubated o/n at 4 ºC under agitation.

Dynabeads-protein G (Invitrogen) was used to immunoprecipitation through magnetic separation technology. 20 µl of magnetic beads per ml were added to samples after o/n sample-antibody incubation. Protein-antibody-Dynabeads mix was incubated for 2-4 h at 4 ºC. Following magnetic beads were separated through a magnet and washed 3 times for 5 min with 1 ml of lysis buffer. Mix were suspended in Laemmli sample buffer which was heated at 95 ºC for 5 min to separate antibodies and proteins to Dynabeads which were removed using a magnet and at the end the samples were loaded in SDS-PAGE minigel.

3.4.3. Chromatin immunoprecipitation

Cells were fixed in 1% FPA for 10 min and fixation blocked with 125 mM Glycine for 5 min. Cells were washed with cold PBS and lysed in lysis buffer (0.7% SDS, 10 mM EDTA, 50 mM TrisHCl pH8) for 30 min. Cell lysates were sonicated in Bioruptor sonicator for 30 min at 4 ºC (15 pulses of 30 sec) to fragment DNA to lengths among 300 and 600 bp. Lysates were centrifuged at 12,000 rpm for 10 min at 4 ºC and supernatant was aliquoted and diluted 7-fold in dilution buffer (1% TritonX100, 1.2 mM EDTA, 16.7 mM TrisHCl pH8, 167 mM NaCl). Moreover, 20 µl of supernatant were separated to be used as input.

ChIP was performed by using magnetic beads coupled to specific antibody and IgG as control. To reduce nonspecific background, Dynabeads were previously incubated with salmon sperm DNA at 4 ºC for 1 h. Then, the mixture Dynabeads-salmon sperm was incubated with lysates o/n at 4 ºC and washed once for 5 min at RT with low salt wash buffer (1% TritonX100, 2 mM EDTA, 20 mM TrisHCl pH8, 150 mM NaCl), high salt wash buffer (1% TritonX100, 2 mM EDTA, 20 mM TrisHCl pH8, 500 mM NaCl), LiCl wash buffer (0.25 M LiCl, 1% NP40, 1 mM EDTA, 10 mM TrisHCl pH8) and twice with TE buffer (10 mM TrisHCl pH8 and 1 mM EDTA). Chromatin was eluted with 200 µl of elution buffer (0.1 M $NaHCO_3$, 10% SDS), added NaCl and RNase and keeping 30 min at 37 ºC. Finally, it was decrosslinked o/n at 65 ºC. Then 10 µl of 0.5 M EDTA, 20 µl 1 M TrisHCl pH6.5 and 2 µl of 10 mg/mL Proteinase K (Roche) were added to samples and incubated for 1 h at 45 ºC. DNA was purified using Qiaquick columns (Qiagen).

Not immunoprecipitated input aliquots were also decrosslinked and DNA-purified to be used as controls.

RT-qPCR of the eluted DNA was performed with the primers showed in Table 3.5 and Table 3.6.

Table 3.5. Primers used to validate chromatin immunoprecipitation assays by RT-qPCR.

Gene	Sp.	Primer sequence (5'-3')	Amplicon size	Annelling T[a]
-1,7 Kb *MYC* promoter	Rat	AAATCCGAGAGCCACAACC GGTGCGCATTGTTCAAAGTA	234	56
-1 Kb *MYC* promoter	Rat	GGCATATTCTCGCGTCTAGC CGGTCTACACCCCATACACC	155	56
-300 bp *MYC* promoter	Rat	GCCCGAACAACTGTACAGAAA CTCCCCTCCCGACCTCTA	232	56
-1,8 Kb *MYC* promoter	Mouse	AAGCATCTTCCCAGAACCTG ATCCCTAGTCTGCGTTTTGC	200	56
-1 Kb *MYC* promoter	Mouse	GAAAGCTTGGGTTTGTCCTG AATCCTCTTTGCCCCTGTG	234	56
+2.2 Kb *MYC* promoter	Mouse	ATCTGCGACGAGGAAGAGAA ACCGCAACATAGGATGGAGA	161	56
Lamp3 promoter	Human	AAGAAAGGAGGAGACCCAGGGTATGA AGAAACCTACCTGTGCCGGAGAAA	241	56
-2 Kb *MYC* promoter	Human	AGGAACCGCCTGTCCTTC ATCGCTATGCTGGATTTTGC	215	56
-1 Kb *MYC* promoter	Human	CACAAGGGTCTCTGCTGACTC CACACGGAGTTCCCAATTTC	232	56
-700 bp *MYC* promoter	Human	CTCTGGAACAGGCAGACACA CTCCCATTGCATTTGTTGG	208	56
-200 bp *MYC* promoter	Human	GTAGTTAATTCATGCGGCTCTCTTACT GGGCAGCCGAGCACTCTA	227	56
+1 bp *MYC* promoter	Human	GGAGGGATCGCGCTGAGTA TCTGCCTCTCGCTGGAATTAC	78	56
+190 bp *MYC*	Human	GCCGCATCCACGAAACTTT TCCTTGCTCGGGTGTTGTAAG	74	56
+393 bp *MYC*	Human	CGGGTAGTGGAAAACCAGGTAA TCGACTCATCTCAGCATTAAAGTGA	84	56
+5 Kb *MYC*	Human	AAGTACATTTTGCTTTTTAAAGTTGATT GCTCAATGATATATTTGCCAGTTATTT	80	56
+6 Kb *MYC*	Human	TCCCCATATTAGAAGTAGAGAGGGAA CTTGGGCATGTGGATGAGTCT	61	56
+7 Kb *MYC*	Human	ATCGGGAAGGTGTTAGTCTGAATC CACTCTCTCCTATTCTGAGGGCTT	62	56
+11,5 Kb *MYC*	Human	TGAAGGATGTTGGAGCATGAGTA TCTCTTCCCAGTTGAGTCTTGAAA	80	56

Table 3.6. Primers used to validate ChIP-seq data analysis by RT-qPCR. Corresponding UPL probes (Universal Probe Library, Roche) are shown. (Primers designed by Flor Pérez-Campo).

Gene	Sp.	Primer sequence (5'-3')	Probe	Annelling T[a]
ERBB4 (1)	Rat	GCACCACCAGCCTGCTATAC AACCAGCACCATTTCCAGAT	UPL 41	60

ERBB4 (2)	Rat	TGCTTTCCAAGATTAAATACATGC CCTGGCAACAGTTGAACACTAT	UPL 44	60
ERBB4 (4)	Rat	CCCTAAGTTCATAGCACACATCA TGCTTGCCTTTATAAGCAAATCT	UPL 76	60
FANCC (1)	Rat	CACTCCTGCAGAGATGAAACA AGTGGGCAGATGGTTCTAGG	UPL 60	60
FANCC (2)	Rat	AGGACTCTAGGTTCCCATCAGC CTTGCTTTGTTTGCCCTCAC	UPL 56	60
FANCC (3)	Rat	ACTGTTGTGAGTGCAGCTGTAAG CCTGGGGAACCAAGAGTGT	UPL 56	60
SOX13 (2)	Rat	GTCAGGGTCAGGAAGTCAGG GTCTTTATTGCTGCATAACTCAGG	UPL 110	60
SOX13 (4)	Rat	TGACGGCTCTGTCTCTCATTT CTGTGCTGGGGCTCACTT	UPL 111	60
SOX13 (5)	Rat	CAGACACCTGGGATCCTCTT GGATTGGATGTGCATTTGTG	UPL 42	60
SOX13 (7)	Rat	GGCATCCGCTCTACCTTTAAGT CACCATGGTCTTTTGCTTAAAAA	UPL 2	60

3.4.4. Immunofluorescence

3.4.4.1. IF in K562/S cells

K562/S cells were grown on coverslips and treated with 20 nM TPA (Sigma) to decrease Myc expression (Delgado, 1995). 24 h after treatment the cells were fixed for 15 min in 3.7% PFA in PBS. Then cells were permeabilized with 0.5% TritonX100 for 30 min, blocked for 30 min at 37 ºC in 3% BSA/PBS/0.01% TritonX100, incubated with primary antibodies o/n at 4 ºC, washed twice in PBS and incubated with the secondary antibodies at RT for 1 h. Subsequently, to detect a second protein in the same sample, the samples were blocked in rabbit-serum (sc-2338 of Santa Cruz Biotechnology) for 1 h and incubated again with primary and secondary antibodies. After several washes, cells were mounted in mounting medium with DAPI (Invitrogen). Images were obtained by means of a confocal microscope.

The primary and secondary antibodies used are shown in Table 3.4.

3.4.4.2. IF in HeLa and MEF

HeLa and MEF cells were grown on coverslips and fixed for 15 min in 3.7% PFA in PBS. Then cells were permeabilized with 0.5% TritonX100 for 30 min and blocked for 30 min at 37 ºC in 3% BSA/PBS/0.01% TritonX100. Then, primary antibodies were applied in blocking buffer o/n at 4 ºC, washed twice in PBS and incubated with the secondary antibodies at RT for 1 h. After several washes, cells were mounted in mounting medium with DAPI. Images were obtained by means of a confocal microscope.

The primary and secondary antibodies used are shown in Table 3.4.

3.4.5. *in situ* Proximity Ligation Assay

3.4.5.1. isPLA in K562/S cells

K562/S cells grown on coverslips were treated with 20 nM TPA (Sigma). 24 h after treatment, the cells were fixed for 15 min in 3.7% PFA in PBS. Then cells were permeabilized with 0.5% TritonX100 for 30 min at RT and incubated with blocking buffer (3% BSA/PBS/0.01% TritonX100) for 2 h at 37 ºC.

After blocking, primary antibodies, shown in Table 3.4, were applied in blocking buffer over night at 4 ºC.

On the following day, samples were washed in low buffered Tris Buffered Saline with Tween20 (TBS-T), which was prepared according to the O-LINK Bioscience recipe. Then, the slices were incubated with the PLA probe solution (containing the secondary antibodies conjugated with the DNA probes) for 1 h at 37 ºC. After the removal of the PLA probe solution, samples were washed in TBS-T and incubated with the hybridization solution containing oligonucleotides that hybridize to the PLA probes for 45 min at 37 ºC. The samples were washed and subsequently incubated in the ligation solution (containing the DNA ligase which allows the ligation of the probes and oligonucleotides to form a round circle DNA strand) for 45 min at 37 ºC. Subsequently, samples were washed in TBS-T and incubated with the amplification solution, containing DNA polymerase for the rolling circle amplification (RCA), at 37 ºC for 90 min. Finally, they were incubated with the detection stock solution (containing Texas Red labelled oligonucleotides that hybridize to the RCA product) for 1 h at 37 ºC, washed in SSC buffer (made up according to the manufacturer's recipe) and ethanol, mounted with DAPI mounting medium and analysed by means of a confocal microscope.

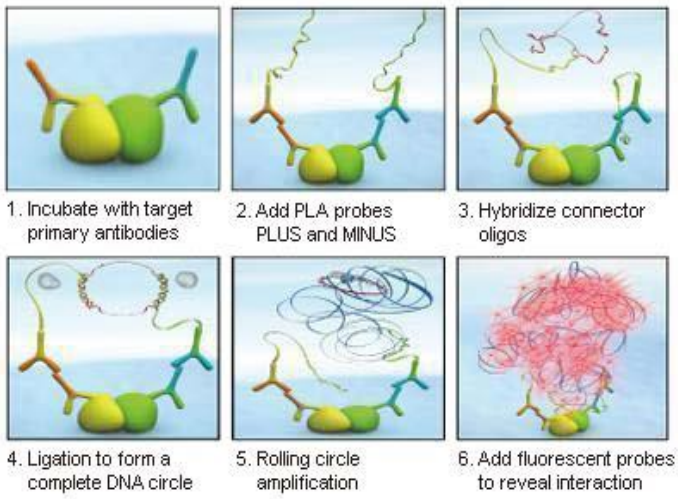

Figure 3.1. isPLA technique. Endogenous protein interactions in cells and tissue can be visualized using regular immunostaining antibodies combined with isPLA technique (or Duolink Kit, OLINK Biosciences).

3.4.5.2. isPLA in Hela and MEF cells

HeLa and MEF cells were grown on coverslips fixed for 15 min in 3.7% PFA in PBS. Then cells were permeabilized with 0.5% TritonX100 for 30 min at RT and incubated with blocking solution for 2 h at 37 ºC. After blocking, primary antibodies (shown in Table 3.4.) were applied in blocking buffer o/n at 4 ºC.

On the following day, samples were washed in TBS-T and incubated with commercial buffers following manufacturer's instructions of Duolink Kit (OLINK Biosciences), and finally mounted with DAPI mounting medium and analysed by means of a confocal microscope.

3.5. Luciferase assay

To analyze transcriptional activity of ERK2 over *MYC* promoter, we constructed some luciferase reporters containing different fragments and mutated fragments of human *MYC* promoter into pBV-luc luciferase vector. Luciferase assays were performed using 1.5 µg of the reporter plasmid (shown in Table 3.7.), 0.5 µg of the plasmid for renilla luciferase (pRL-Null) and 1.5 µg of the ERK2 expression vectors. 12 h after electroporation, the cells were cultured with 0% FBS for 24 h (starved) and then stimulated with DMEN supplemented with 10% FBS (D10F) from 10 min to 30 min and the cells were lysed to determinate the luciferase activity. Notably, stimulation with D10F after starved state involves ERK activation in the nuclei.

36 h after the different transient transfections the cells were washed in PBS and lysed on the plate with 200 µl of the PLB solution ("Passive Lysis Buffer"). Lysates were briefly frozen at -80 °C and then centrifuged at 14,000 rpm for 30 sec to clarify. Luciferase assay was performed using Dual Luciferase Reporter Assay System Kit (Promega) following the manufacturer´s instructions. The luciferase activity was measured in in a luminometer TD-20/20 (Turner Designs). Data were normalized to the values of the Renilla.

Table 3.7. Luciferase reporters used.

Luciferase vector	Insert	Origin	Reference
pRL-Null (renilla)		Promega	
pBV-Luc	Empty vector	Addgene	He, 1998
pBV-Luc-FragA	*MYC* promoter (human) -2394/-1194 from TSS	Addgene	He, 1998
pBV-Luc-FragB	*MYC* promoter (human) -1194/-741 from TSS	Addgene	He, 1998
pBV-Luc-FragD	*MYC* promoter (human) -484/-234 from TSS	Addgene	He, 1998
pBV-Luc-Del1	*MYC* promoter (human) -2394/+106 from TSS	Addgene	He, 1998
pBV-Luc-FragB1	*MYC* promoter (human) -1194/-1098 from TSS	This Thesis	
pBV-Luc-FragB1D2	*MYC* promoter (human) -1194/-1098 (two ERK boxes deleted) from TSS	This Thesis	

pBV-Luc-FragB2	*MYC* promoter (human) -1098/-932 from TSS	This Thesis	

3.6. Bioinformatic analysis

3.6.1. Gene expression analysis by microarray hybridization

Total RNA samples from UR61, UR61-Myc (URMYC) and UR61-MycMax (URMYCMAX3) cells, in differentiating and undifferentiating conditions (± 200 nM Dex for 24h) were purified with the RNA Easy Extraction Kit (Qiagen), converted into cDNA probes and hybridized to Affymetrix chips in the "Unidad de Genómica y Proteómica" of "Centro de Investigación del Cáncer" (CIC) in Salamanca (Spain).

The biotinylated cRNAs were hybridized (at 45 ºC for 16 h) in the Affymetrix Rat GeneChip RAT230 2.0. The hybridized arrays were washed and labeled with the GeneChip fluidics station 400, and scanned with Agilent G2500A GenArray Scanner. The high resolution images files obtained with the Affymetrix GCOS software after the biochip scanning (".CEL" files) were normalized with the dChip software (Li and Wong, 2001) for the mean of intensity, using the PM-MM (Perfect Match-Mismatch) criteria, which removes the background errors from the intensity signal and analyses exclusively those genes with "present calls" (i.e., genes with signal above background). The expression levels were converted to logarithmic scale (log_2).

The analysis of each experimental condition was based on two independent experiments. The replicates were used to calculate means, p-values and standard deviations of expression values of all probes. Each signal was considered valid if it appeared in the two experiments.

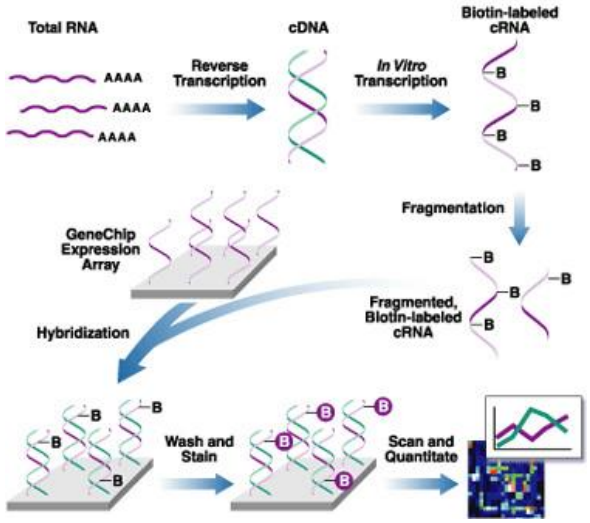

Figure 3.2. An overview of the standard method for analysis of eukaryotic gene expression using Affymetrix microarrays.

Finding biological interaction networks application was performed with Ingenuity Pathways Analysis software (http://www.ingenuity.com/). We analysed all connections, direct and indirect, using as selection criteria a score over 30. Score is a measure that indicates significant connections (high value indicates low probability of connection comes about by chance).

3.6.2. RNA-sequencing

3.6.2.1. Library preparation and sequencing

1 µg of total RNA (of two samples: UR61-MT-Hebo and UR61-MT-Max2324, both treated with 100 µM $ZnSO_4$ for 24 h) were used to construct 250 bp-insert size mRNA libraries using Illumina TruSeq RNA Sample Prep Kit v2 following manufacturer instructions. After quantification, quality control on a 2100 Agilent Bioanalyzer and normalization, a mix of four barcoded libraries per lane were submitted for on a High-Seq 2000 Illumina sequencing platform following a 50 bp Single-End protocol, obtaining a minimum of 40 million reads for each sample.

3.6.2.2. Data analysis

The sequencing reads obtaining for each sample were aligned against the Rat genome (version RGSC3.4.68) using Tophat algorithm (Trapnell, 2009). A collection of genes identified for rat were obtained from RefSeq database (rn4) through NCBI web service that was used to generate a .bed file with the gene coordinates using in house written perl scripts. These gene coordinates were posteriorly used to obtain the number of sequencing reads (with mapping and sequencing quality higher than 20) that overlap each one of the genes using Bedtools suite (Quinlan, 2010). The total number of reads corresponding to each gene, corrected by the total number of reads generated by each sample, were used to identify genes showing significant differential expression using DESeq package for R (Anders, 2010).

3.6.2.3. Gene ontology analysis

Gene Ontology (GO) structures biological knowledge by using a controlled vocabulary consisting in GO terms. GO terms are organized in three general categories: biological process, molecular function and cellular component, and the terms within each category are linked in defined parent-child relationships that reflect current biological knowledge. The ontology analysis of the RNA-seq data obtained was performed using the Babelomics 4.2 (http://www.babelomics.bioinfo.cipf.es/) and Webgestalt (http://www.bioinfo.vanderbilt.edu/webgestalt) software. The analysis were performed in two

groups separately, upregulated and downregulated genes. This software retrieves GO information for input genes and graphically represents the structures information.

3.6.3. ChIP-sequencing

3.6.3.1. Analysis of DNA binding sites from UCSC database (human model)

DNA binding sites for Sin3a and Max proteins identified in K562 human cell line from ENCODE/HAIB project (release of September 2012) and deposited in University of California Santa Cruz database (UCSC, http://www.genome.ucsc.edu/). Similarly, DNA binding sites from Myc protein in K562 and GM12878 cell lines identified from ENCODE/Open Chrom project (release of September 2012) were downloaded from the UCSC database. In order to restrict the analysis to only bona fide binding sites, in the case of Sin3a and Max, only those binding sites present in both technical replicates were used. In the case of Myc, binding sites from two human hematopoietic cell lines (K562 and GM12878) were compared and the analysis was restricted to the common binding sites. To detect those binding sites present in gene promoters, gene information from RefSeq database were downloaded from UCSC database (GRCh37/hg19 RefSeq release February 2009) and one Kb upstream and downstream of the transcription starting site for each gene was extracted.

All downloaded files were homogenized to .bed format using in house written perl and awk scripts. Finally, all comparisons between binding sites of different proteins and with the promoters were performed using intersectBed tool from BedTools suite (http://www.code.google.com/p/bedtools/) (Quinlan, 2010).

A minimum of 10% of sequence overlap between different binding sites was required. The normalization of binding sites per Mb was estimated considering 51.3 Mb of total promoter sequence and 3,500 Mb of total genomic sequence (according to RefSeq).

3.6.3.2. Analysis of DNA binding sites from UCSC database (in mouse model)

DNA binding sites for Sin3a, Myc, Max, Pol2, Smc3, CTCF and Znf384 proteins identified in CH12 mouse cell line from ENCODE/HAIB project (release of September 2012) and deposited in University of California Santa Cruz database (UCSC, http://www.genome.ucsc.edu/) and were downloaded from the UCSC database. In order to restrict the analysis to only bona fide binding sites, only those binding sites present in both technical replicates were used. To detect those binding sites present in gene promoters, gene information from RefSeq database were downloaded from UCSC database (GRCm38/mm9 release July 2007) and one Kb upstream and downstream of the transcription starting site for each gene was extracted.

All downloaded files were homogenized to .bed format using in house written perl and awk scripts. Finally, all comparisons between binding sites of different proteins and with the promoters were performed using intersectBed tool from BedTools suite (http://www.code.google.com/p/bedtools/) (Quinlan, 2010).

A minimum of 10% of sequence overlap between different binding sites was required. The normalization of binding sites per Mb was estimated considering 48.4 Mb of total promoter sequence and 3,500 Mb of total genomic sequence (according to RefSeq).

3.6.3.3. ChIP-seq of UR61-MT-Hebo and UR61-MT-Max2324

3.6.3.3.1. Library preparation and sequencing

A minimum of 10 ng of immunoprecipated DNA (together with control DNA inmunoprecipitated with anti-IgG antibody) were used to construct 250 bp insert size DNA libraries using Illumina ChIP-seq Sample Preparation Kit following manufacturer instructions. After quantification, quality control on a 2100 Agilent Bioanalyzer and normalization, a mix of six barcoded libraries per lane were submitted for on a High-Seq 2000 Illumina sequencing platform following a 50 bp Single-End protocol, obtaining between 20 and 30 million reads per sample.

3.6.3.3.2. Data analysis

The sequencing reads obtaining for each sample were aligned against the rat genome (version RGSC3.4.68) using BWA algorithm (Li and Wong, 2001). Enrichment regions were identified from the aligned data of both experimental and control sample using MACS algorithm (Zhang Y, 2008) constructing the model with peaks with a fold between 5 and 30, a minimum p-value of 0.05, and with the options –on-auto and –to-large. Those peaks that overlap regions contained in RepeatMasker database for rat were discarded. Posteriorly the coverage of each peak in each experimental and control sample were calculated using Bedtools suite (Quinlan, 2010) and those peaks in the experimental sample that contains not more than 2 reads in the control sample were selected as positive enrichment regions. Finally, the relative location of the positive peaks respecting the rat annotated genes was annotating using Ensembl perl API tools (http://www.ensembl.org/).

These peaks detected were analysed with Integrative Genomics Viewer (http://www.broadinstitute.org/igv/) to evaluate enrichment and select genes to validation.

4. RESULTS

PART I: MYC AND MAX TARGET GENES AND DIFFERENTIAL EXPRESSION ANALYSIS USING MICROARRAYS, RNA-SEQ AND CHIP-SEQ

4.1.1. Myc-dependent gene expression in Max-deficient cells

It has been demonstrated by our group that Myc blocks Ras-mediated differentiation of UR61 cells and that this effect is mediated by inhibition of c-Jun upregulation (see Introduction). UR61 cells do not express wild type Max, but a truncated form (Max^{PC12}) unable to bind MYC. This is most interesting as it represents the unique known example of Myc function independent of Max.

UR61 sublines with constitutive Myc expression (URMYC) and constitutive both Myc and Max (URMYCMAX3) were generated in our lab (Pablo Garcia, PhD Dissertation).

In this part we set out to study the mechanisms by which Myc exert this biological effect (the blocking of differentiation) with and without Max and identify their target genes. For this, we compare transcriptomes of UR61, URMYC and URMYCMAX3 treated and untreated with dexamethasone (Table 4.1) using Affymetrix chip hybridization as described in Materials and Methods.

Table 4.1. Samples analysed by microarrays. The analysis of each experimental condition was based on two independent experiments (Experiment-1 and Experiment-2) for each condition. In total, twelve RNA samples were hybridized and analysed.

Experimental samples	Ref. Exp-1	Ref. Exp-2
1.- UR61	05	08
2.- UR61 +200 nM Dex for 24h	05	08
3.- URMYC	05	08
4.- URMYC +200 nM Dex for 24h	05	08
5.- URMYCMAX3	08	Nov08
6.- URMYCMAX3 +200 nM Dex for 24h	08	Nov08

Chip hybridization data was collected for all the above samples using Affymetrix Rat230 2.0 platform. The hybridization reactions were processed and scanned according to standard Affymetrix protocols. From each cell line and condition, two independent experiments with cell harvests, labelling and chip hybridization experiments were performed.

Firstly, the expression mRNA levels of Myc, Max, Gap43 and c-Jun was assessed by RT-qPCR as control of the cellular model (Figure 4.1.). The results showed that as described c-Jun expression was dramatically upregulated in response to Ras-mediated differentiation and that Myc abrogated this upregulation. They also confirmed the lack of expression of *MAX*, except in URMYCMAX cells, and interestingly, the transient upregulation of endogenous and ectopic Myc shortly after differentiation, likely due to a posttranscriptional mechanism.

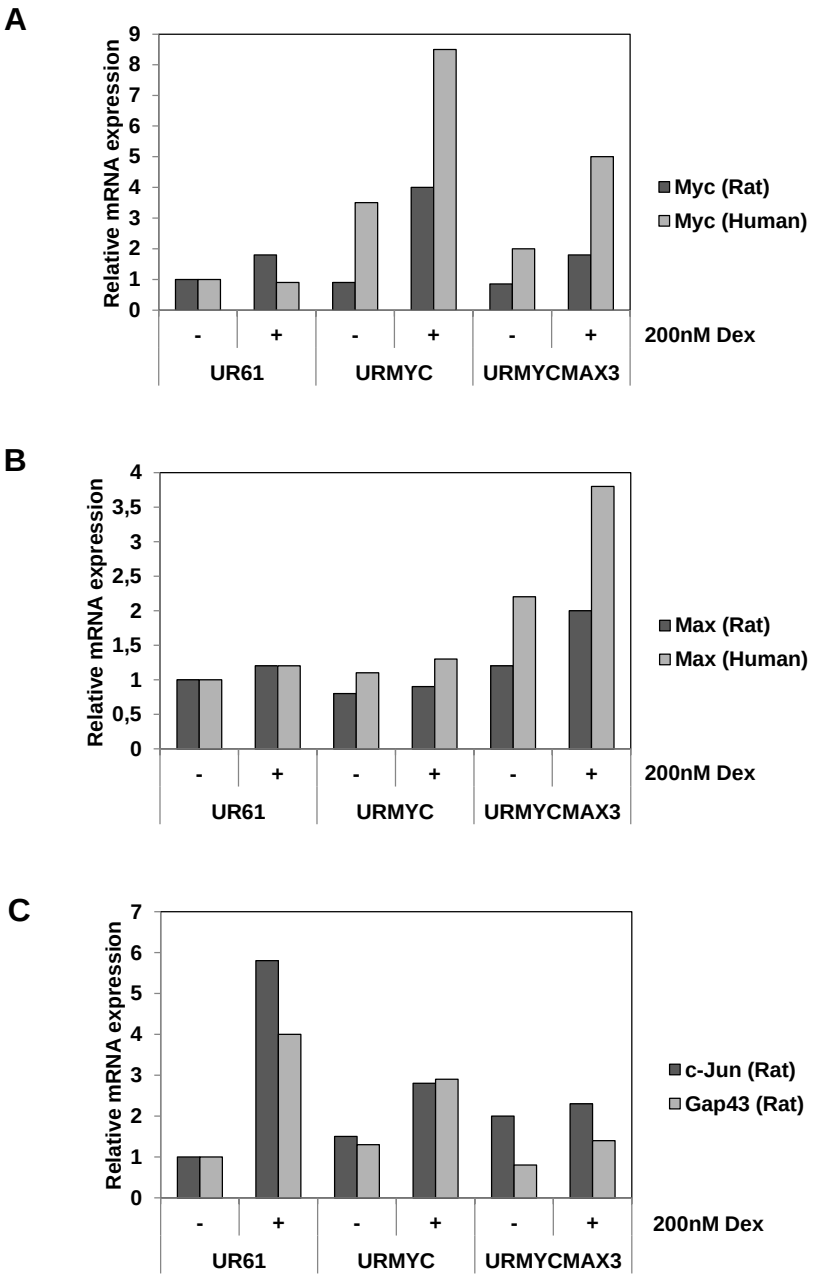

Figure 4.1. Relative mRNA expression of Myc, Max and differentiation markers. (A) Cells were treated for 24 h with 200 nM Dex as indicated. Relative mRNA expression of Myc and **(B)** Max, endogenous (rat) and exogenous (human) levels, were measured by RT-qPCR as control of experiment previous to validation. **(C)** Relative mRNA expression of endogenous c-Jun and Gap43, as control of differentiated condition, are shown. To allow comparisons, the residual Max expression has been given value 1. Data are means from two independent experiments.

dChiP software was used to bioinformatic analysis. In a first joint analysis of all samples clearly two groups were distinguished, untreated and treated cells (Figure 4.2.), and also we found a good clustering between duplicates. The analysis shows that there are not extensive differences between URMYC and URMYCMAX3 transcriptomes. In fact, the bioinformatic tools clustered both samples together (Figure 4.2.). The clustering indicates that gene profiling of the two independent experiments of each treatment or cell line are similar enough to allow the analysis as "duplicates" through the dChip platform.

The expression profiles were compared among different cell lines and experimental conditions separately with dChip software (see below). The value obtained in each analysis for each gene is the "fold change", calculated as "mean baseline expression of experimental sample/mean baseline control sample". It has been transformed at logarithmic scale (log_2) and the values have been considered significant over 2.3-fold (> $log_2$1.2) (complete list of genes differentially expressed appears in Annex 1).

Validation of microarray results was done using RT-qPCR on a subset of genes (Table 4.2.) Altogether we could validate the 90% of expression changes detected by microarray hybridation plus dChip statistical analysis.

Table 4.2. Subset of genes included in the validation of microarray data.

Symbol	Gene
Aqp3	Aquaporin 3
Chga	Chromogranin a
Klf5	Kruppel factor 5
LdhB	Lactate dehydrogenase B
Mdm2	Mdm2 p53 dinding protein
Ndrg1	N-Myc downstream regulated gene 1
Ngfr	Nerve growth factor receptor
Pak1	P21-activated kinase 1
Ret	Ret proto-oncogene
Rgs4	Regulator of G.protein signalling 4
Syp	Sinaptophysin
Tspan2	Tetraspanin 2
Tspan5	Tetraspanin5
Vgf	Nerve growth factor inducible

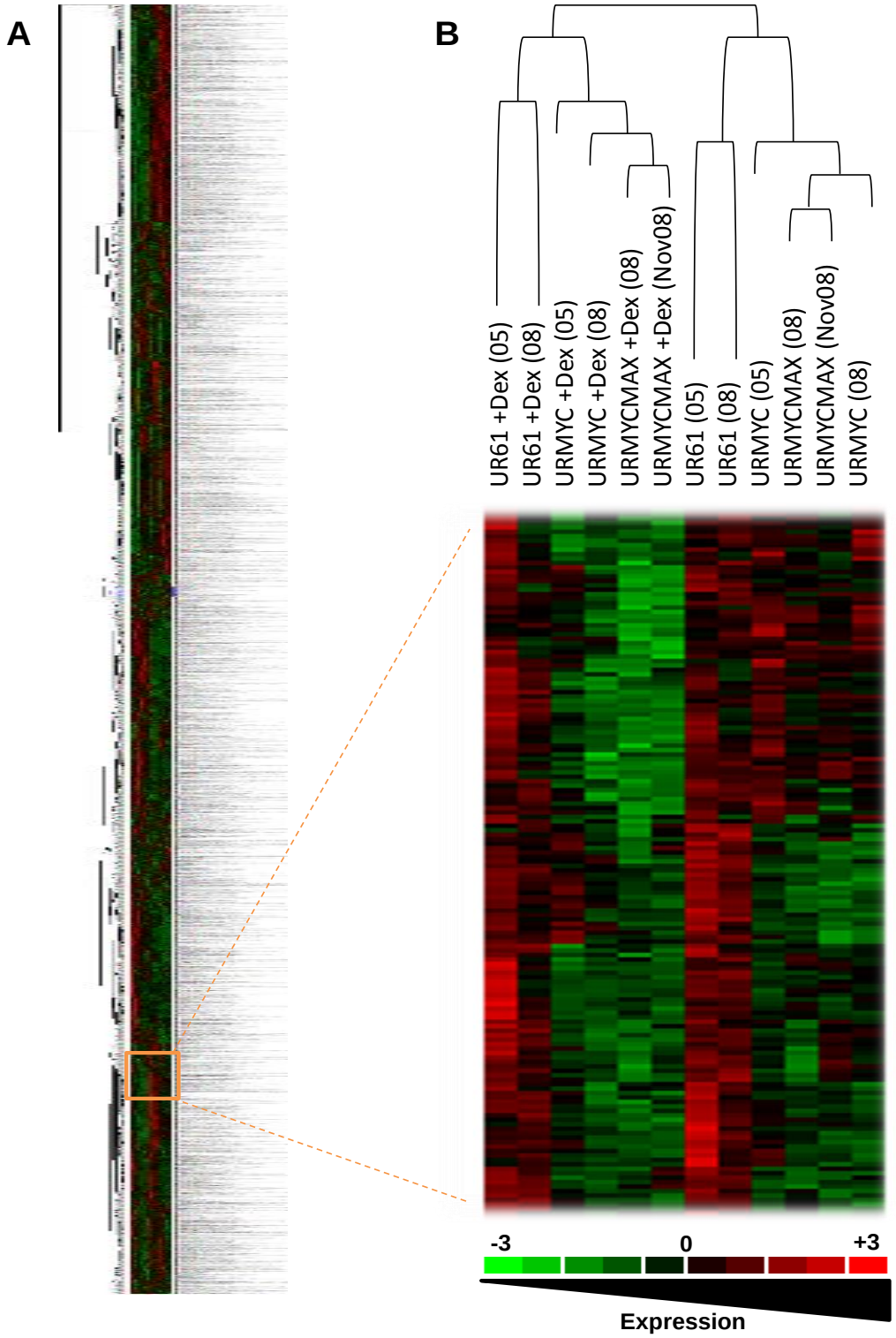

Figure 4.2. Hierarchical clustering analysis of gene expression profiles. (A) Hierarchical clustering of genes and samples by differential gene expression. 31099 probesets were detected corresponding to 14788 annotated genes filtered by RepeatMasker. **(B)** The samples, used by duplicate, correspond to UR61, UR61 +Dex for 24 h, URMYC, URMYC +Dex for 24 h, URMYCMAX3 and URMYCMAX3 +Dex for 24 h. The gene expression is shown in logarithmic scale from green (lower expression) to red (higher expression) as indicated at the bottom of the panel.

4.1.2. Gene expression profile induced by Ras during UR61 differentiation.

To know the gene expression profile of UR61 cells before and after Ras-induced differentiation we used the Affymetrix hybridization analysis. The results are shown in Figure 4.3., which show a dramatic change in gene expression in differentiating cells (24 h after Ras induction by dexamethasone).

As expected, most of selected genes for validation as Ret, Vgf, Ngfr, Chga, Klf5, Rgs4 and Mdm2 are induced in neuronal-like differentiation (Figure 4.3.B), which were validated by RT-qPCR (Figure 4.3.C).

Next, we used Ingenuity Pathways software to performed network analysis with the validated data, which revealed that c-Jun transcription factor is the main node located in the middle of network when compare differentiated and undifferentiated cells (Figure 4.4.) suggesting that the neuronal differentiation phenotype in this rat pheochromocytome model is mediated by this transcription factor.

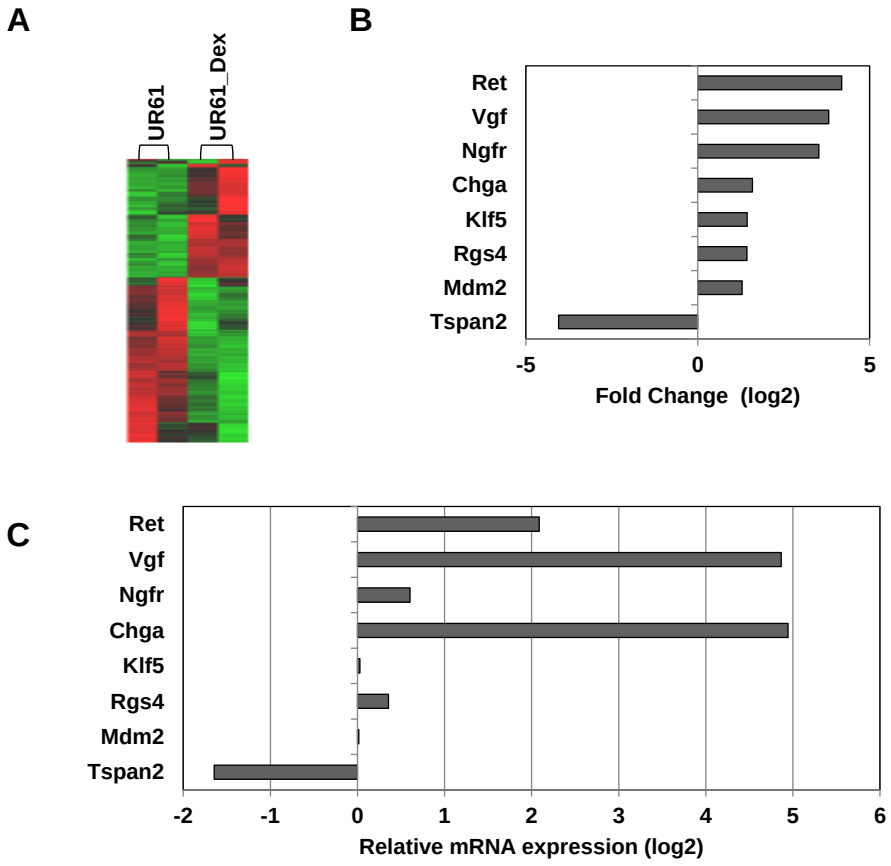

Figure 4.3. Genes regulated in Ras-induced differentiation in UR61 model. (A) Heat-map showing 1790 probesets which expression has changed due to neuronal-like differentiation with an expression change > 2.3-fold. The duplicates clustered, where the genetic expression is shown in $\log_2$ scale from green (lower expression) to red (higher expression). These cells were treated for 24 h with 200 nM of

dexamethasone and compared with untreated cells. **(B)** Expression changes of selected genes from the microarrays data. **(C)** The relative expression of these genes was confirmed by RT-qPCR. The values are means from two independent experiments.

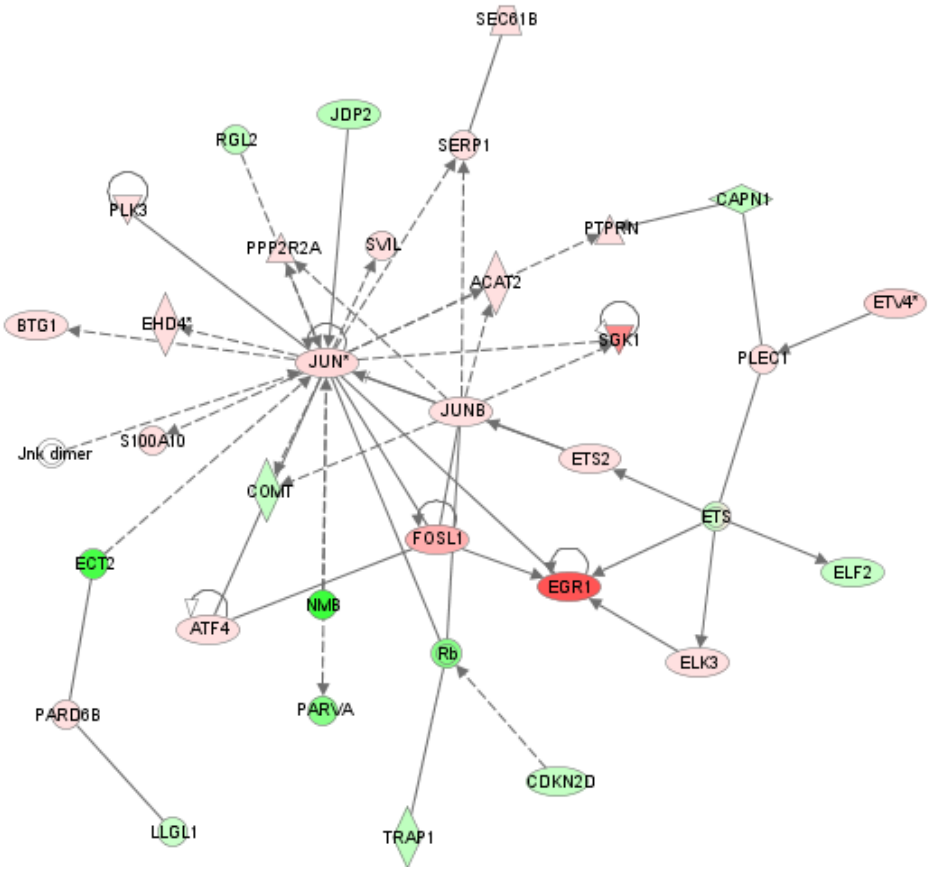

Figure 4.4. c-Jun regulates neuronal-like differentiation. Network obtained from analysis of comparison UR61 vs. UR61 +Dex performed by Ingenuity Pathways software, which shows c-Jun transcription factor as main regulator of neuronal-like differentiation in this model. The network score is significant (score 34 by Ingenuity Pathways) and correspond with behaviour, nervous system, development and gene expression pathways. Green colour indicates downregulated and red colour upregulated signature genes.

4.1.3. Gene expression profile induced by Myc in UR61

We next used this Max-deficient cell model to study whether Myc overexpression results in changes in gene expression. For this purpose we compared the gene expression profiles based in microarray data of controls cells and cells overexpressing human Myc, and the results are shown in Figure 4.5.B.

The validation by RT-qPCR confirmed that Pak1 and Ndrg1 are upregulated, whereas Chga, Vgf, Syp, Ngfr, Rgs4 and Ret are downregulated in URMYC growing cells (Figure 4.5).

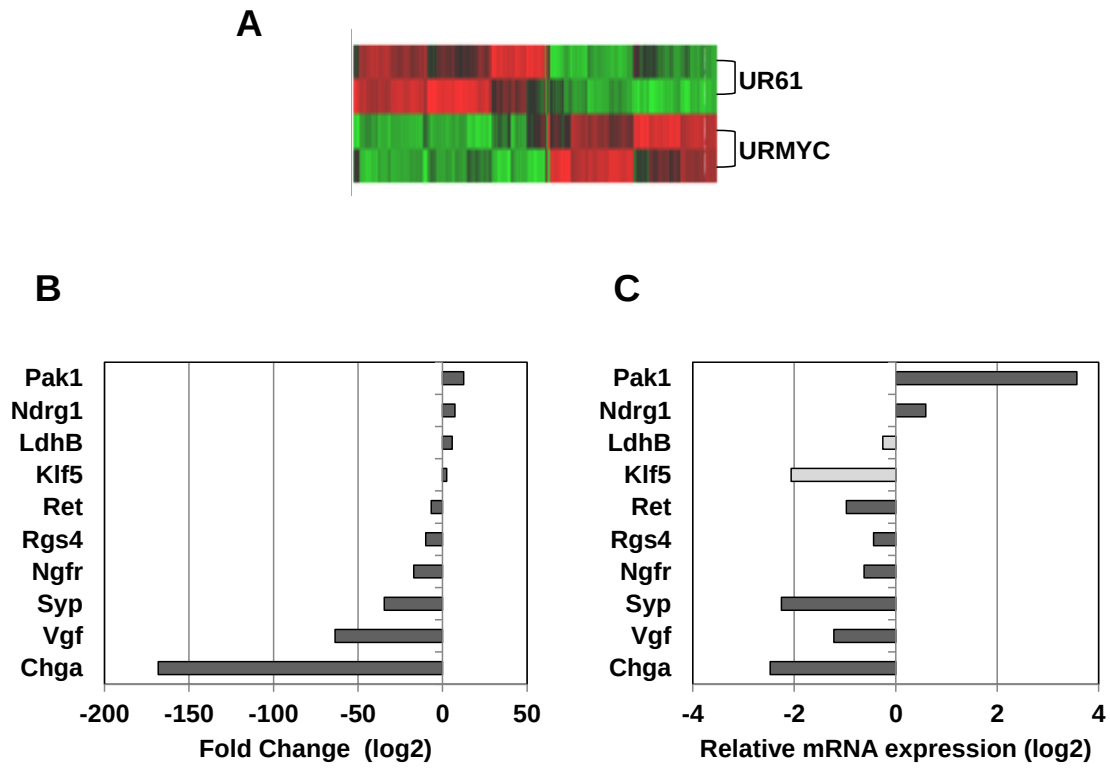

Figure 4.5. Genes regulated by Myc in URMYC cells. (A) Heat-map showing 1457 probesets which expression has changed due to presence of Myc in growing cells with an expression change > 2.3-fold. The duplicates clustered, where the genetic expression is shown in $\log_2$ scale from green (lower expression) to red (higher expression). **(B)** Expression changes of selected genes from the microarrays data after comparison UR61 vs. URMYC growing cells. **(C)** mRNA expression of the indicated genes were determined by RT-qPCR. The values are means from two independent experiments. Grey bars indicate expression levels obtained by RT-qPCR which do not correspond with microarray data.

4.1.4. Myc-mediated differential gene expression during UR61 differentiation.

Most of the genes regulated by Myc in growing URMYC cells (Pak1, Chga, Vgf, Syp, Ngfr and Rgs4) are genes reported as specific of neuronal linage (Figure 4.6). This result confirms that Myc provokes an arrest in neural differentiation of UR61 cells.

Also, Ingenuity Pathways analysis showed Myc as a major transcription factor involved in blocking neuronal-like differentiation in URMYC cells (Figure 4.7.).

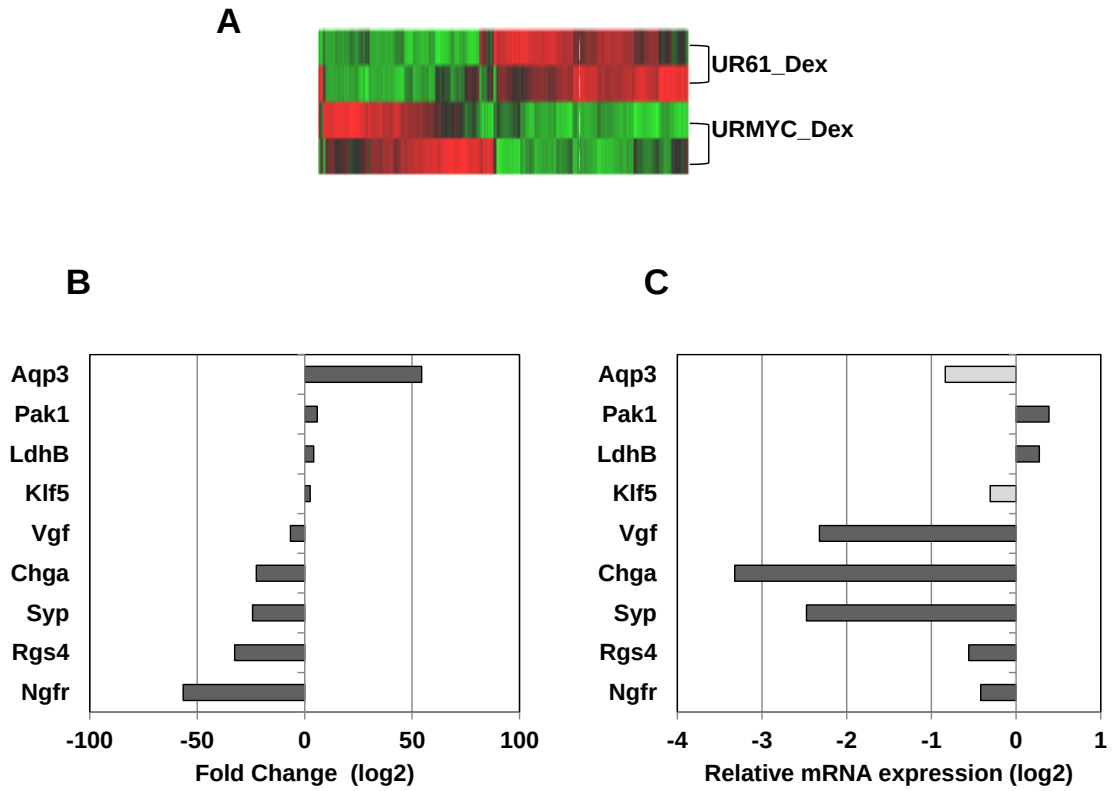

Figure 4.6. Genes regulated by Myc in differentiated URMYC cells. (A) Heat-map showing 1630 probesets which expression has changed in presence of Myc during differentiation in UR61 cells with an expression change > 2.3-fold. The duplicates clustered, where the genetic expression is shown in $\log_2$ scale from green (lower expression) to red (higher expression). **(B)** Expression changes of selected genes from the microarrays data after comparison between UR61 and URMYC cells, both treated with 200 nM Dex **(C)** mRNA expression levels of the indicated genes were determined by RT-qPCR. The values are means from two independent experiments. Grey bars indicate expression levels obtained by RT-qPCR which do not correspond with microarray data.

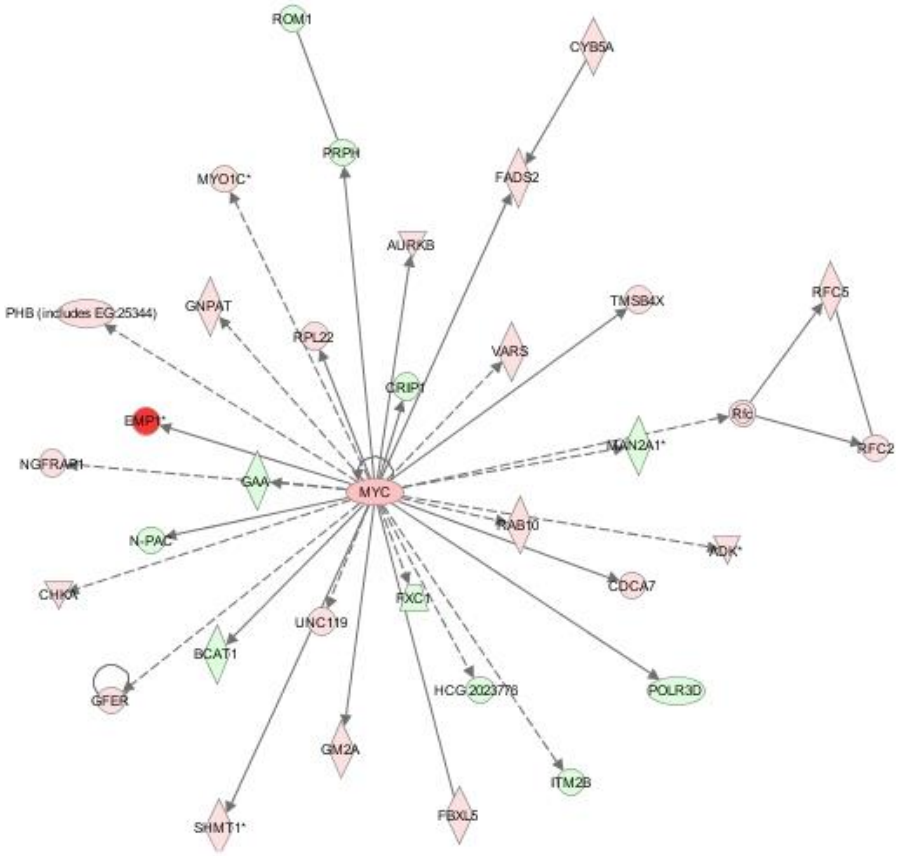

Figure 4.7. Myc-blocked neuronal-like differentiation in URMYC cells. Network obtained from analysis of comparison UR61 +Dex vs. URMYC +Dex with Ingenuity Pathways software, which shows Myc as main regulator of blocked neuronal-like differentiation in this model. The network score is significant (score 41 by Ingenuity Pathways) and correspond with amino acid metabolism, small molecule biochemistry and cell cycle pathways. Green color indicates downregulated and red color upregulated signature genes.

4.1.5. Max-mediated differential gene expression in Myc-expressing cells.

We also used this cell model to study whether Max overexpression results in changes in gene expression profile. For this purposes we compared the gene expression profiles of Myc-expression cells with cells overexpressing human Myc and human Max (Figure 4.8.).

Only 192 probesets were found with an expression change > 2.3-fold in this comparison, which are represented in the heat-map from Figure 4.8.A. Mdm2 and Tspan2 are upregulated by Max in Myc-expressing cells, whereas Ndrg1 and Tspan5 are repressed (Figure 4.8.B). All of them were validated by RT-qPCR (Figure 4.8.C).

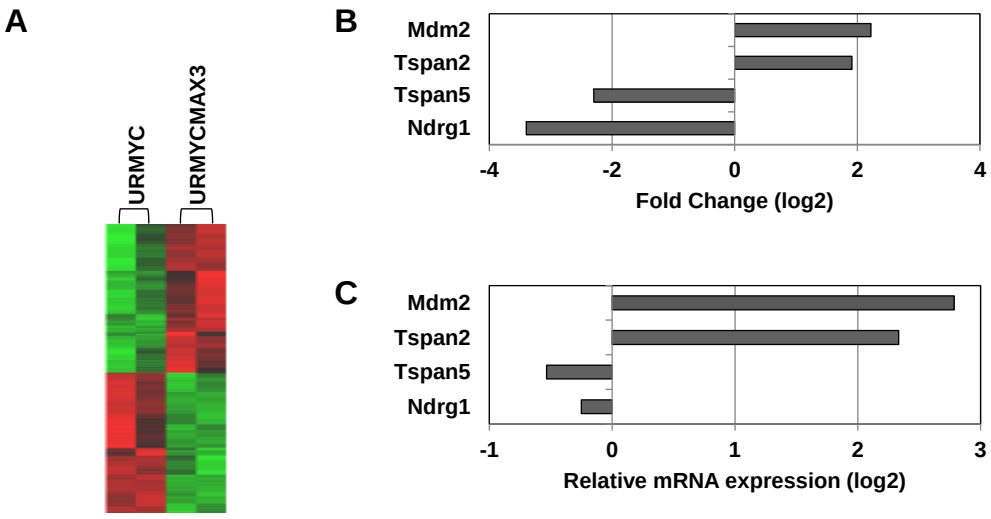

Figure 4.8. Genes regulated by Max in Myc-expressing cells. (A) Heat-map showing 192 probesets which expression has changed in presence of Max with an expression change > 2.3-fold. The duplicates clustered, where the genetic expression is shown in $\log_2$ scale from green (lower expression) to red (higher expression). **(B)** Expression changes of selected genes from the microarray data after comparison URMYC vs. URMYCMAX3 growing cells. **(C)** Expression of these genes determined by RT-qPCR. The values are means from two independent experiments.

4.1.6. Max-mediated differential gene expression during UR61 differentiation.

We investigated the role of Max in this model during neuronal-like differentiation. We confirmed that Chga, Aqp3, Tspan5 and Ndrg1 expression levels are lower in differentiated URMYCMAX3 cells with respect to differentiated URMYC cells, whereas Mdm2 is overexpressed (Figure 4.9.). Ingenuity Pathways analysis revealed that in presence Max, Myc continues being in the central node of networks, suggesting that Myc is the responsible for the change of gene expression in this model when the neuronal differentiation is blocked also in presence of Max (Figure 4.10).

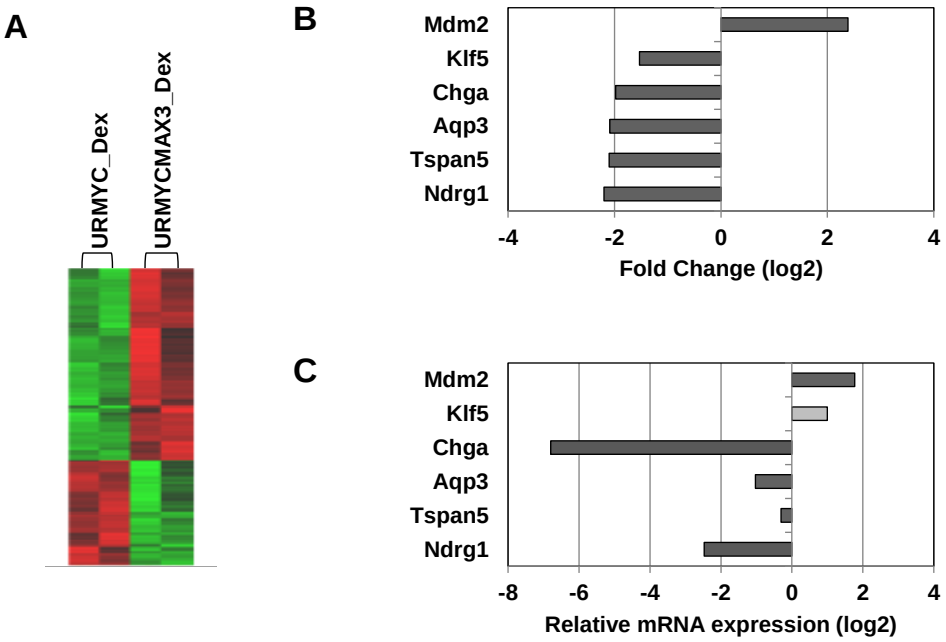

Figure 4.9. Genes regulated by Max for blocking of Ras-induced differentiation. (A) Heat-map showing 628 probesets which expression has changed in presence of Max during differentiation in these cells with an expression change > 2.3-fold. The duplicates clustered, where the genetic expression is shown in $\log_2$ scale from green (lower expression) to red (higher expression). **(B)** Expression changes of selected genes from the microarrays data microarray data after comparison URMYC vs. URMYCMAX, both treated with 200 nM Dex, are illustrated. **(C)** Expression of these genes determined by RT-qPCR. The values are means from two independent experiments. Grey bars indicate expression levels obtained by RT-qPCR which do not correspond with microarray data. The values are means from two independent experiments.

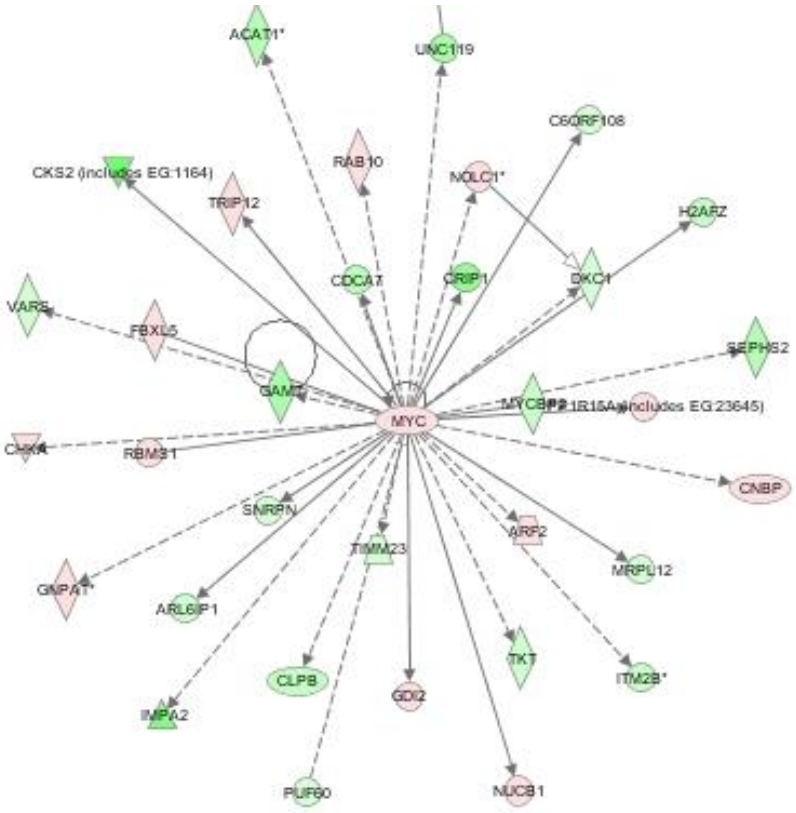

Figure 4.10. Myc is in the central node in the network obtained when Myc blocks neuronal-like differentiation in presence of Max. Network obtained from analysis of comparison URMYC +Dex vs URMYCMAX +Dex with Ingenuity Pathways software. The network score is significant (score 42 by Ingenuity Pathways) and correspond with molecular transport and protein trafficking pathways.

4.1.7. Gene expression profile induced by Max in UR61.

After several failed attempts to generate a cell line expressing constitutive Max, we decided to generate a UR61 subline with zinc-inducible expression of this protein. For the generation of this subline, UR61 cells were transfected with pHebo-MT-Max vector in which the full-length human Max cDNA was cloned in the sense orientation, and pHebo-MT-empty vector as control (as described in Materials and Methods)

After transfection and selection, we performed a pool of two clones Max inducible (identified as 23 and 24) which called UR61-MT-Max2324. These cells were expanded and analyzed for Max expression by western blot after 24 h with 80-120 µM $ZnSO_4$ (Figure 4.11).

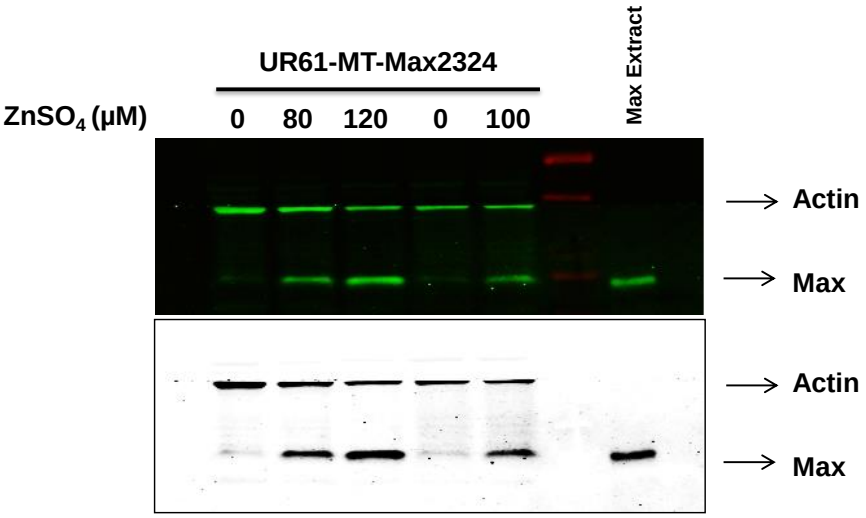

Figure 4.11. Generation of Max-inducible system. Immunoblot analysis of inducible Max expression in UR61-MT-Max2324 cells after treatment with 100 µM $ZnSO_4$ for 24 h. It was analyzed by western blot with anti-Max and anti-Actin (antibodies are shown in Table 3.4.of Materials and Methods).

Next we analysed gene expression profiles by RNA-seq using the Illumina Genome Analyzer to study particular functions of Max and its potencial targets genes. As the UR61-MT-Max2324 expressed detectable levels of Max even in the absence of inducer (Figure 4.11), we compared the transcriptome of Zn^{2+} treated UR61-MT-Max2324 cells with that of cells transfected with the empty vector (UR61-MTHebo) also treated. RNA-libraries of UR61-MT-Hebo and UR61-MT-Max2324 treated with 100 µM $ZnSO_4$ for 24 h by duplicate were constructed as described in Materials and Methods.

After normalization, the obtained data suggested significant differences in Max-expressing cells. Thus, we selected a subset of genes (Table 4.3.) to validate by RT-qPCR. All the expression changes detected by RNA-seq were confirmed (Figure 4.12.).

Table 4.3. Subset of genes included in the validation of RNA-seq data.

Symbol	Gene
Scg2	Secretogranin II
Chga	Chromogranin A
Th	Tyrosine hydroxylase
Snap25	Synaptosomal-associated protein, 25kDa
Ppp1r14c	Protein phosphatase 1, regulatory (inhibitor) subunit 14C
Msn	Moesin
Rgs2	Regulator of G-protein signaling 2, 24kDa
Fgfr1	Fibroblast growth factor receptor 1
Ptn	Pleiotrophin

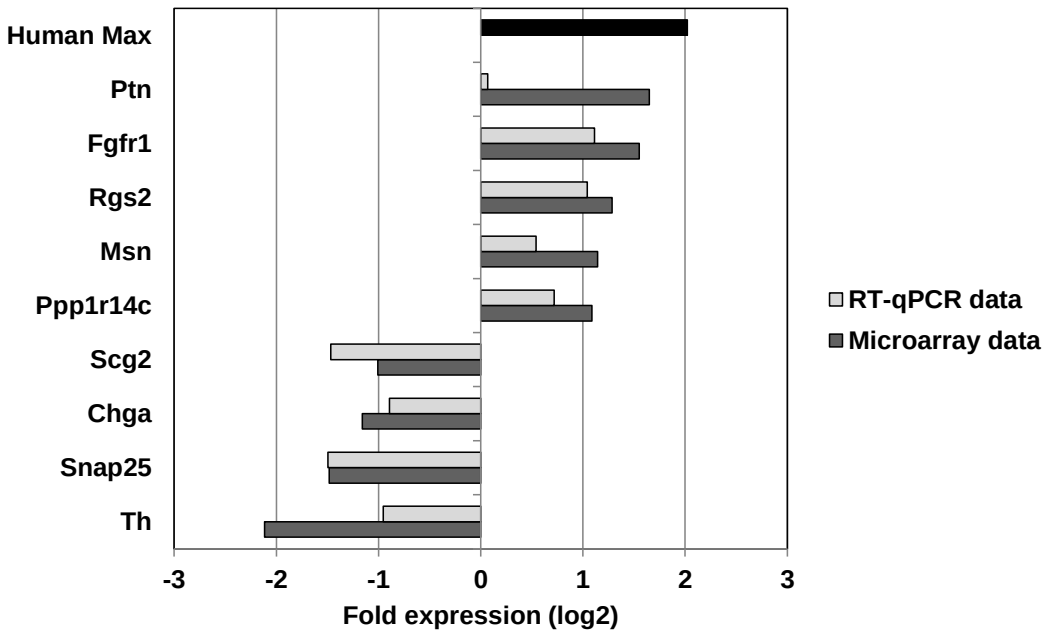

Figure 4.12. RNA-seq data validated by RT-qPCR. The expression levels of all the analysed genes were confirmed by RT-qPCR in Max-expressing cells, which induction was also confirmed (black bar). The values are means from two independent experiments.

Statistical analysis showed 519 annotated genes over p-value 0.05 (Annex 2), 258 downregulated and 261 upregulated in presence of Max, whose ontology was analysed separately by two independent software, Webgestalt and Babelomics 4.2., with similar results.

The gene ontology analysis of upregulated genes in Max-expressing cells showed several significant biological processes involved, most of them related with cellular adhesion and mobility (Figure 3.1.14). Moreover, the list of significantly enriched KEGG pathways includes: axon guidance (adjP=0.0002), cell adhesion (adjP=0,00003), regulation of actin cytoskeleton (adjP=0.001), Wnt signalling (adjP=0.0118) and cancer (adjP=0,0002).

Also, the majority of genes downregulated in Max-expressing cells are related mainly with metabolic pathways (djP=0.0140) and different components of synapsis and cytoskeleton.

4.1.8. Myc and Max binding sites on the genome found by ChIP-seq.

The goal of ChIP-Seq data analysis is to find those genomic regions that are enriched in a particular transcription factor.

Regions of high sequencing read density are referred to as “peaks” to evoke the visual impression of many reads mapping to a specific region compared to few reads mapping to the genomic background.

In a parallel approach we will carry out ChIP of UR61 cells and analyse Myc and Max binding sites at the genome level by ChIP-seq. As this is the only cell line known to lack Max, it will be most interesting to identify Myc binding sites on the genome that occur in the absence of Max and compare with Max-expressing cells.

UR61-MT-Max2324 cells were treated with 100 µM $ZnSO_4$ for 24 h to induce Max expression and then they were harvested, fixed and immunoprecipitated with Myc antibody and IgG as control. Parental cells, UR61-MT-Hebo (e.v.), were also treated with $ZnSO_4$ to control possible zinc-mediated gene regulation effects.

After quality controls, libraries were performed from these DNAs and sequenced using the Illumina Genome Analyzer. The sequencing reads obtaining for each sample were aligned against the rat genome and MACS algorithm was used to identify enrichment regions.

The listed genes were filtered by score >50, coverage sample >20 and location inside gene or promoter, which we defined as 2 Kb upstream from TSS. Also, we discard genes whose control has not 0 reads in their control sample.

In Max-deficient cells, Myc-peaks were found in 271 annotated genes (Annex 3.A). In Max-expressing cells Myc-peaks were identified on 120 annotated genes (Annex 3.B). These peaks were visualized with Integrative Genomics Viewer (IGV) (http://www.broadinstitute.org/igv/) to evaluate enrichment and select genes to validation, which are shown in Table 4.4. An example of images obtained from IGV of the peaks located on the selected genes is showed in Figure 4.13.A.

Table 4.4. Genes included in the validation of ChIP-seq data.

Symbol	Gene
Erbb4	v-erb-b2 avian erythroblastic leukemia viral oncogene homolog 4
Sox13	SRY (sex determining region Y)-box 13
Fannc	Fanconi anemia, complementation group C protein

It is well-known that Myc and Max co-occupy sites on the genome in Max-expressing cells. However in absence of Max, our results suggested that Myc binds to different sites and with less intensity to DNA.

Chip-seq data showed many genomic sites bound by Myc in controls cells (without Max) and not bound in Max-expressing cells. However Myc binding in all of these sites was not confirmed by individual ChIP analysis using different amplicons for the tested DNA regions. On the other hand, we found a number of genes bound in Myc-Max expressing cells but not in Myc only-cells. These were putative Myc-Max target genes and we assayed individually the Myc binding on the promoters of *ERBB4, SOX13* and *FANCC* genes (Fig 4.13.B)

A

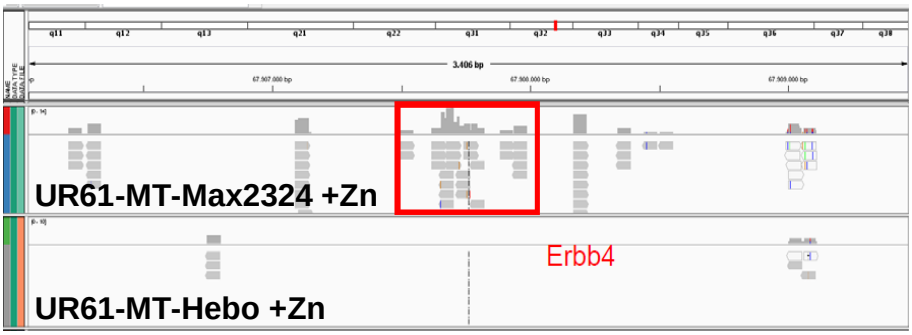

B

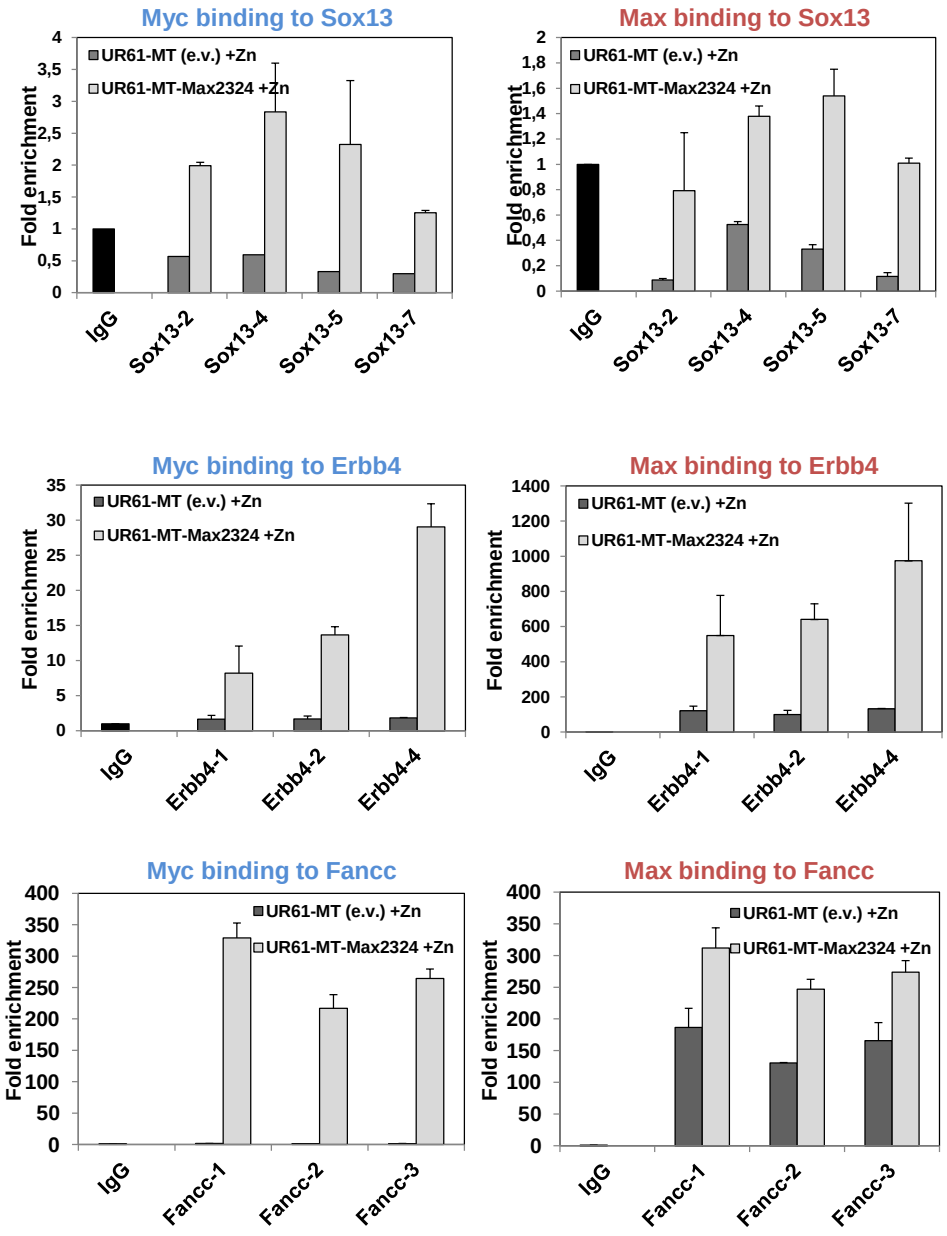

Figure 4.13. Validation of ChIP-seq data analysis. (A) The chromatin of UR61-MT-Hebo and UR61-MT-Max2324 cells, both treated with 100 µM $ZnSO_4$ was immunoprecipitated with Myc antibody.

After sequencing, the data obtained was visualized with IGV, i.e. *ERBB4* are shown. Grey signal represents reads. **(B)** ChIP experiments were carried out on UR61-MT-Hebo and UR61-MT-Max2324, both treated with 100 µM $ZnSO_4$ to induce Max expression in UR61-MT-Max2324. Chromatin was immunoprecipitated using antibodies against Myc and Max and it was analysed by RT-qPCR at the amplicons indicated surrounding the *ERBB4* (ChIP-seq score 52.3), *FANCC* (ChIP-seq score 68.1) and *SOX13* (ChIP-seq score 41). Data indicate the fold enrichment at each amplicon (detailed in Materials and Methods) against rabbit anti-IgG. Shown are the mean values ±SEM obtained from replicate experiments with error bars indicating the range of values. (Experiments performed in collaboration with Flor Pérez-Campo in Dr. León's laboratory).

PART II: ERK BINDS *MYC* PROMOTER INCREASING THEIR TRANSCRIPTION

4.2.1. *MYC* promoter is enriched in ERK-Boxes

It has been reported that ERK2 binds at active promoters of genes involved in metabolic pathways and cell-cycle progression, many of which are essential for survival, proliferation or pluripotency of hESCs. It has been proposed that sequence specific DNA-binding activity of ERK2 is independent of its kinase activity. Moreover, DNA-binding of ERK2 correlates with the occurrence of specific DNA sequence motifs identified as C/G-AAA-C/G (ERK-Boxes hereafter) and binding sites for the transcription factor Elk1 (see Introduction).

Therefore, we looked for ERK-Boxes on the human *MYC* gene and we found that these boxes are located above all in their promoter (Figure 4.14.A) and they are highly conserved in mouse and rat (Figure 4.14.B).

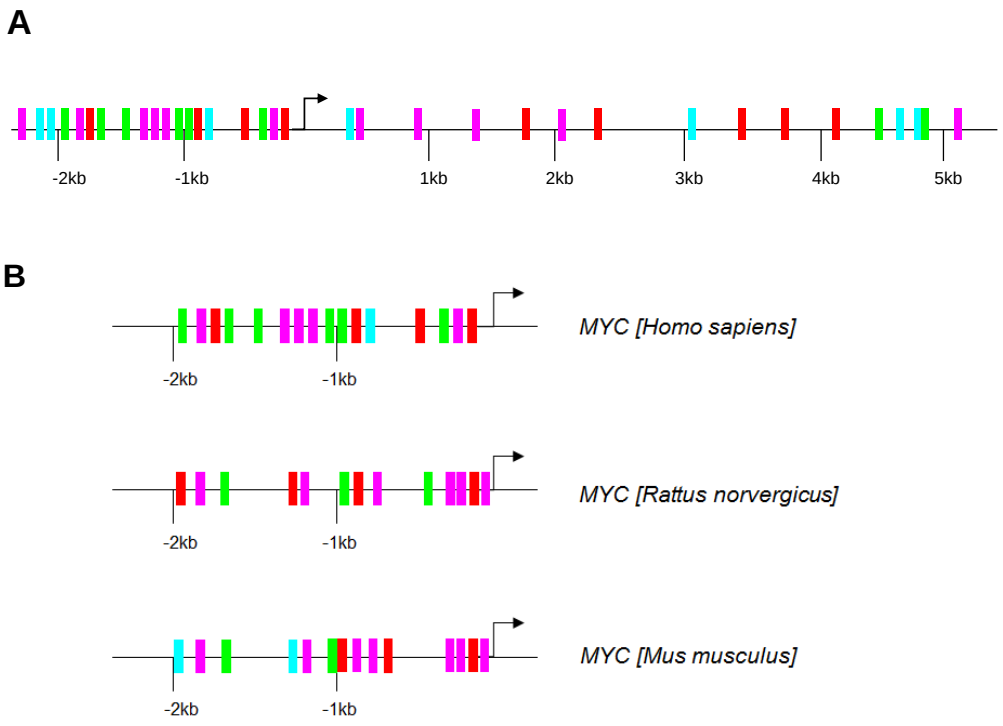

Figure 4.14. Distribution of ERK-Boxes on *MYC*. (A) ERK-Boxes on human *MYC* gene and their promoter, defined as 2 Kb upstream from the TSS. **(B)** ERK-Boxes distribution on promoters of rat, mouse and human *MYC*. ERK-Boxes are illustrated in green (CAAAC), red (CAAAG), pink (GAAAG) and blue (GAAAC), as defined in Hu, 2009.

4.2.2. ERK2 binds to *MYC* promoter

NGF-induced differentiation of PC12 cells, and its derivatives, is dependent on Ras-MEK-ERK activation (Cowley, 1994). Consistently, MEK1/2 inhibitors, as PD98059 or UO0126, also suppress PC12 differentiation (Hamada, 2009).

On the rat *MYC* promoter we found three conserved regions enriched in ERK-Boxes, located at -300 bp, -1 Kb and -1.7 Kb from the TSS. ChIP assays in UR61 cells showed binding of ERK2 to their specific DNA sequence motifs when ERK was activated by Ras. The same experiment was performed in URMYC cells and the results reported that Myc partially blocks ERK activation and there are lower DNA-binding (Figure 4.15.).

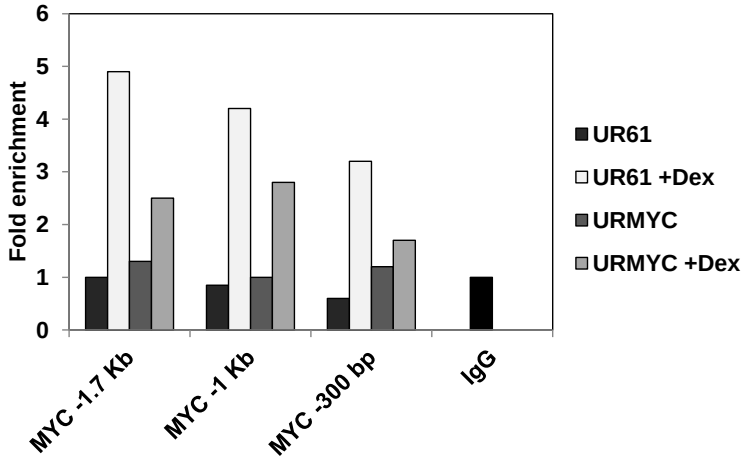

Figure 4.15. ChIP experiments show significant ERK-binding on rat *MYC* promoter. ERK was activated by Ras in UR61 and URMYC cells through treatment with 100 nM Dex for 4 h. The chromatin was immunoprecipitated and the DNA subjected to RT-qPCR for the showed amplicons along *MYC* promoter. The amplicons of the PCR reactions are described inMaterials and Methods. The results are expressed as fold enrichment of DNA in chromatin immunoprecipitated with ERK2 antibody (above the signal with rabbit anti-IgGs).

We also found high rate of specific DNA binding sites on human and mouse *MYC* promoter and it was correlated with DNA binding of ERK2 in human cells (HeLa or 293T) and in mouse immortalized embryonic cells (MEF).

First, HeLa cells were treated with interferon-γ (IFN-γ) to active ERK expression, which was validated by ChIP of ERK on *LAMP3* promoter as positive control (Hu, 2009) (Figure 4.16.A). In the same experiment we studied ERK-binding to different positions of *MYC* promoter (-2 Kb and -1 Kb from TSS), which showed enrichment in ERK-Boxes, and other region without ERK-Boxes as negative control (+2.2 Kb from TSS) (Figure 4.16.A). Also, we performed ChIP experiments in 293T and MEF cells deprived of serum for 24h (starved) and stimulated with 10% FBS until 30 min to induce ERK activation. The results showed significant binding of ERK2 on regions

analyzed on human and mouse *MYC* promoters, defined as 2 Kb upstream from TSS (Figure 4.16.B and Figure 4.17.).

In summary, ChIP assays suggested that ERK binds to ERK-Boxes situated around 1 Kb upstream from *MYC* TSS in human cells, whereas that in mouse cells, ERK binds to other conservative region surrounding 1.8 Kb upstream.

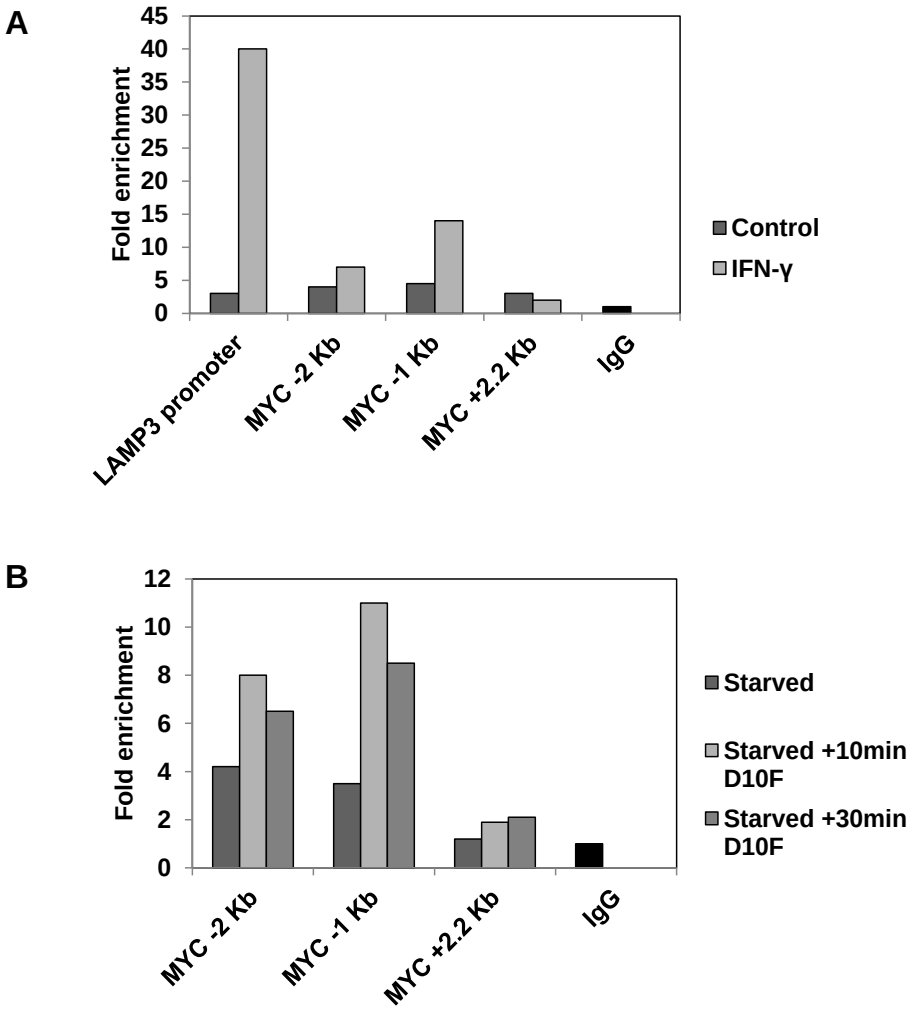

Figure 4.16. ChIP experiments show significant ERK-binding on human *MYC* promoter. (A) HeLa cells were culture in normal media supplemented with 10,000 U of IFN-γ to activate ERK. **(B)** 293T cells were deprived of serum for 24 h (starved) and stimulated for 10 and 30 min with 10% FBS. In both cases, the chromatin was immunoprecipitated with ERK2 antibody or IgG and the DNA subjected to RT-qPCR for the shown amplicons along *MYC* promoter. The amplicons of the PCR reactions are described in Materials and Methods. The results are expressed as fold enrichment of DNA in chromatin immunoprecipitated with ERK2 antibody (above the signal with rabbit anti-IgGs). Values are means from two independent experiments.

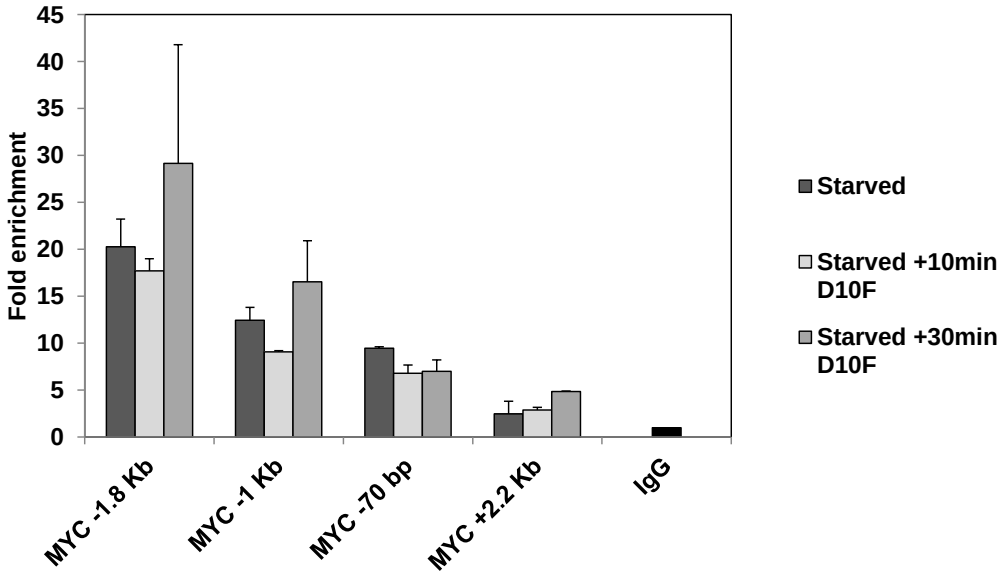

Figure 4.17. ChIP experiments show significant ERK-binding on mouse *MYC* promoter. MEF cells were deprived of serum for 24 h (starved) and stimulated for 10 and 30 min with 10% FBS. The chromatin was immunoprecipitated with ERK2 antibody or IgG and the DNA subjected to quantitative PCR for the shown amplicons along *MYC* promoter. The amplicons of the PCR reactions are described in Materials and Methods. The results are expressed as fold enrichment of DNA in chromatin immunoprecipitated with ERK2 antibody (above the signal with rabbit anti-IgGs). Data are means ±SEM from three independent experiments.

4.2.3. Activated ERK increases Myc expression levels

Thus, we determined the mRNA expression level of Myc when ERK is activated and bound to *MYC* gene. After serum deprivation for 24 h, 293T cells were stimulated with 10% FBS for 10 and 30 min (Figure 4.18.A). Also, 293T were transfected with ERK-NLS, a constitutively active and nuclear form of ERK (Rodriguez, 2010) (Figure 4.18.B). In both cases, activated ERK is correlated with Myc overexpression, as assessed by RT-qPCR. The same occurred in mouse cells (Figure 4.19.).

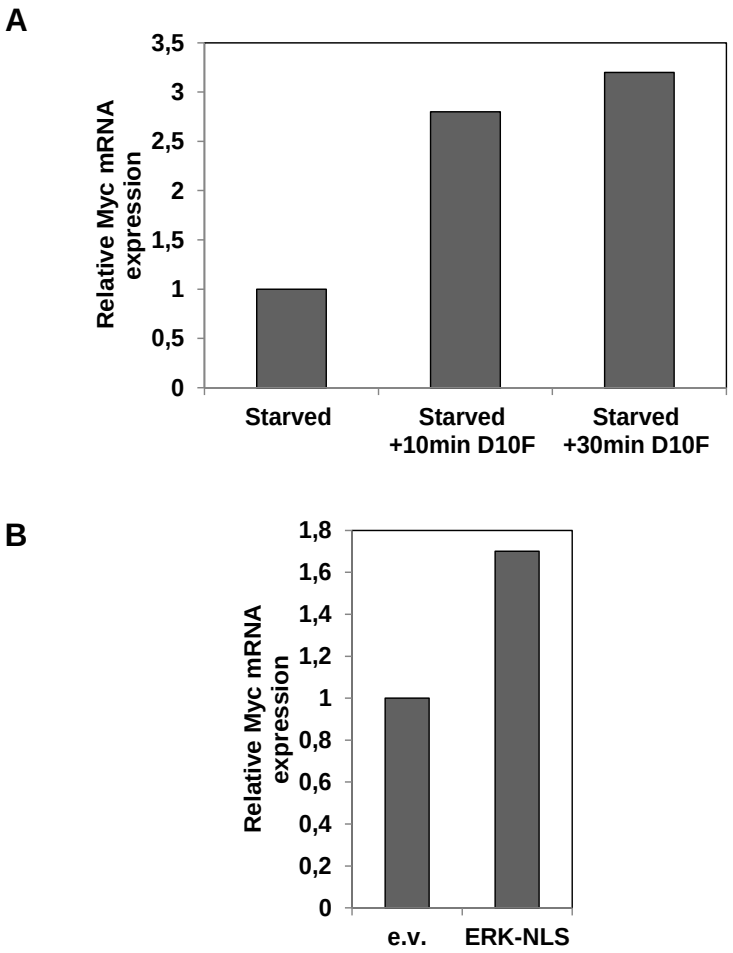

Figure 4.18. Activated ERK increases Myc mRNA expression levels in human cells. (A) Myc mRNA levels were measured by RT-qPCR in 293T cells deprived of serum for 24 h (starved) and stimulated with 10% FBS for 10 and 30 min to activate ERK. **(B)** 293T cells were transfected with ERK-NLS and deprived of serum for 24 h. β-actin mRNA levels were used for normalization. Values are means of two independent experiments.

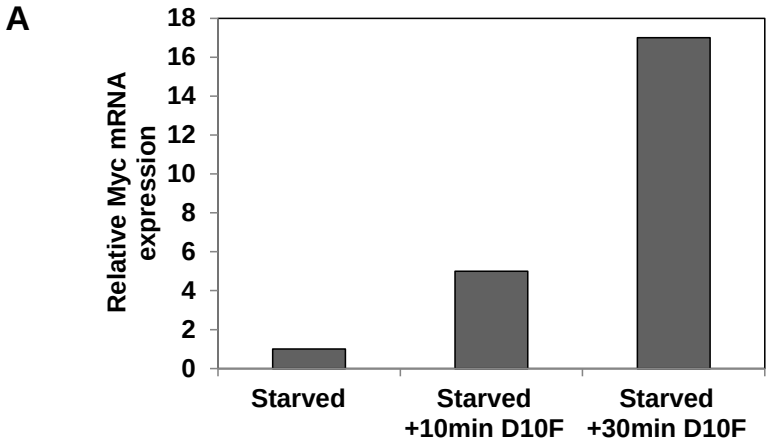

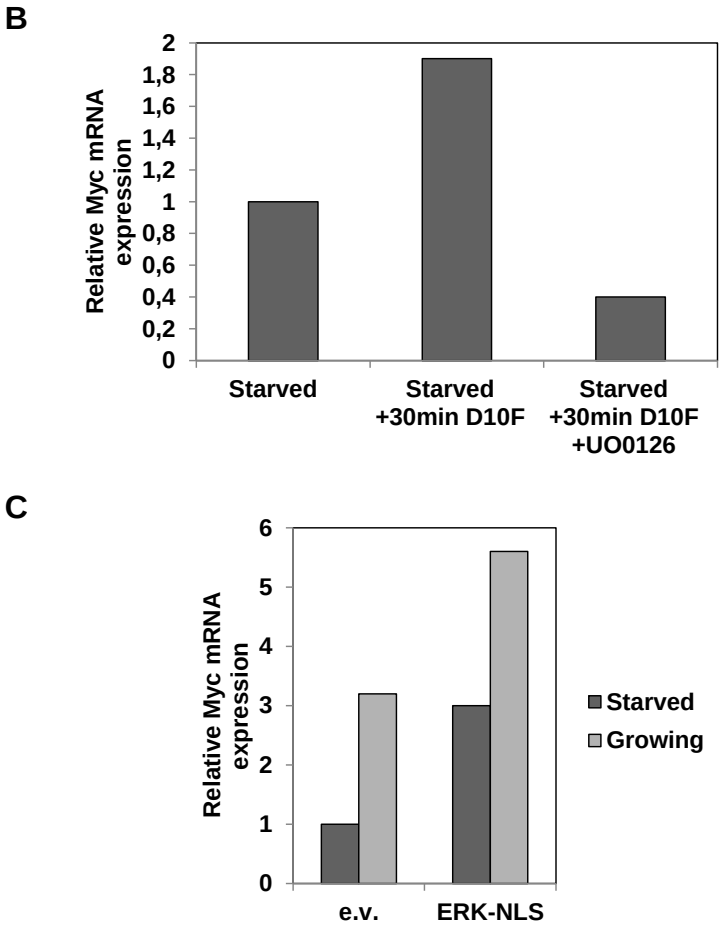

Figure 4.19. Activated ERK increases Myc mRNA expression in mouse cells. (A) Myc mRNA levels were measured by RT-qPCR in MEF cells deprived of serum for 24 h (starved) and stimulated with 10% FBS for 10 and 30 min. **(B)** Transfected and deprived of serum for 24 h 3T3 cells were stimulated with 10% FBS for 30 min and also treated with 10 μM UO0126 for 1 h before harvested. **(C)** 3T3 cells were transfected with ERK-NLS or the corresponding empty vector (e.v.), deprived of serum for 24 h and compared with growing transfected cells. RP-S18 mRNA levels were used for normalization. Values are means from two independent experiments.

Although it was known that Ras-ERK stabilizes and thus upregulates Myc protein, work in Dr. Crespo's laboratory has shown that this effect is independent of ERK kinase activity because transfection with the mutant ERK2-DK, lacking kinase activity, also showed increased levels of Myc protein (not shown).

4.2.4. ERK binds ERK-Boxes increasing transcriptional activity

To analyze transcriptional activity of ERK on *MYC* promoter, we constructed luciferase reporters containing different fragments (A, B, D and Del1) of human *MYC* promoter (Figure 4.20.) into

pBV-luc vector. Luciferase assays were performed using 1.5 µg of the reporter plasmid, 0.5 µg of the plasmid for renilla (pRL-Null) and 1.5 µg of the expression vectors of ERK. 12 h after electroporation, the cells were cultured without serum for 24 h. Cells were cotransfected with luciferase reporter and renilla and after starvation they were stimulated with culture media supplemented with 10% FBS for 10 and 30 min.

The results suggest that the critical region for ERK-dependent transactivation is located around -1 Kb from TSS of *MYC* corresponding with FragB construction (Figure 4.21.A and 4.21.C), which coincides with the promoter region bound to ERK2 detected by ChIP assays (see above).

Then, we also generated mutants of pBV-FragB-luc, called pBV-FragB1-luc, pBV-FragB1D2 and pBV-FragB2-luc (Figure 4.20.). Next luciferase experiments showed that pBV-FragB1-luc had higher activity in presence of activated ERK than others mutants in HeLa cells (Figure 4.21.B). This pBV-FragB1-luc contains two ERK-Boxes located around -1 Kb from TSS of human *MYC* (Figure 4.20.).

Moreover, in presence of MEK1/2 inhibitor (UO0126), the luciferase activity is reduced (Figure 4.22.).

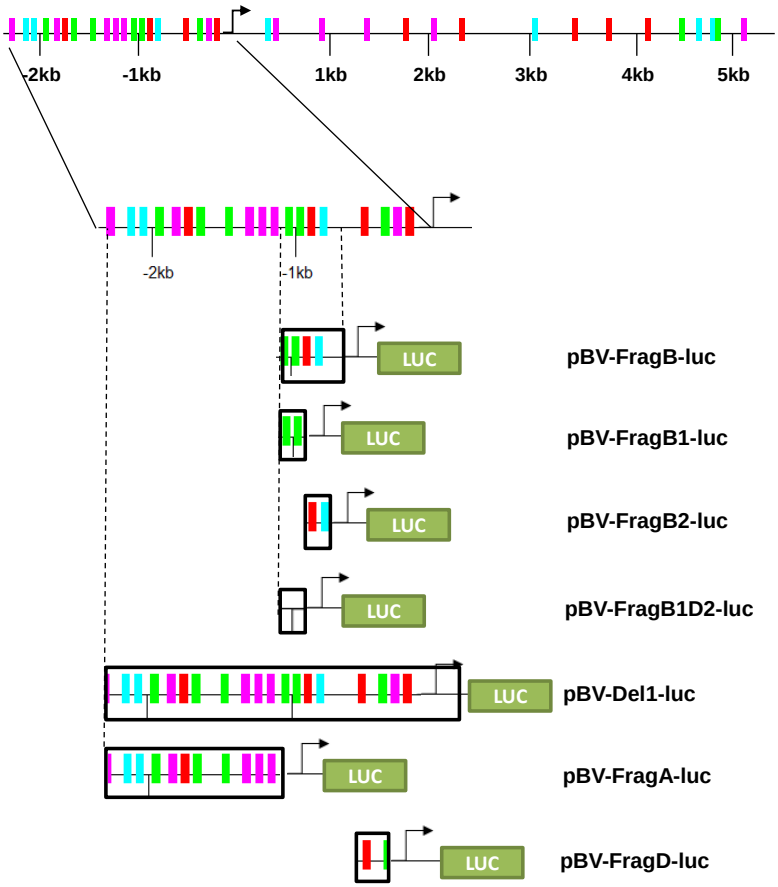

Figure 4.20. Map of luciferase reporters of human *MYC* promoter used. ERK-Boxes are illustrated in green (CAAAC), red (CAAAG), pink (GAAAG) and blue (GAAAC), as defined in Hu, 2009. The specific coordinates of each one are showed in Materials and Methods.

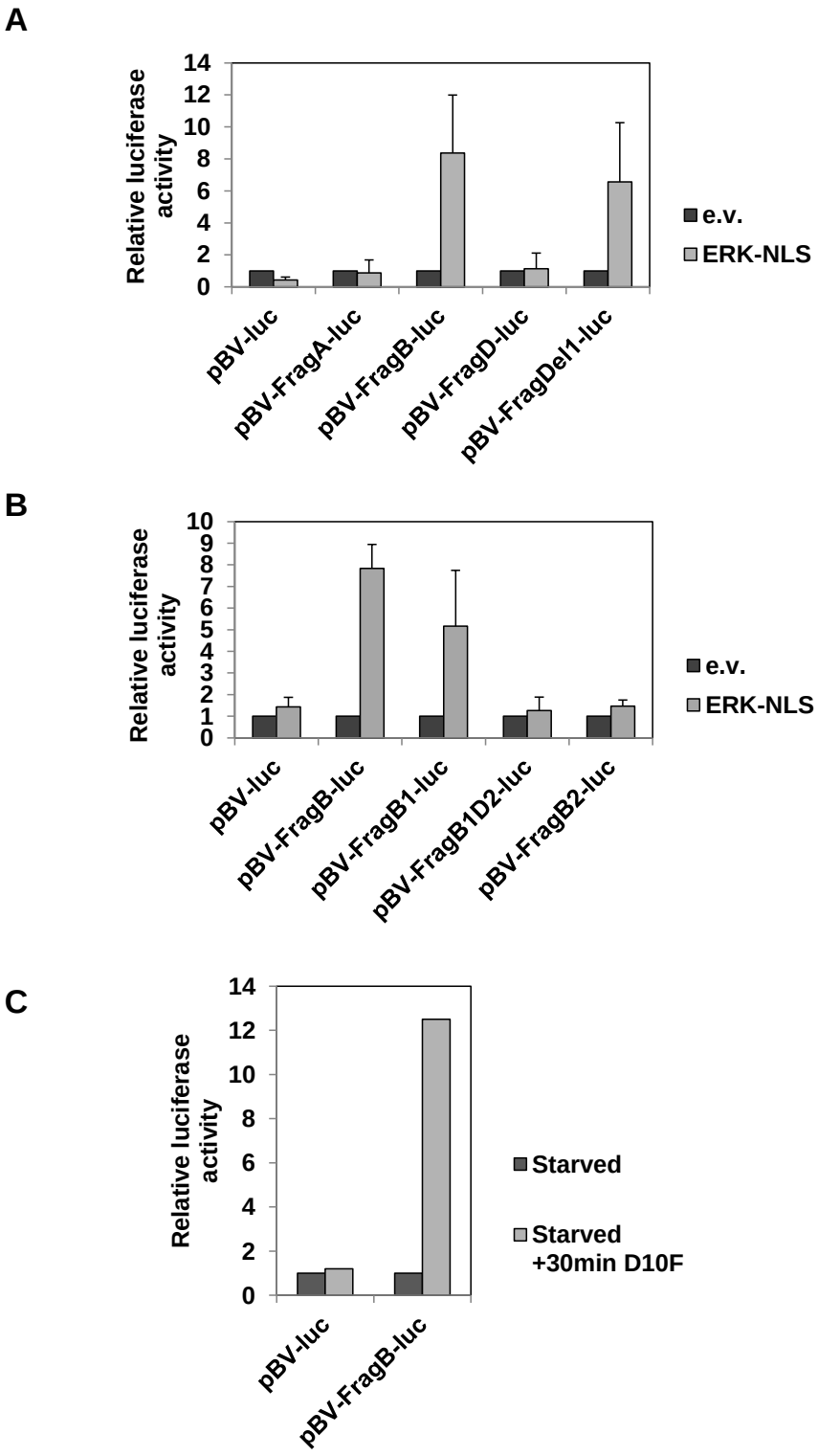

Figure 4.21. Relative luciferase activity of ERK in human cells. (A) Relative luciferase activity of ERK in HeLa cotransfected with ERK-NLS and different luciferase reporters of *MYC* promoter, and **(B)** cotransfected with ERK-NLS and mutants of pBV-FragB-luc. **(C)** Luciferase activity of ERK in HeLa cells transfected with pBV-FragB, starved and then stimulated with 10% FBS for 30 min. Luciferase activity was measured 36 h after transfection and normalized against the renilla value. The means ±SEM from three independent experiments are shown.

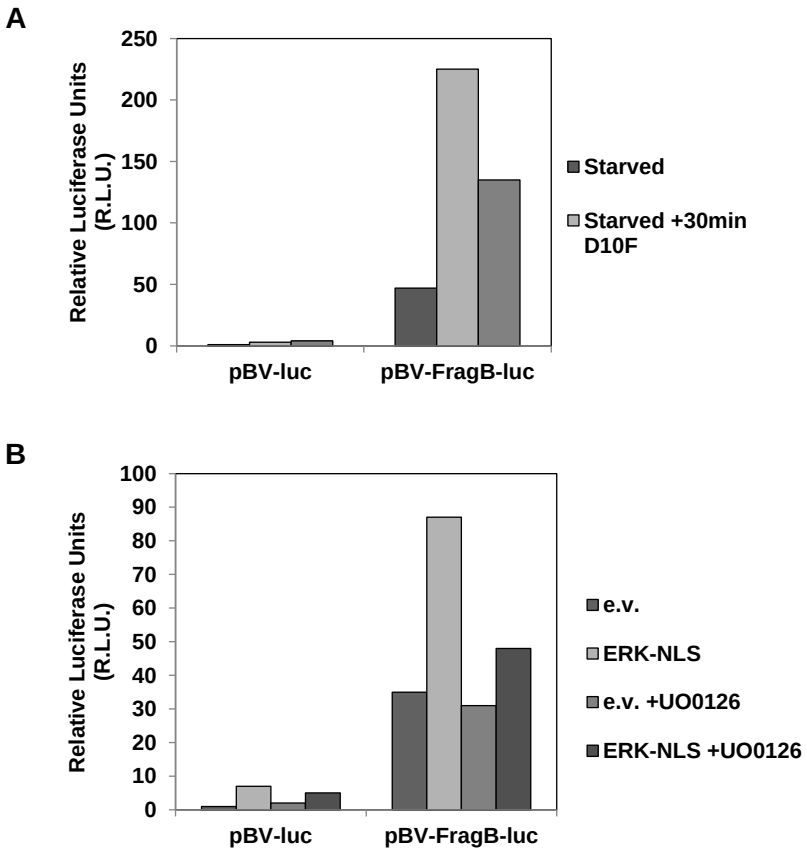

Figure 4.22. Relative luciferase activity of ERK in 293T cells. (A) 293T cells were transfected with luciferase reporters (pBV-luc and pBV-FragB-luc) and, 12 h post-transfection, the cells were deprived of serum for 24 h. Then, cells were stimulated or not with 10% FBS. **(B)** 293T cells were cotransfected with expression vectors for ERK-NLS or empty vector (e.v.) and luciferase reporters (pBV-luc and pBV-FragB-luc) and treated or not with 10 µM UO0126 for 1 h before harvested. Luciferase activity was measured 36 h post-transfection and normalized against the renilla value. The means from two independent experiments are shown.

4.2.5. ERK2 genome-wide coincides with Elk1 and CDK9

ERK lacks DNA interaction motif, and thus we assumed that ERK needs other partners for the transcriptional regulation of *MYC* described above. Thereby, we investigate the role of Elk1 as ERK cooperator because it has been reported differences between ERK2 and Elk1 DNA-binding and their genome-wide localization showing ERK2 colocalization with Elk1 at promoters (see Introduction).

For this purpose we analysed the genome data generated by the ENCODE project and made public through the UCSC browser. There are not ChIP-seq data for ERK1/2 in ENCODE project (UCSC browser), but the ChIP-seq data for Elk1 in several cell lines (GM12878, K562 and HeLa) is available. These data showed enrichment of Elk1-binding in three regions of human *MYC* promoter, the first one mapping at -700 bp, the second at -1.1 Kb and third region is close to -2 Kb from TSS of human *MYC* (Figure 4.23.).

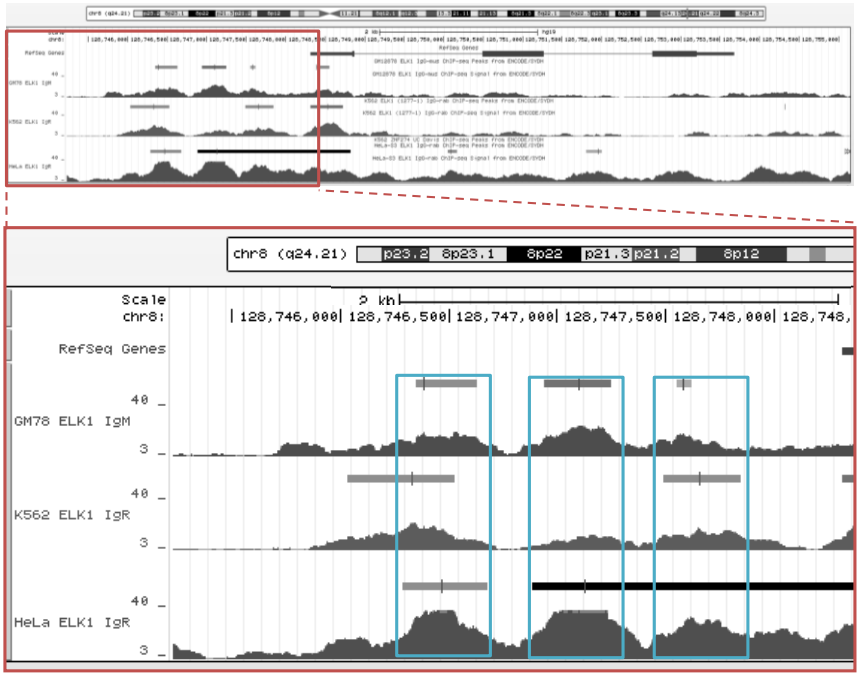

Figure 4.23. Elk1 genome-wide at human *MYC* promoter. Chip-seq data for Elk1 (data of ENCODE project, UCSC browser) is illustrated on human *MYC* promoter in K562, GM12878 and HeLa cells. Three peaks are detected between -500 bp and -2 Kb from TSS.

Also it has been reported that Myc generally plays a role in RNA polymerase II (Pol II) pause release and does so through recruitment of pTEFb (formed by CDK9 and CyclinT1). CDK9 is responsible for phosphorylation of Ser5-Pol II, which is the form associated with initiation of transcription (see Introduction).

It has been described that CDK9 colocalize with Ser5-phosphorylated Pol II (Pol II-Ser5P) around TSS of *MYC,* whereas Ser2-phosphorylated Pol II (Pol II-Ser2P) is associated with elongation and is bound to 3' end of genes (Larochelle, 2012; Ghamari, 2013). We have performed ChIP experiments for CDK9, Pol II-Ser5P and Pol II-Ser2P and we have also found binding on the described sites along human *MYC* (Figure 4.24.), confirming a recent report (Larochelle, 2012). Next, we studied DNA-binding of ERK2 and Elk1 in these sites in growing human cells, whose results showed that CDK9 also localize before TSS, close to binding region of ERK2 and Elk1 around to -1 Kb from *MYC* TSS (Figure 4.24.).

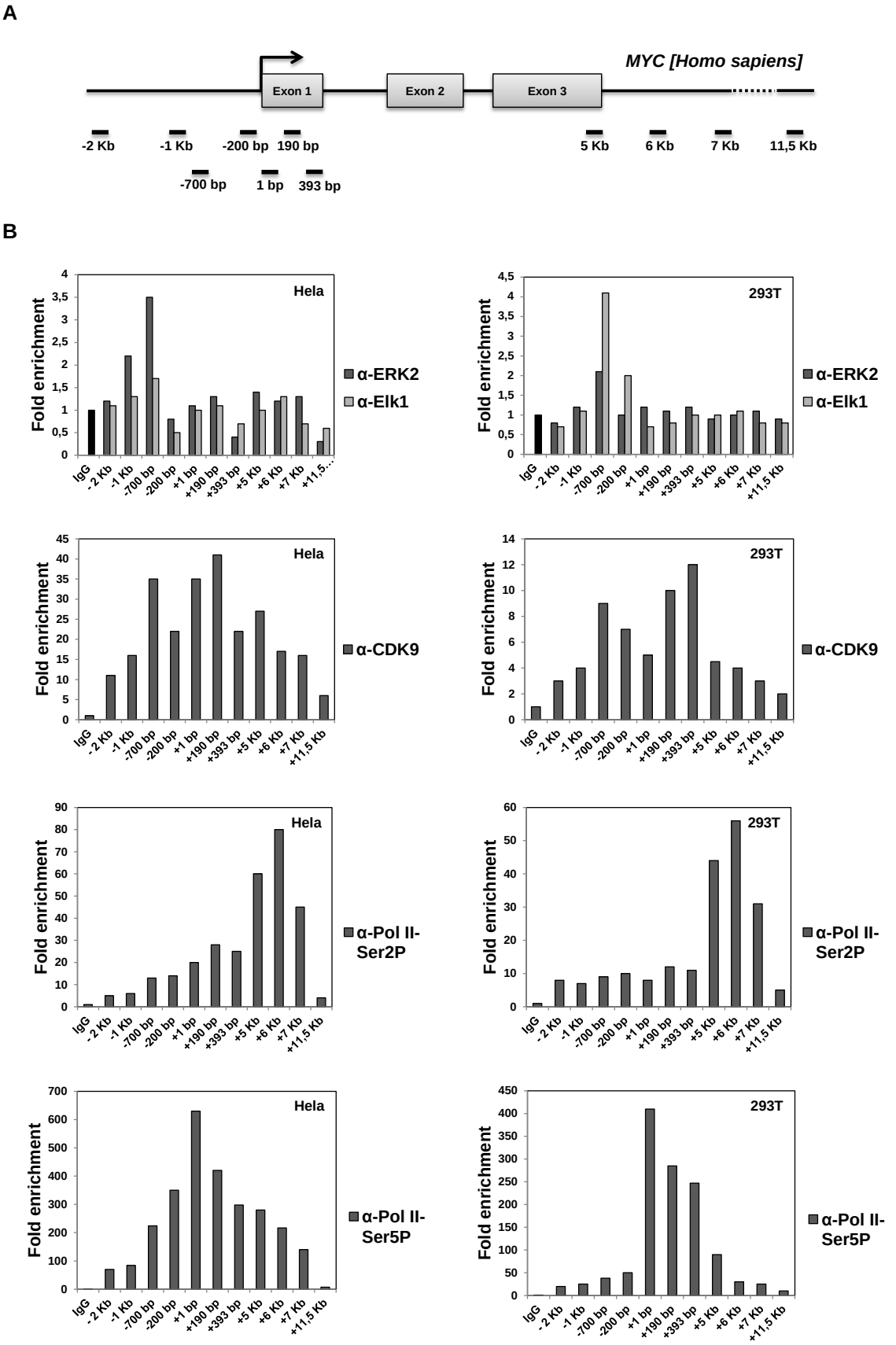

Figure 4.24. CDK9, ERK2 and Elk1 are bound to chromatin on human *MYC* promoter. (A) Map of studied amplicons on human *MYC*, which sequences are showed in Materials and Methods. **(B)** Chromatin

of HeLa and 293T was immunoprecipitated with anti-Pol II-Ser2P, anti-Pol II-Ser5P, anti-CDK9, anti-ERK2 and anti-Elk1 and the DNA subjected to RT-qPCR for the amplicons mapping at the coordinates indicated at the graph bottom. The results are expressed as fold enrichment of DNA in chromatin immunoprecipitated above the signal with anti-IgGs.

4.2.6. ERK2 interacts with CDK9

The above ChIP results suggested that ERK2 and CDK9 might be interacting bound to specific chromatin regions. To explore this hypothesis we performed *in situ* Proximity Ligation Assay (isPLA).

First, we performed immunofluorescence to confirm the colocalization of ERK2 and CDK9 into the nuclei in HeLa and MEF cells (data not shown). The isPLA demonstrated the interaction between CDK9 and ERK2, where we used the Myc-Max interaction as positive control and the interaction between ERK2 and CDK2 and sample without primary antibody as negative controls (Figure 4.12).

Also the interaction between ERK2 and CDK9 (but not CDK7 and CDK8) has also been demonstrated by coinmmunoprecipitation experiments. Moreover, the interaction region of CDK9 responsible of interacting with ERK2 was identified (results obtained by Javier Rodríguez in Dr. Crespo's laboratory).

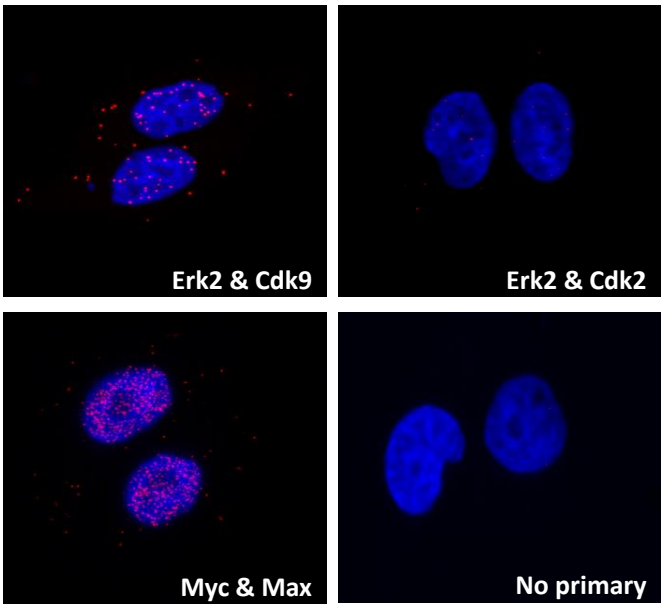

Figure 4.25. CDK9 and ERK2 interact *in situ* in HeLa cells. Interaction between ERK2 and CDK9 in HeLa cells by isPLA. Myc-Max interaction is the positive control, whereas ERK2-CDK2 and no primary antibody are negative controls. The same experiment was performed in MEF cells with similar results (not shown). (Experiments performed in collaboration with Lorena Agudo, from Dr. Crespo's laboratory).

RESULTS PART III: MYC INHIBITS RAS-MEDIATED SENESCENCE

4.3.1. Myc inhibits Ras-mediated senescence in UR61 cell (lacks Max protein)

UR61 is a PC12-derived cell line with inducible expression of the N-Ras oncogene. Previous experiments in our lab showed that Myc impairs the neuronal-like differentiation induced by Ras blocking c-Jun upregulation (Vaqué, 2008). This model provides the opportunity to analyse the activity and functions of Myc in absence of Max.

The accumulation of oncogenic Ras is initially mitogenic but over time an antiproliferative response ensues and cells acquire a characteristic senescent morphology. Ras-induced senescence absolutely requires the activation of Raf-MEK-ERK signalling cascade, which provides cells with constitutive mitogenic signals and after also triggers Ras-induced cell cycle arrest through accumulation of p16, p21 or p53 (see Introduction).

Therefore, we have used UR61 as senescence model by accumulation of N-Ras after Dex treatment and in this part we also have studied the role of Myc on this Ras-induced senescence in the UR61-MYC cell line (URMYC hereafter) that shows constitutive expression of Myc protein.

At least five or six days are needed to develop senescence in most cellular models. Therefore UR61 and URMYC cells were grown over matrigel to get optimum growth conditions during this time and to avoid detachment and death of senescent cells (see Materials and Methods).

Time-lapse video microscopy experiments showed that most of the cells undergo differentiation in response to Ras, although the neurite-extension process is transient and can last longer or shorter depending on the individual cell (Figure 4.26.). After differentiation, UR61 cells showed a senescent-like morphology subsequently to described Ras-induced neuronal differentiation, whereas apparently URMYC cells had a quiescent state at the end, but not senescent. This was also showed in SA-β-gal assays (Figure 4.27) and crystal violet staining (Figure 4.28.).

However, endogenous and even exogenous Myc expression in URMYC cell line is rather low and when growing on artificial matrix (i.e., matrigel), there are a higher fraction of cells that undergo differentiation in response to Ras that on plastic (not shown), which become senescent after differentiation. This is showed in Figure 4.26., where a differentiated URMYC cell (illustrated with blue dot) becomes senescent after differentiated state, in contrast to another cell, not differentiated (illustrated with orange dot).

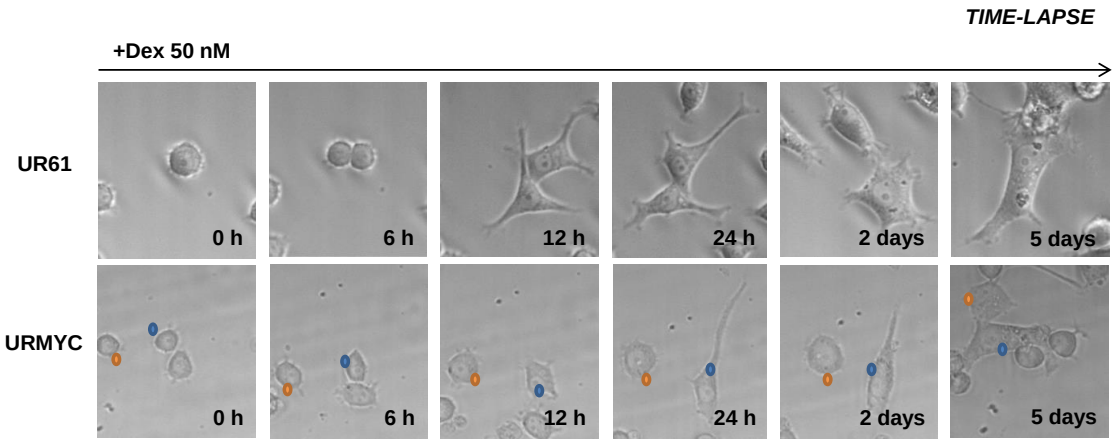

Figure 4.26. Captures of time-lapse video microscopy. UR61 and URMYC were cultured over matrigel and treated with 50 nM Dex for over five days. Orange dot shows a quiescent URMYC cell, in contrast to differentiated and then senescent cell, marked with a blue dot.

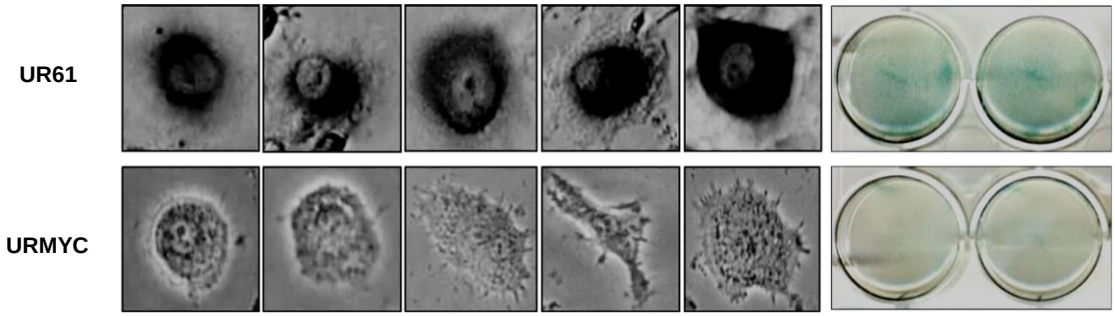

Figure 4.27. Ras-induced senescence in UR61 cell line, whereas do not in URMYC. SA-β-gal assay in UR61 and URMYC treated with 100 nM Dex for six days. Senescent UR61 and quiescent URMYC cells are shown after SA-β-gal staining. These cells were culture in T6 plates, which were scanned after assay and they show a positive activity as blue colour in treated UR61 cells.

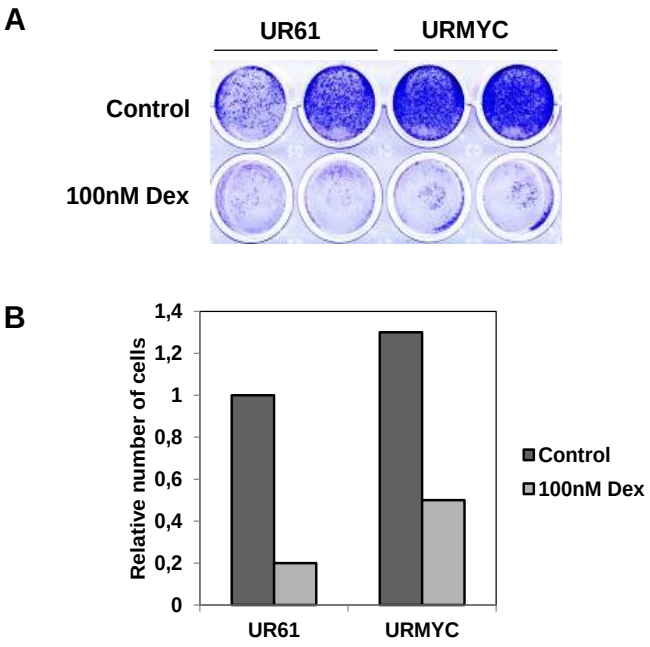

Figure 4.28. Ras-induced cell cycle arrest in UR61. (A) Cristal violet staining of UR61 and URMYC treated and untreated for six days with 100 nM Dex. They were cultured in T24 plates by duplicate. **(B)** Quantification of crystal violet experiments showed in A. The data are mean values from two independent experiments.

It has been reported that Ras transactives p21 promoter through the Raf-MEk-ERK pathway, whereas Myc antagonizes the Ras-mediated growth arrest, at least partially, by impairing p21 upregulation (Vaqué, 2005). It has also been shown that high levels of constitutively active Raf and MEK can activate p21 expression *per se*, indicating that, at least, the Ras-Raf-MEK pathway can bring about p21 upregulation. To repress p21 expression, Myc forms a complex with the zinc finger protein Miz1, which binds to their proximal promoter (see Introduction).

p21 has been described as a senescence marker and we also have demonstrated in the UR61 cells that the induction of N-Ras for five days results in the overexpression of p21 and senescence phenotype, whereas that Myc impairs this upregulation (Figure 4.29.A), suggesting that Myc mediates the inhibition of Ras-induced senescence. However, the results could just reflect the direct action of Myc on p21 promoter rather than a consequence of senescence inhibition. Thus we studied expression levels of other described senescence marker as p16 and the results showed that p16 is also upregulated in treated UR61 cells and Myc impairs this overexpression (Figure 4.29.B).

Then, we can conclude that the accumulation of N-Ras induces senescence in this rat feochromocitome model and Myc blocks it independently of Max. However, the molecular mechanism by which Myc impairs Ras-mediated senescence in this model is still unknown.

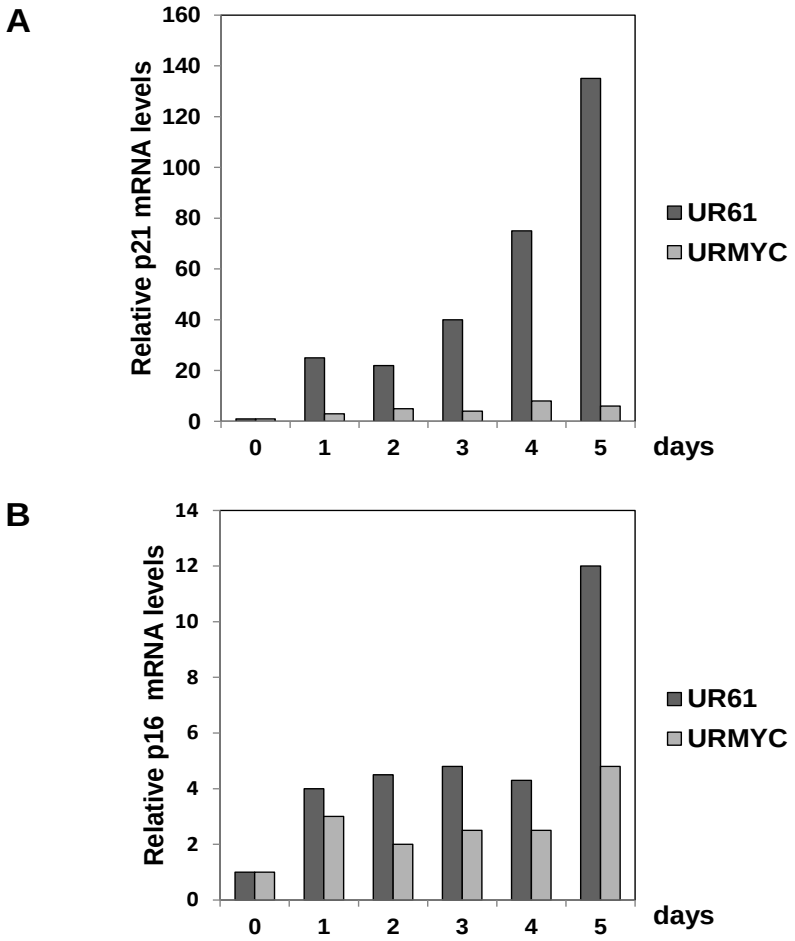

Figure 4.29. p16 and p21 are upregulated in UR61 senescent cells and Myc impairs this overexpression. (A) Relative expression of mRNA levels of p21 and **(B)** p16 in UR61 and URMYC treated cells with 100 nM Dex along five days. The graph shows mean values from two independent experiments.

4.3.2. Myc blocks secretion of interleukins related with secretome of senescent cells independently of Max protein

Senescent cells secrete a complex mixture of secreted and extracellular factors usually called senescence-associated secretory phenotype (SASP) and this is related to wound healing, inflammatory response and cytokine and chemokine signalling. This secretome includes extracellular proteases, growth factors and proinflamatory cytokines and chemokines (see Introduction). Thereby, we studied the expression of several factors related with this secretome as IL-1α, IL-1β and IL-6 and in all cases we found higher expression levels in UR61 cells than URMYC (Figure 4.30.). Therefore, the N-Ras-induced senescence in UR61 is related with the following secretion of several interleukins, whereas that the results suggest that Myc impairs this senescence-associated secretory phenotype.

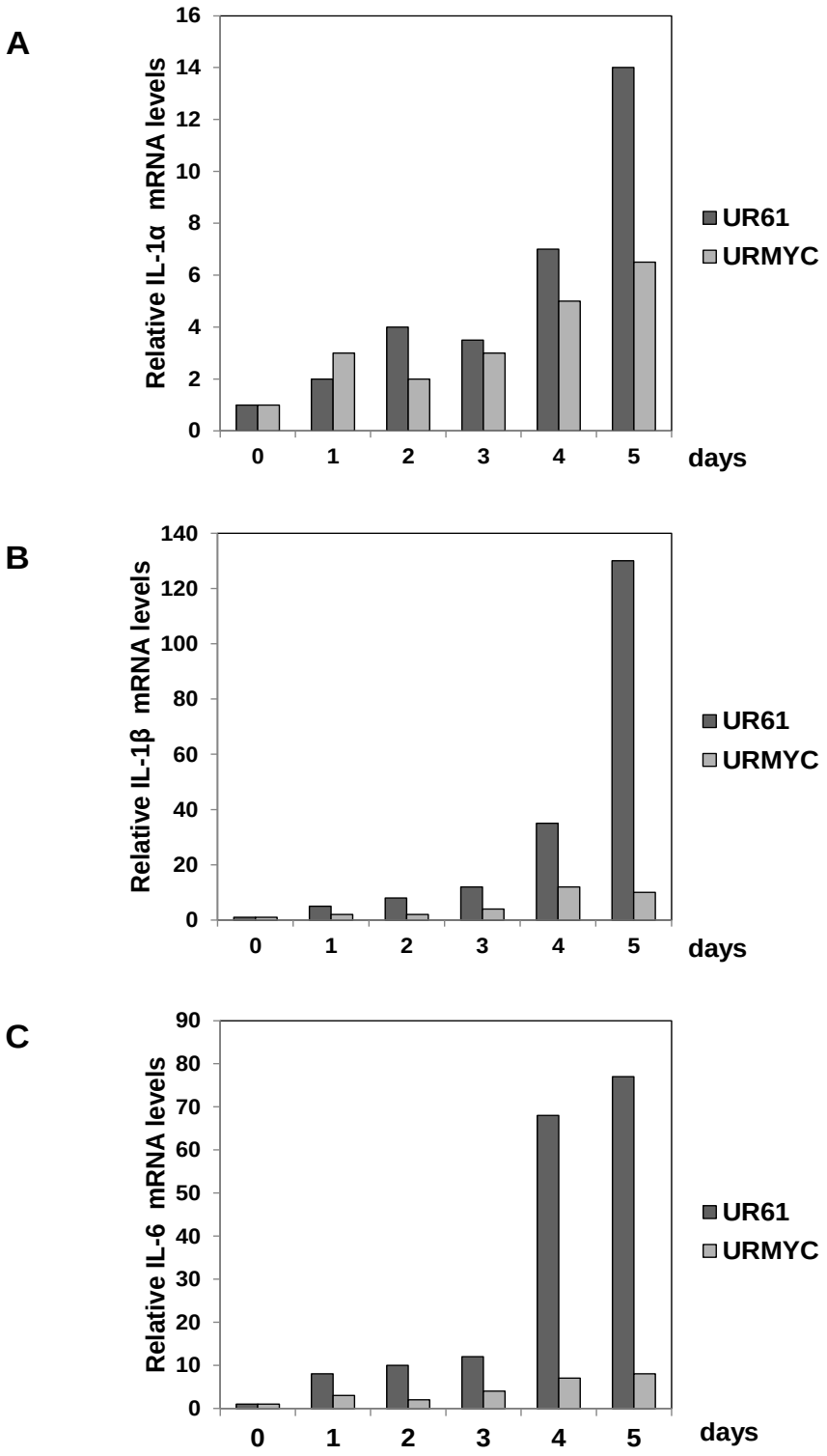

Figure 4.30. Ras induces overexpression of some factors related with secretome and Myc blocks its expression. (A) Relative mRNA levels of IL-1α, **(B)** IL-1β and **(C)** IL-6 in UR61 and URMYC cells treated with 100 nM Dex along five days. The graph shows the mean values of two independent experiments.

4.3.3. UR61 senescent cells shows high caspase-1 activity, do not impairs by Myc

On the other hand, it is believed that the secretion of proinflamatory cytokines by senescent cells initiates an innate immune response *in vivo*.

Inflammasomes are molecular platforms activated upon cellular stress that trigger the maturation of proinflamatory cytokines such as IL-1β. Generation of IL-1β via cleavage of its proform requires the activation of caspase-1, therefore we determined caspase-1 activity by fluorometric assay in our model. The results showed higher activity in cells treated with 100 nM Dex for eight days than untreated cells (Figure 4.31.). However, we did not find significant differences in presence of Myc, at least along this period time.

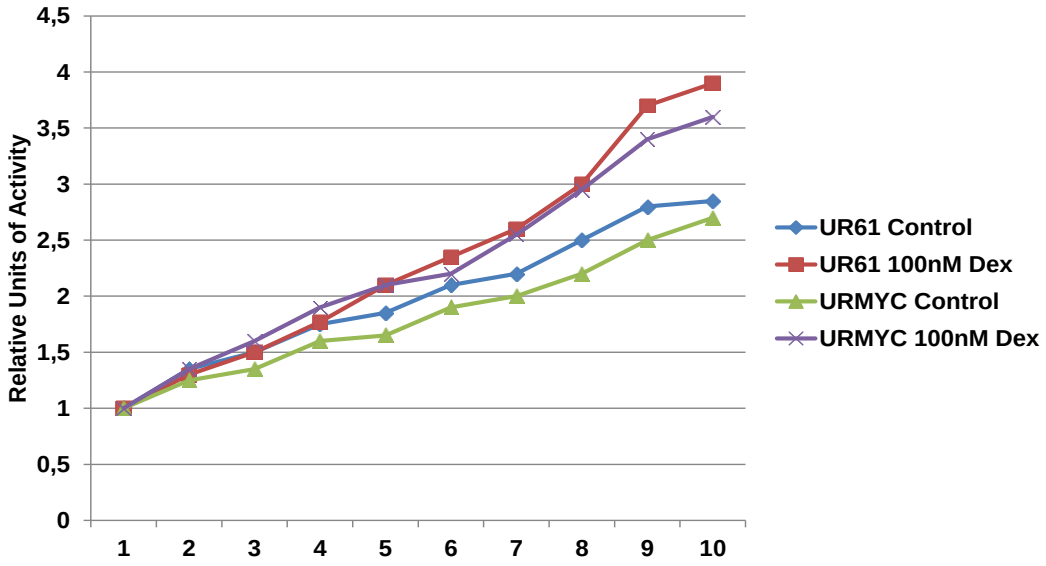

Figure 4.31. Senescent cells show highest caspase-1 activity. UR61 and URMYC cells were treated and untreated with 100 nM Dex for eight days. The fluorometric was performed taking lectures each 30 min until ten lectures.

Moreover, UR61 and URMYC cells were seeded in T24 plates and treated with 100 nM caspase-1 inhibitor and 100 nM Dex. The cells were fixed six days after seeding and the plates were stained with crystal violet, which was extracted and quantified. The treatment with caspase-1 inhibitor partially prevented the cell cycle arrest observed during Ras-induced senescence (Figure 4.32.), which suggests that caspase-1 is related with the senescence development in these cells. Again, there are not significant differences in caspase-1 activity in Myc-expressing cells.

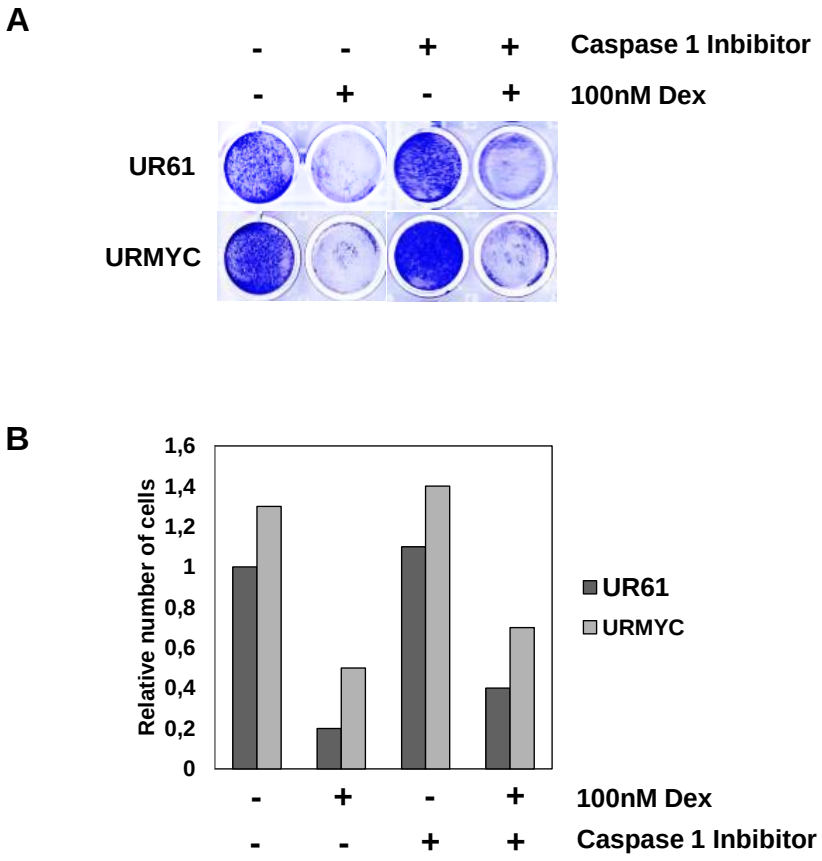

Figure 4.32. Caspase-1 inhibitor partially prevented the cell cycle arrest observed during Ras-induced senescence in UR61 and URMYC. (A) Crystal violet staining of cells cultured for six days in T24 plates and treated with 100 nM Dex and 100 nM caspase-1 inhibitor. **(B)** Quantification of crystal violet shown in A. The graph shows the mean values of two independent experiments.

4.3.4. Primary human fibroblast as model to study Ras-Myc relationship in senescence

To better understand the Myc-Ras relationship in senescence we used IMR90 primary human fibroblasts, an established senescence cellular model (Acosta, 2013). These experiments were performed using early passage IMR90 cells to prevent confounding effects of replicative senescence.

IMR90-MycER, stable cell line derived from IMR90, expresses the conditional MycER fusion protein. The fusion of Myc to a modified version of the ligand-binding domain of the estrogen receptor allows the selective activation of Myc by the addition of the synthetic estrogen analog 4OHT (4-O-Hidroxy-Tamoxifen).

At first, IMR90-MycER were infected with retroviruses of RasV12 and their corresponding empty vector (e.v.) and selected with their respective antibiotic to get stables cell lines (IMR90-MycER-e.v. and IMR90-MycER-RasV12). After selection, these cells were cultured with 10% FBS and with or without 200 nM 4OHT to active Myc expression.

By using this system, we have studied Ras-Myc relationship in senescence and identified genes whose expression is modified by Myc in Ras expressing cells.

Three days after infection, expression levels of p15, p16, p21 and proinflamatory cytokines or chemokines as IL-6 and IL-8 were assessed by RT-qPCR. Our results confirmed that Ras induce accumulation of senescence markers as p15, p16 and p21 in primary human fibroblasts (Figure 4.33.A). In contrast, the activation of Myc by 4OHT has not clear effect on the expression of these proteins, although Myc-Ras cooperation results in p15 upregulation. Otherwise, Myc blocked IL-6 and IL-8 expression induced by Ras (Figure 4.33.B) in parallel with the results observed in rat model (see above).

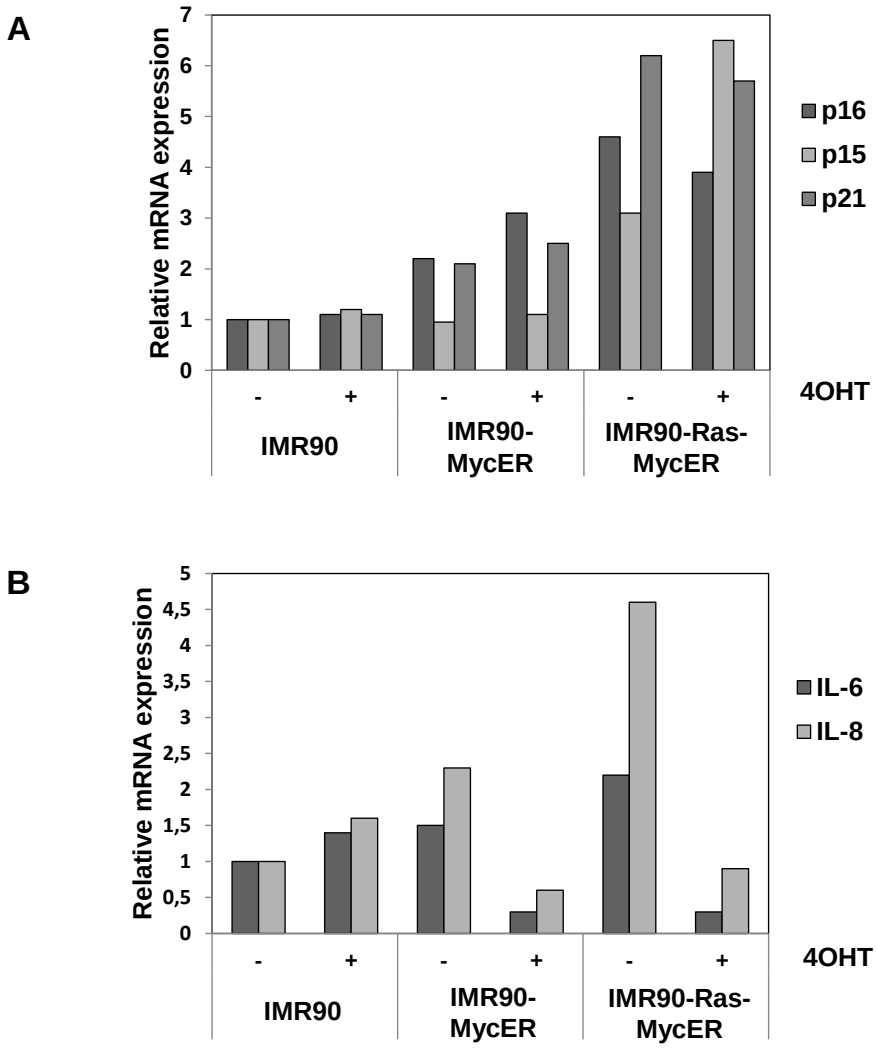

Figure 4.33. Effect of Myc on the expression of senescence-related genes. (A) Relative mRNA expression of senescence markers as p16, p15 and p21 and **(B)** interleukins 6 and 8 in stable IMR90 derived cells treated with or without 200 nM 4OHT to induce Myc activation.

Moreover, these IMR90 derived cells were cultured supplemented with or without 200nM 4OHT for eight days and then they were fixed and stained with crystal violet to study Myc-Ras relationship in proliferation (Figure 4.34.). Apparently there is a basal level of Myc-dependent transformation due to the leakiness of the MycER system (Figure 4.34.A) and, surprisingly, after induction with 4OHT, there was an extensive cell death due to high Myc levels (Figure 4.34.A and Figure 4.35.A). On the other hand, Ras expression arrested IMR90 cells causing senescence phenotype (Figure 4.35.B) accompanied by upregulation of senescence markers (see above). SA-β-gal staining also revealed an increase of positive senescent cells in Ras-expressing cells (Figure 4.35.B).

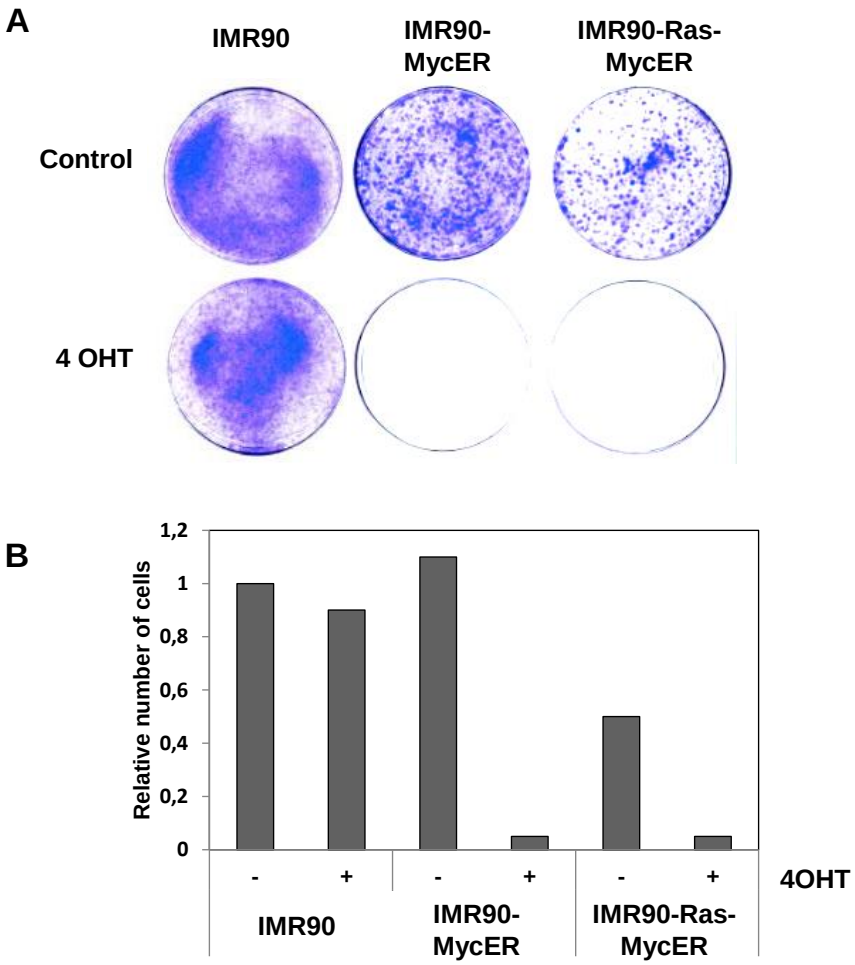

Figure 4.34. Ras-induced cell cycle arrest in IMR90 cells and IMR90-MycER cells dead after induction with 4OHT of high levels of Myc independently of Ras. (A) Stable IMR90 derived cell lines were seeded in p100 plates and fixed after treatment with or without 200 nM 4OHT for eight days to stain with crystal violet. **(B)** These samples were quantify, which are illustrated.

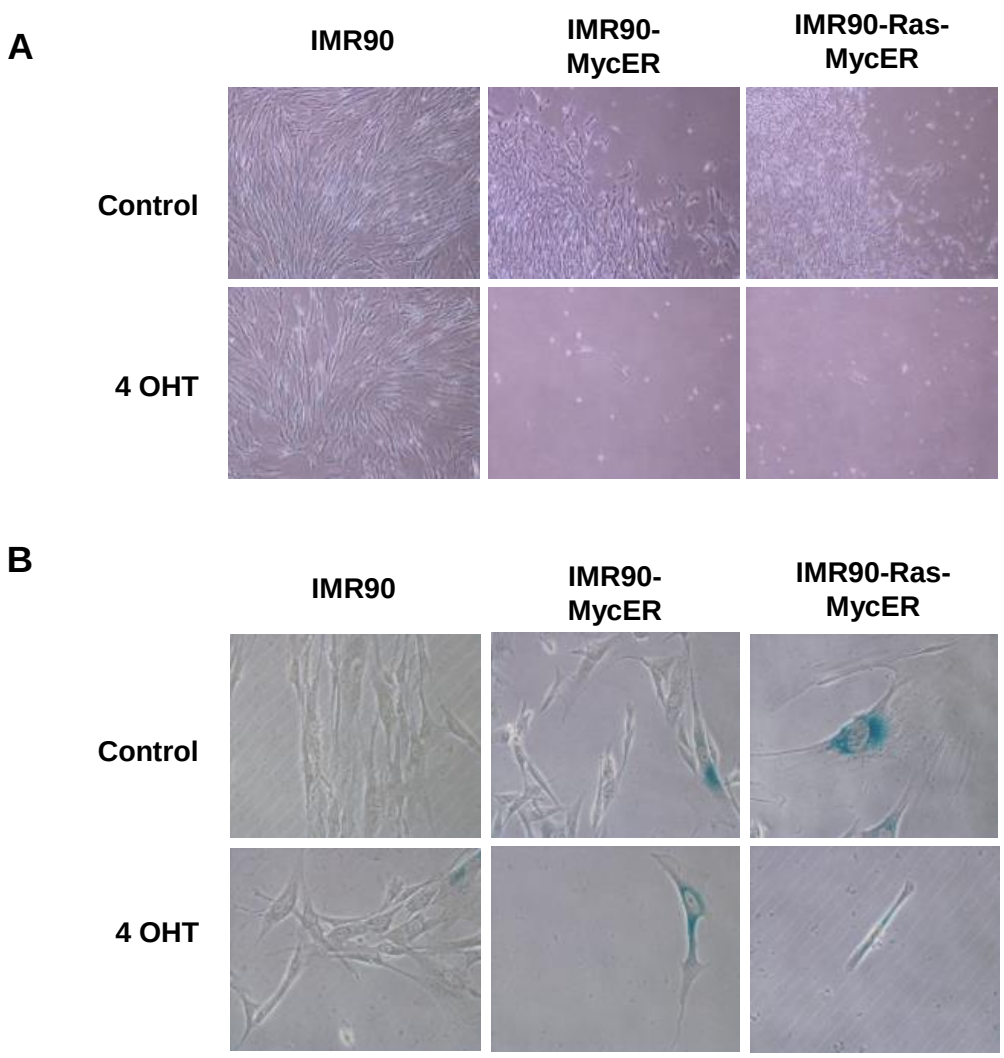

Figure 4.35. Morphology of IMR90, IMR90-MycER and IMR-Ras-MycER. These cells were cultured for eight days with or without 200 nM 4OHT. **(A)** Images of growing cells (4x) and **(B)** fixed cells to SA-β-gal assay (10x) by means of Zeiss microscope.

RESULTS PART IV: MYC INTERACTS WITH SIN3

In view of the results observed in the UR61 (Max deficient) model, we considered the possibility that one of the keys for the multiple and varied effects of Myc is its ability to interact with other proteins different from Max.

In order to identify any of these potential new proteins it was performed in our laboratory a screening yeast two-hybrid assay, using as bait complete Myc protein (Pablo García-Sanz, PhD Dissertation). One of the positive clones contained a plasmid whose sequence corresponds to a region of the Sin3b protein (amino acids 5-194). This region contains the PAH1 domain and part of the PAH2 domain of this protein. PAH domains are involved in protein-protein interaction.

The study of this positive clone was particularly attractive to us because Sin3b has an important role in the regulation of transcription and has been implicated in the transcriptional repression mediated by Mxd a protein with which interacts physically.

After confirming the specificity of the interaction between Myc and Sin3b in yeasts, this interaction was also studied in animal cells. Firstly, this interaction was shown by co-immunoprecipitation in 293T transfected cells with expression vectors of human Myc and Sin3b proteins. Moreover, the interaction between Myc and Sin3b also was detected in UR61 cells (which do not express Max wild type protein), indicating that Myc does not need to form heterodimers with Max to interact with Sin3b (Pablo García-Sanz, PhD Dissertation).

4.4.1. Interaction between endogenous Myc and Sin3b

We next asked whether endogenous Myc and Sin3b interacted in the cells. We selected for this purpose the human myeloid leukemia K562 cells, as they are known to express high levels of Myc and, in contrast to 293T cells, express endogenous Sin3b. We conducted immunoprecipitation with Myc and Sin3b antibodies. Myc was detected in Sin3b immunoprecipitates and Sin3b was also detected in Myc immunoprecipitates, although at lower levels, in agreement with the lower Sin3b expression in these cells as compared to Myc (Figure 4.36.). The results showed that at least a fraction of endogenous Myc and Sin3b proteins interact in the cells. Moreover, endogenous HDAC1 is detected in both immunoprecipitates, which is consistent with the described interaction between Sin3b and HDAC (Figure 4.36.)

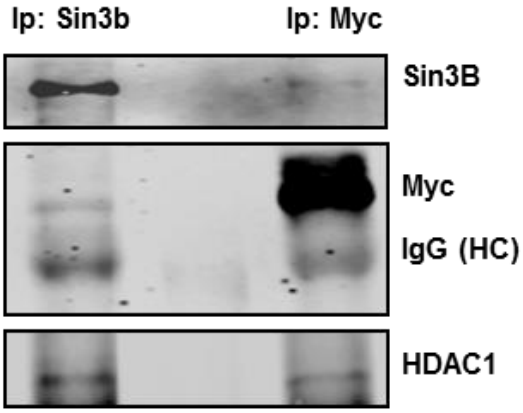

Figure 4.36. Endogenous Myc and Sin3b interacts in human leukemia cells. Lysates from K562/S cells were immunoprecipitated with Sin3b and Myc anti-rabbit antibodies and the levels of Sin3b and Myc were analysed by western blot using anti-mouse antibodies. IgG HC, rabbit heavy chain (anti-mouse IgG slightly cross react against rabbit IgG). Also, HDAC1 was detected in both immunoprecipitates. Antibodies used are shown in Materials and Methods.

Most of Myc and Sin3b localize in cell nuclei and the expectation would be that the Myc-Sin3b complexes would be also nuclear. By immunofluorescence we showed that Myc and Sin3b colocalize in the cell nuclei of K562/S cells (Figure 4.37.).

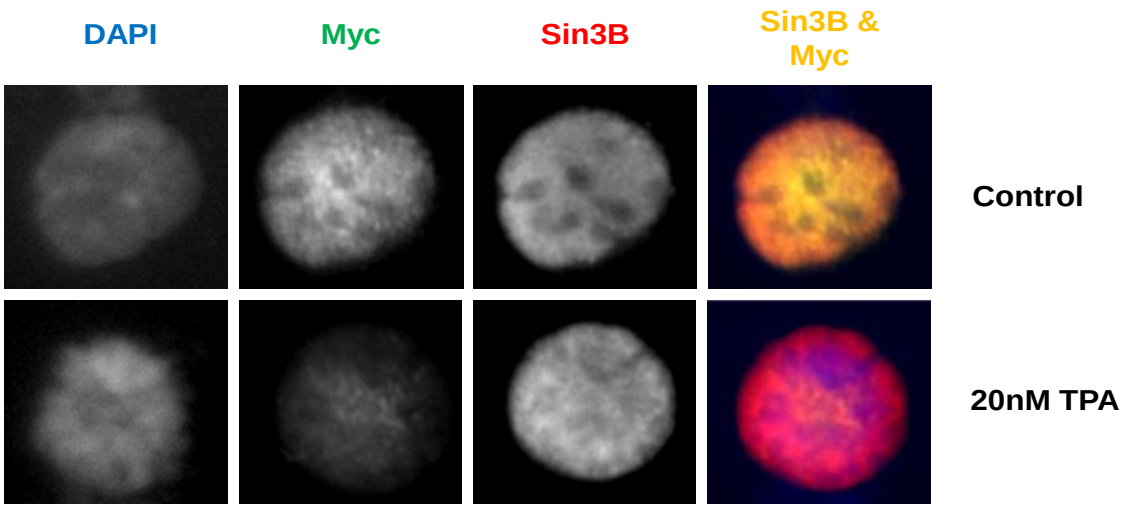

Figure 4.37. Myc and Sin3b colocalize in the nuclei of K562/S cells. Immunofluorescence of the indicated proteins in K562/S cells treated or not with 20 nM TPA for 24 h. Antibodies used are shown in Materials and Methods.

The total expression of Myc and Sin3b was assessed by western blot (Figure 4.38.). As control, K562/S cells were treated for 24 h with 20 nM TPA to reduce Myc expression (Delgado, 2005).

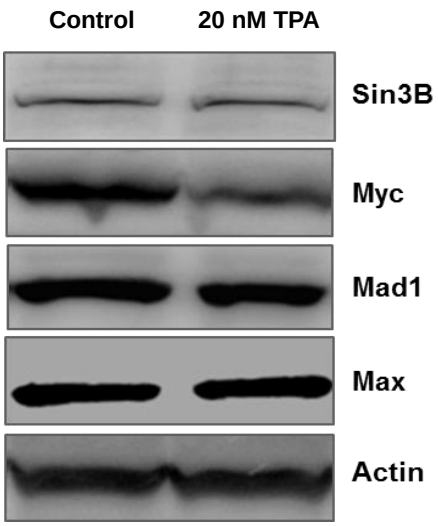

Figure 4.38. TPA reduce Myc levels in leukemia cells, whereas do not affect to Sin3b, Max and Mxd1 expression. Immunoblot of Myc, Sin3b, Mxd1 and Max expression in K562/S cells untreated and treated with 20 nM TPA for 24 h. Antibodies used are shown in Materials and Methods.

To confirm the interaction between endogenous proteins and the localization, we performed *in situ* Proximity Ligation Assay (isPLA) in K562/S cells. The basics of this method of detecting protein interactions are described in Materials and Methods of this work.

We achieved isPLA in growing cells and in TPA-treated cells. isPLA was performed with antibodies against Myc and Sin3b. As positive controls we also tested the interaction between Myc and Max and between Mxd1 and Sin3b. The results showed that endogenous Myc and Sin3b interact in the cell nuclei as expected (Figure 4.39.A). Consistently with the lower Myc expression in TPA-treated cells, the level of interaction was also reduced in these cells, as demonstrated by the quantification of the corresponding signals (Figure 4.39.B).

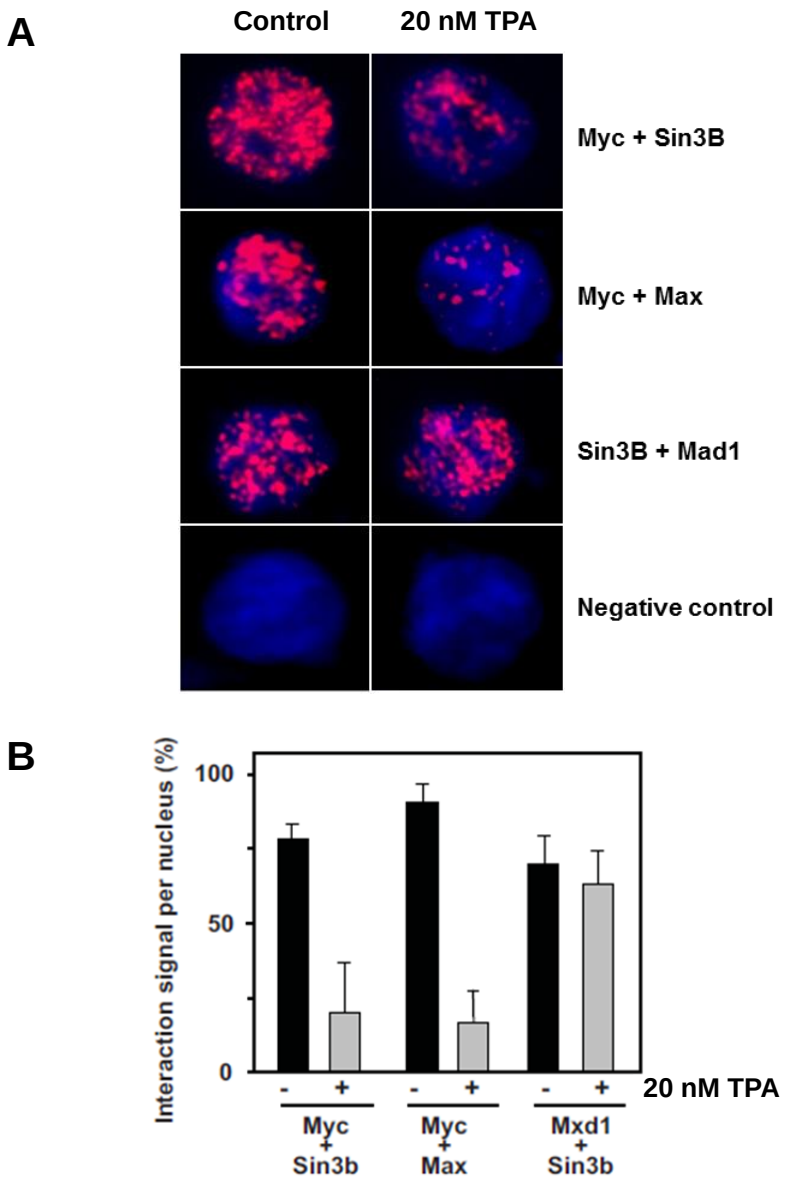

Figure 4.39. Detection of endogenous Myc-Sin3b interaction by isPLA. (A) A representative nuclei is shown for each pair of interactive proteins assayed. Nuclei were counterstained with DAPI. **(B)** Quantification of the isPLA signals. At least 200 nuclei were scored for each pair of assayed proteins. 100% means that the positive signal covers the entire nucleus. Data are mean values of four independent experiments. Error bars are SEM.

4.4.2. Sin3a also binds Myc

The data shown so far argues for a Myc-Sin3 DNA binding in the cell nucleus. Myc binds to DNA E-Boxes to regulate expression, but we did not know whether both proteins can be form complexes while bound to chromatin. We asked whether Sin3 should also be found on a fraction of the Myc-bound chromatin sites as assessed by ChIP assays. For this purpose we analysed the genome data generated by the ENCODE project and made public through the

University of California Santa Cruz browser (UCSC). There are no ChIP-seq data for Sin3b in the data of ENCODE project, but the Chip-seq data for Sin3a in several cell lines is available.

The genome-wide pattern of Sin3a and Myc binding, as determined by ChIP-seq, in several human cell lines are deposited in UCSC as part of the ENCODE project. The bioinformatic analysis revealed that Sin3a is present in ~20% of the Myc sites on the human genome. Interestingly, the colocalization of Myc and Sin3a is 40-fold more frequent in the chromatin region surrounding the transcription start site of the genes (Figure 4.40.). Chip-seq data for Max, the Myc heterodimerization partner, is also available. The analysis revealed all Myc+Sin3a sites are also occupied with Max (Figure 4.40.C).

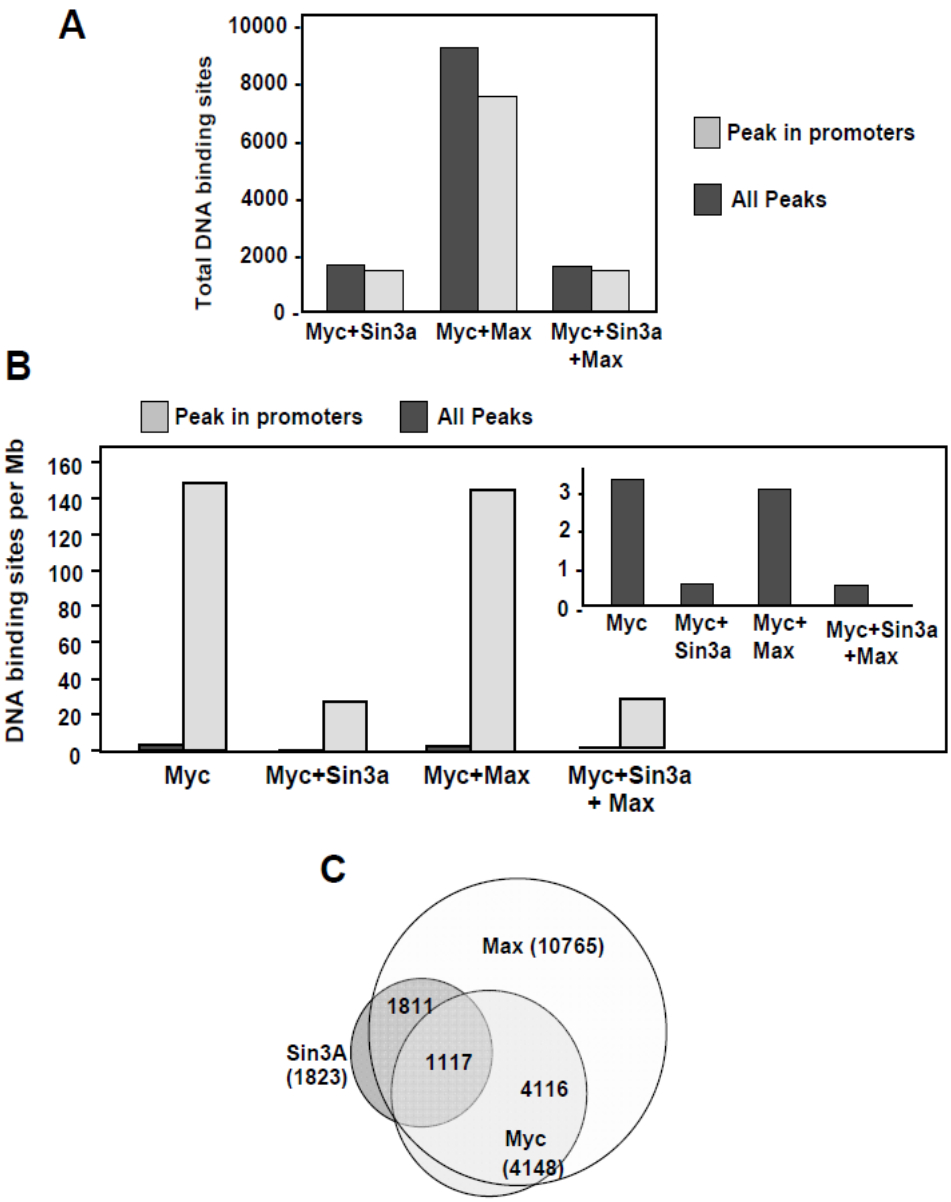

Figure 4.40. Co-localization of Myc and Sin3a on human chromatin binding sites on the genome of K562 cells shared by Myc, Max and Sin3a. (A) The black bars refer to the total sites and the grey bars to

the number of sites in the promoter, defined as 1 Kb upstream and downstream from TSS. **(B)** Number of sites normalized per Mb of genomic DNA. **(C)** Venn diagram indicating the number of promoters showing colocalization of Sin3b, Myc and Max. More than one ChIP-positive site may be present in the promoters.

Although the ChIP data do not demonstrate the interaction, it is in agreement with the hypothesis that Myc and Sin3a/b are in the same complex in the cells. This was directly assessed in our lab by performing re-ChIP in K562 cell line (performed by Lucía García-Gutierrez) and the results showed that Sin3b colocalize with Myc on the E-box containing promoter region of two typical Myc target genes (*CAD* and *LDHB*, data not shown).

After ChIP-seq analysis, we tried to found a correlation between binding and expression level associating ChIP-seq and RNA-seq data of K562 cells. There are more genes with Myc binding in their promoters than Sin3 (Figure 4.41.A). However there was not a correlation among the three groups of genes and differences in their level expression depending on whether Myc, Sin3b or both are bound to their promoter (Figure 4.41.B).

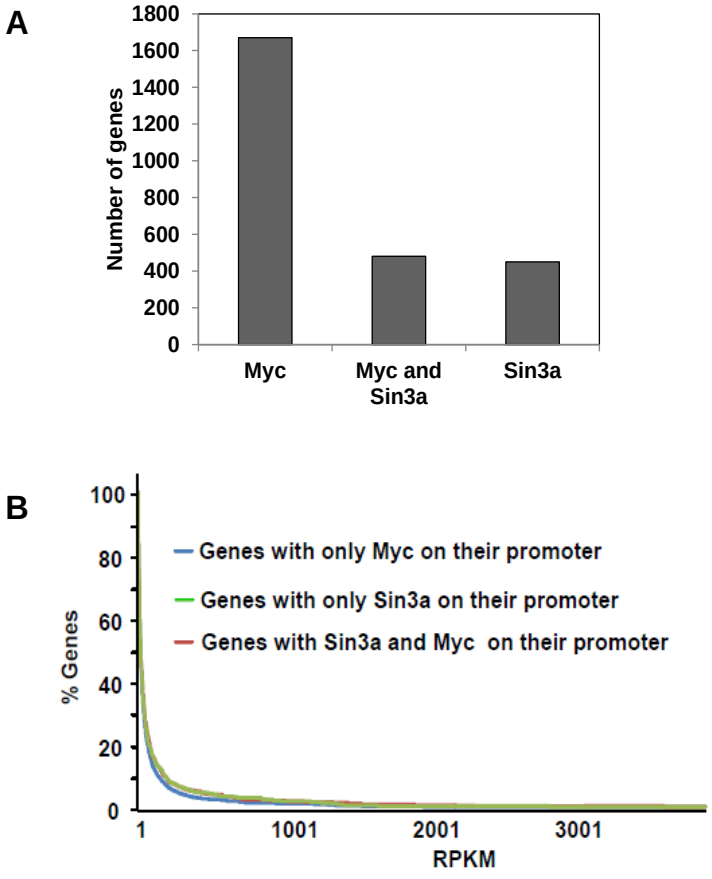

Figure 4.41. Correlation between gene expression and DNA-binding of Myc and Sin3b on the promoters of K562 cells. (A) Number of genes with Myc, Sin3a or both bound to their promoter, defined as 1 Kb upstream and downstream from TSS. **(B)** The graph shows the RKPM (reads per Kb per million of mapped reads) from the RNA-Seq data against the percentage of expressed genes, normalized for each immunoprecipitated protein.

Likewise, we also analysed the co-occupation of Myc and Sin3a on mouse genome (CH12, B-cell lymphoma cell line) and again we found a significant fraction of genomic sites occupied by both factors, and this fraction dramatically increases in the regions around the TSS (Figure 4.42.).

Moreover, on mouse genome we have studied co-occupied sites by Myc and other proteins as Max, Sin3a, Pol2, as well as, Smc3, CTCF and Znf384 as negative controls (Figure 4.43), to demonstrate the Myc-Max and Myc-Sin3b bound-enrichment in promoters. The results in mouse cells, as it occurred in human cells, are that more that 60% of the Myc bound regions also contained Sin3a.

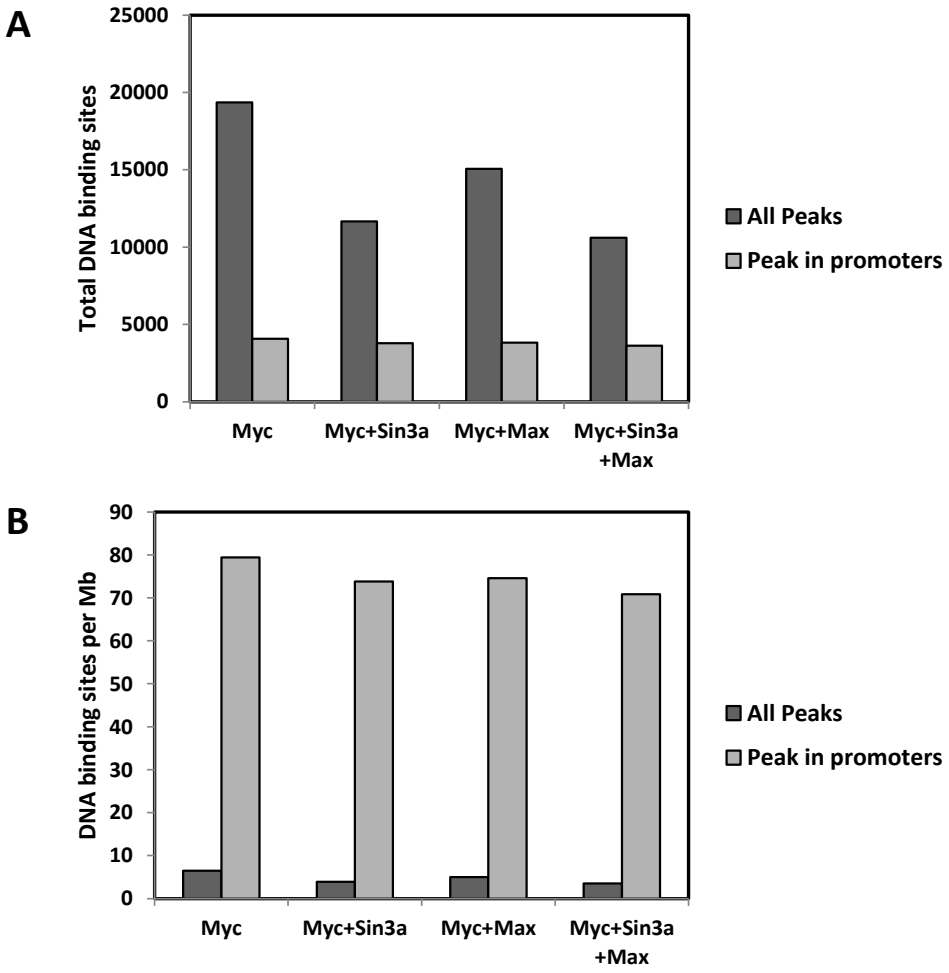

Figure 4.42. Co-localization of Myc and Sin3a proteins on mouse chromatin in CH12 cells. **(A)** Binding sites in the genome of CH12 cells shared by Myc, Max and Sin3a. The black bars refer to the total sites and the grey bars to the number of sites in the promoter, defined as 1 Kb upstream and downstream from TSS. **(B)** Number of binding sites occupied by the indicated proteins normalized per Mb of genomic DNA.

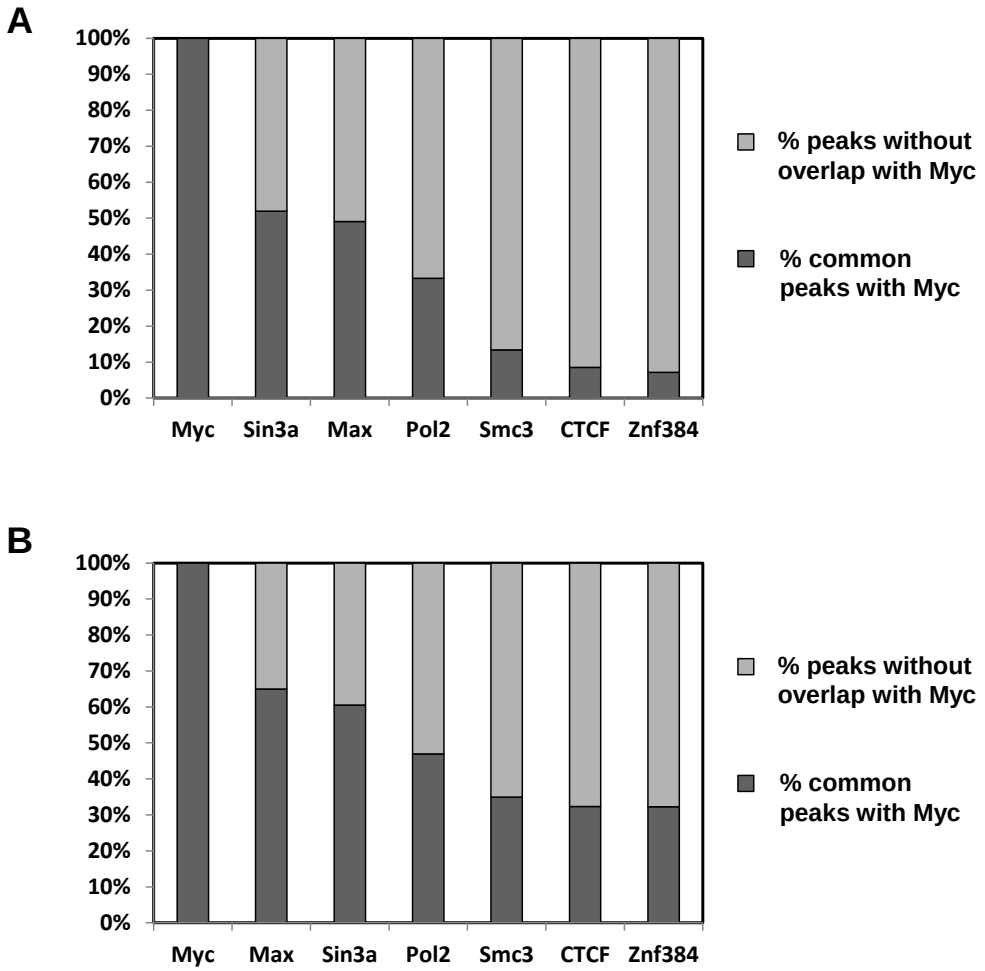

Figure 4.43. Overlapping between peaks of Myc and peaks of Max, Sin3a and others factors on mouse genome. **(A)** Overlap on complete mouse genome and **(B)** on promoters, defined as 1 Kb upstream and downstream from TSS.

5. DISCUSSION

5.1. DISCUSSION-PART I: Myc and Max target genes and differential expression analysis using microarrays, RNA-seq and ChIP-seq

It has been demonstrated by our group that Myc blocks Ras-mediated differentiation of UR61 cells and that this effect is mediated by inhibition of c-Jun upregulation. UR61 cells do not express wild type Max, but a truncated form (Max^{PC12}) unable to bind Myc. This is most interesting as it represents the unique example of Myc function independent from Max. Therefore, Myc should have different functions and target genes in absence of Max.

Therefore we have compared transcriptomes of UR61, URMYC and URMYCMAX3 treated and untreated with dexamethasone (to induce Ras-mediated differentiation) using Affimetrix microarrays. The validation of microarray data was done by RT-qPCR on a subset of genes with 90% efficiency. This has provided data to study the mechanisms by which Myc exerts this biological effect (the blocking of differentiation) with and without Max and identify their target genes.

dChiP software was used to bioinformatic analysis. In a first joint analysis of all samples clearly two groups were distinguished, untreated and treated cells (Figure 4.2.), and also we found a good clustering between duplicates. However, the analysis shows that there are not significant differences between URMYC and URMYCMAX3 transcriptomes, but a significant number of genes changed in their expression (Figure 4.8). However, the gene expression changes were more profound when comparing UR61 vs. URMYC than when comparing URMYC vs. URMYCMAX (Figure 4.5 and Figure 4.8). It must be noted that these two cell lines are stable tranfectants obtained after selection and multiple passage in culture. So it is possible that some differences among these cell lines reflect not only the presence of Max but also clonal differences.

The expression profiles were compared among different cell lines and experimental conditions separately with dChip software. Then, data was analysed with Ingenuity Pathways software, which suggested that c-Jun transcription factor has an important role into neuronal-like differentiation process, whereas that Myc was found as central node of blocked differentiation network in Myc and in Myc-Max expressing cells.

To better characterize the network of genes that mediate Max signalling effects in target genes, we generated UR61 cells that express Max inducible by $ZnSO_4$, called UR61-MT-Max2324. These cells were used to search for Max-dependent changes in transcript levels.

According to transcript profiling obtained from RNA-seq and its subsequently gene ontology analysis, Max has a significant function related with cellular adhesion, axon guidance, mobility and cytoskeleton.

We also used the Max-inducible cells to identify direct Myc and Max binding sites by ChIP-seq in regulatory regions of the genes.

The compared ChIP-seq data between UR61 expressing Myc-only and Myc+Max showed a number of genomic sites where Myc apparently bound without the concourse of Max. However, we could confirm this result in independent ChIP experiments using selected amplicons of about 20 promoters under study. Because of the relevance of the pathways where the genes participate, we chose three genes for a more detailed analysis. These were *ERBB4*, which codes for Erbb4 (v-erb-b2 avian erythroblastic leukemia viral oncogene homolog 4), *SOX13*, which codes for Sox13 (SRY-box 13), and *FANCC*, which codes for Fancc (Fanconi anemia group C) (Figure 4.13). Thus, we suggest that these three genes can be novel *MYC* target genes involved in key functions of cellular physiology.

5.2. DISCUSSION-PART II: ERK binds MYC promoter increasing their transcription

It has been described that activated ERK translocates to the nucleus, where it phosphorylates its interaction partners and induces changes in gene expression (Khokhlatchev, 1998; Bonni, 1999) through a mechanism that involves protein phosphorylation and stabilization. We have also found this increase in Myc levels after ERK activation in several cell lines. Interestingly, in Dr. Crespo's laboratory it has been shown that ERK-NLS increases protein levels of Myc in 3T3 cells and that this effect is independent of ERK kinase activity as transfection with the kinase-dead mutant ERK2-DK, also increased the levels of Myc protein (Javier Rodriguez, unpublished results).

We next asked whether ERK binds DNA on the recently described ERK-Boxes (C/G-AAA-C/G) (Hu, 2009). Therefore, we looked for ERK-Boxes on the human *MYC* gene and we found that most of these boxes are located on their promoter and moreover they are highly conserved in mouse and rat (Figure 4.14). Moreover, ChIP analysis at selected loci along *MYC* gene revealed that activated ERK binds to DNA in rat, human and mouse cells.

To study the transcriptional activity of ERK, we used several luciferase reporters of fragments of *MYC* promoter (He, 1998). Luciferase assays showed that activated ERK increases the activity of two luciferase reporters called FragB and FragDel1, both containing a region of ~500 bp located surrounding 1 Kb upstream from TSS containing four ERK-Boxes. Then, we generated mutants of FragB reporter to define more accurately ERK-binding sites. The results suggested that ERK binds two ERK-Boxes situated around 1 Kb upstream from *MYC* TSS, a highly conserved region in rodents and human genomes. Consistently, MEK1/2 inhibitors, as UO0126, repress *MYC* transcription.

ERK lacks DNA interaction motif, and thus we assumed that ERK needs other partners for the transcriptional regulation of *MYC* described above. Thereby, we investigate the role of Elk1 as ERK cooperator because it has been reported differences between ERK2 and Elk1 DNA-binding and their genome-wide localization showing ERK2 colocalization with Elk1 at promoters (Goke, 2013).

For this purpose, firstly we analyzed the ChIP-seq data for Elk1 project in several cell lines (GM12878, K562 and HeLa) generated by the ENCODE project. These data showed enrichment of Elk1-binding in three regions of human *MYC* promoter (Figure 4.23) and one of them coincide with the previously identified ERK-binding site by luciferase assays.

Another protein related with the increasing of transcription is CDK9, which is associated with active RNA polymerase II. CDK9 phosphorylates RNA Pol II-Ser5 to allow transcriptional elongation (Marshall, 1996; Yamada, 2006). The genome-wide binding of CDK9 coincides with initiating RNA Pol II-Ser5P in the promoter region, close to TSS (Larochelle, 2012; Ghamari, 2013), which is according to our ChIP results on *MYC* gene (Figure 4.24). The results suggested that ERK and CDK9 might be interacting bound to specific chromatin regions.

To explore this hypothesis we performed isPLA, whose results showed positive interaction between ERK2 and CDK9 (Figure 4.25) (results obtained in collaboration with Lorena Agudo in Dr. Crespo's laboratory). Moreover, in the Dr. Crespo's laboratory they have been confirmed this interaction by CoIP experiments and the interaction region of CDK9 responsible of interacting with ERK2 has been identified. Altogether the results argue for an interaction between ERK2 and CDK9 on specific chromatin regions.

5.3. DISCUSSION-PART III: Myc inhibits Ras-mediated senescence

Using this model, we have confirmed that UR61 undergo senescence after differentiation in response to N-Ras activation, whereas this senescence is blocked in Myc expressing cells, as showed by SA-β-gal activity and by time-lapse video microscopy.

URMYC is a derived UR61 stable cell line generated by selection of positive clones with constitutive expression of Myc, and, it has been described that Myc inhibits Ras-mediated differentiation (Vaqué, 2008). However the rate of differentiation is higher when the cells are grown on artificial matrix (i.e., matrigel). Thus there is a fraction of URMYC cells not undergoing differentiation in response to Ras.

It has been described that cellular senescence is a state of irreversible growth arrest. Thus we seeded UR61 and URMYC, and after four days under Ras induction conditions, we seeded these cells on new culture plates to normal growth, in which senescent UR61 were completely arrested, whereas that a significant percentage of URMYC followed growing, suggesting that Myc partially impairs senescence and allows that this cells continues growing. Also, crystal violet staining has shown that Myc can prevent cell cycle arrest mediated by Ras (Figure 4.28).

This Ras-induced senescence occurs accompanied of overexpression of p16 and p21, which have been described as markers senescence. Furthermore, senescent cells develop a complex senescence-associated secretory phenotype (SASP), which includes high level secretion of inflammatory cytokines as IL-6. IL-1α and IL-1β are a multifunctional cytokines that regulate inflammatory and immune responses primarily by initiating a signal transduction cascade that ultimately induces cytokine secretion. IL-1β is active solely as a mature secrete form, whereas IL-1α is rarely secreted at high levels (Apte, 2006). We verified the senescence-associated rise in expression by quantifying mRNA levels. The RT-qPCR results showed that, relative to untreated controls, transcripts encoding these proteins increased steadily along five days in UR61 cells in contrast to Myc-expressing cells, both treated with Dex to Ras-induction. However, the mechanisms by which Myc blocks the inflammatory response and secretion of cytokines in remain unknown. IL-1α and IL-1β are synthesized as precursors. In particular, pro-IL-1β is inactive until processed by the inflammasome, a multiprotein complex comprising of caspase-1 and several adapter molecules (Schroder and Tschopp, 2010). UR61 undergoing Ras-induced senescence displayed caspase-1 activity, relative to growing untreated cells. In this case, it could be expected that caspase-1 activity was blocked by Myc, but there were not significant differences in caspase-1 activity in the presence of Myc (Figure 4.31). Also the caspase-1 inhibitor treatment showed a reduced growth arrest, independently of Myc (Figure 4.32). It is known that the cells show peaks of caspase-1 activity, thus a possible explanation could be that our experiment was performed in cells treated for eight days with Dex to induce Ras and then the activity peak in this cellular model under senescence conditions could occur probably earlier.

To better understand the Myc-Ras relationship in senescence we used IMR90 primary human fibroblasts, an established senescence cellular model (Acosta, 2013). Ras expression in IMR90 cells caused senescence phenotype accompanied by upregulation of senescence markers and components of inflammasome (Figure 4.33). However, the role of Myc in senescence remains unclear, because our Myc-inducible system by 4OHT (IMR90-MycER) does not work properly because there was a basal level of Myc-dependent transformation due to the leakiness of the MycER system. Surprisingly, after induction with 4OHT, there was an extensive cell death due to high Myc levels. After these results, it would be useful to generate an IMR90 derived cell line with constitutive expression of Myc and inducible expression of Ras (IMR90-Myc-RasER) to study Myc-Ras relationship in senescence and proliferation.

In conclusion, Ras induces senescence in both UR61 and IMR90 models, whereas Myc, impairs this Ras-mediated senescence and also inhibits secretion of several components of inflammasome. In conclusion, we show for the first time that this activity of Myc is independent from Max, although further work is required to dissect out the underlying mechanisms.

5.4. DISCUSSION-PART IV: Endogenous Myc interacts with Sin3

The interaction between Myc and Sin3b was initially discovered by yeast two-hybrid screening in our lab, which was confirmed by CoIP experiments in transfected 293T and UR61 cells. However, it was unknown whether this interaction took place between endogenous proteins. We showed that endogenous Myc and Sin3b also interact in K562/S cells, as shown by CoIP (Figure 4.36) and by isPLA (Figure 4.39). The isPLA has been recently introduced as a technique that allows the detection of protein interactions inside the cells. Conversely to FRET, which requires the transfection of labeled proteins, this technique detects interactions between endogenous proteins. Our data does not allow to discriminate between direct or indirect binding as two target proteins can be separated a theoretical maximum distance of 30-40 nm to give a positive PLA signal. However, taken together the PLA, CoIP and two hybrid screening, the results strongly argues in favor of a direct interaction between Myc and Sin3b. In fact, the signal intensity of isPLA positive controls (Myc+Max and Sin3b+Mxd1 described direct interactions) is similar to that detected in Myc+Sin3b. As a control of CoIP, we have also detected endogenous HDAC1 in both immunoprecipitates Myc and Sin3b, which is consistent with the described interaction between Sin3b and HDAC1.

Although Sin3a did not appear in our initial two-hybrid screening, it was later shown that Sin3a also coimmunoprecipitated with Myc. In addition, the genome-wide ChIP-seq data available in the UCSC database from ENCODE project reveals that Sin3a and Myc colocalize in a relevant fraction of chromatin sites on human and mouse genome, often in the chromatin region surrounding the TSS of the genes. The analysis showed that most of these sites also can be occupied by Max. Though the ChIP data *per se* do not demonstrate the interaction, it is in agreement with the hypothesis that Myc and Sin3a/b are in the same complex in the cells, and a significant part of these complexes are also bound to chromatin.

Even though Sin3 proteins have been described as transcriptional co-repressors, the combined analysis of ChIP-seq and RNA-seq data generated by the ENCODE consortium revealed that, at least in K562 cells, the coincidence of Myc and Sin3a in the proximal promoters does not correlate with a lower expression with respect to genes with Myc alone (Figure 4.41).

In general, a chromatin remodelling complex binds to a coactivator or corepressor to bridge between sequence-specific transcription factors and basal transcription factors. It has been described that Mxd1 antagonizes the transactivation function of Myc-Max into Myc-Max-Mxd1 network, and further Mxd1 binds to Sin3b to be recruited to the basal corepressor complex possessing histone deacetylase activity (HDAC1). Although the mechanisms of regulation are still unclear, there are several hypotheses that could explain the Myc repressive action through its direct interaction with Sin3 proteins. It has been suggested that Sin3a stabilizes Myc by promoting its deacetylation (Nascimento, 2011) and a similar mechanism can be operative for Sin3b. Thus, if a direct repressive effect of Sin3-Myc on chromatin is ruled out, Sin3b could limit the Myc activity through two complementary activities: Mxd-dependent gene repression and reduction of Myc levels. Therefore, Sin3 could shift between Mxd- or Myc-complexes to achieve

a similar biological readout, i.e., a decrease in Myc activity. However we do not know whether the affinity of Sin3 for Myc is higher or lower than that for Mxd to support this model of transit between Myc or Mxd complexes. In conclusion, we have discovered a new interaction between Myc and Sin3, which could be relevant for Myc activity.

6. CONCLUSIONS

1. There are not extensive differences between the transcriptomes of UR61 cells expressing Myc but not Max and UR61 cells expressing both Myc and Max, suggesting that many genes are regulated by Myc without the concourse of Max.
2. Bioinformatic analysis of the protein interaction networks of the regulated genes showed that c-Jun transcription factor has an important role into neuronal-like differentiation process, whereas that Myc was found as central node of blocked differentiation network in Myc- and in Myc-Max-expressing cells.
3. UR61-MT-Max2324, a UR61 subline with Max inducible expression by $ZnSO_4$, was generated and used for RNA-seq analysis to show that Max regulates genes related with cellular adhesion, axon guidance, mobility and cytoskeleton.
4. ChIP-seq analysis showed that Myc binding profile is different in Max-lacking cells with respect to cells expressing Myc and Max.
5. *ERBB4*, *SOX13* and *FANCC* genes were identified as putative novel Myc target genes, being regulated by Myc+Max, but not by Myc in Max-deficient cells.
6. ERK binds to *MYC* promoter in a region mapping around 1 Kb upstream from TSS, increasing *MYC* transcription.
7. Genome-wide ENCODE data analysis showed ERK2 colocalization with Elk1 and CDK9 in human cells suggesting that these proteins might be interacting bound to specific chromatin regions.
8. Interaction between endogenous ERK2 and CDK9 was confirmed using isPLA in HeLa and MEF cells.
9. Oncogenic N-Ras induces senescence in Max-deficient UR61 cells, whereas this senescence is blocked in Myc expressing cells.
10. Ras-mediated senescence is accompanied by upregulation of several components of associated secretome (IL-1α, IL1-β and IL-6), all of them are repressed in Myc overexpressing cells.
11. Endogenous Myc and Sin3b interacts *in situ* in K562/S cell and genome-wide ENCODE data analysis revealed that Sin3a and Myc colocalize in a relevant fraction of chromatin sites on human and mouse genome, often in the chromatin region surrounding the TSS of the genes.

7. BIBLIOGRAPHY

Acosta JC, Ferrándiz N, Bretones G, Torrano V, Blanco R, Richard C, O'Connell B, Sedivy J, Delgado MD, León J (2008). Myc inhibits p27-induced erythroid differentiation of leukemia cells by repressing erythroid master genes without reversing p27-mediated cell cycle arrest. Mol Cell Biol 28:7286-95.

Acosta JC, Gil J (2012). Senescence: a new weapon for cancer therapy. Trends Cell Biol 22:211-9.

Acosta JC, Banito A, Wuestefeld T, Georgilis A, Janich P, Morton JP, Athineos D, Kang TW, Lasitschka F,Andrulis M, Pascual G, Morris KJ, Khan S, Jin H, Dharmalingam G, Snijders AP, Carroll T, Capper D,Pritchard C, Inman GJ, Longerich T, Sansom OJ, Benitah SA, Zender L, Gil J (2013). A complex secretory program orchestrated by the inflammasome controls paracrine senescence. Nat Cell Biol.

Albert T, Urlbauer B, Kohlhuber F, Hammersen B, Eick D (1994). Ongoing mutations in the N-terminal domain of c-Myc affect transactivation in Burkitt's lymphoma cell lines. Oncogene 9:759-63.

Albert T, Wells J, Funk JO, Pullner A, Raschke EE, Stelzer G, Meisterernst M, Farnham PJ, Eick D (2001). The chromatin structure of the dual c-myc promoter P1/P2 is regulated by separate elements. J Biol Chem 276:20482-90.

Alland L, Muhle R, Hou H Jr, Potes J, Chin L, Schreiber-Agus N, DePinho RA (1997). Role for N-CoR and histone deacetylase in Sin3-mediated transcriptional repression. Nature 387:49-55.

Amati B, Dalton S, Brooks MW, Littetlewood D, Evan, Land H (1992). Transcriptional activation by the human c-Myc oncoprotein in yeast requires interaction with Max. Nature 359:423-426.

Amati B, Littlewood TD, Evan GI, Land H (1993). The c-Myc protein induces cell cycle progression and apoptosis through dimerization with Max. Embo J 12:5083-5087.

Amati B, Frank SR, Donjerkovic D, Taubert S (2001). Function of the c-Myc oncoprotein in chromatin remodeling and transcription. Biochim Biophys Acta 1471:135-45. Embo J 24:336-46.

Amundson SA, Zhan Q, Penn LZ, Fornace AJ Jr (1998). Myc suppresses induction of the growth arrest genes gadd34, gadd45, and gadd153 by DNA-damaging agents. Oncogene 17:2149-2154.

Anders S, Huber W (2010). Differential expression analysis for sequence count data. Genome Biology 11:R106.

Apte RN (2006). The involvement of IL-1 in tumorigenesis, tumor invasiveness, metastasis and tumor-host interactions. Cancer Metastasis Rev 25:387-408.

Arabi A, Wu S, Ridderstrale K, Bierhoff H, Shiue C, Fatyol K, Fahlén S, Hydbring P, Söderberg O, Grummt I, Larsson LG, Wright AP (2005). c-Myc associates with ribosomal DNA and activates RNA polymerase I transcription. Nat Cell Biol 7:303-10.

Arsura M, Deshpande A, Hann SR, Sonenshein GE (1995). Variant Max protein, derived by alternative splicing, associates with c-Myc in vivo and inhibits transactivation. Mol Cell Biol 15:6702-6709.

Arvanitis C, Felsher DW (2006). Conditional transgenic models define how Myc initiates and maintains tumorogenesis. Semin Cancer Biol 16:313-317.

Askew DS, Ashmun RA, Simmons BC, Cleveland JL (1991). Constitutive c-myc expression in an IL-3-dependent myeloid cell line suppresses cell cycle arrest and accelerates apoptosis. Oncogene 6:1915-22.

Axelson H, Henriksson M, Wang Y, Magnusson KP, Klein G (1995). The amino-terminal phosphorylation sites of C-MYC are frequently mutated in Burkitt's lymphoma lines but not in mouse plasmacytomas and rat immunocytomas. Eur J Cancer 31A:2099-104.

Ayer DE, Kretzner L, Eisenman RN (1993). Mad: a heterodimeric partner for Max that antagonizes Myc transcriptional activity. Cell 72:211-22.

Ayer DE, Lawrence QA, Eisenman RN (1995). Mad-Max transcriptional repression is mediated by ternary complex formation with mammalian homologs of yeast repressor Sin3. Cell 80:767-76.

Bacon TA, Wickstrom E (1991). Daily addition of an anti-c-myc DNA oligomer induces granulocytic differentiation of human promyelocytic leukemia HL-60 cells in both serum-containing and serum-free media. Oncogene Res 6:21-32.

Barbacid M (1987). Ras genes. Annu Rev Biochem 56:779-827.

Barr LF, Campbell SE, Bochner BS, Dang CV (1998). Association of the decreased expression of alpha3beta1 integrin with the altered cell: environmental interactions and enhanced soft agar cloning ability of c-myc-overexpressing small cell lung cancer cells. Cancer Res 58:5537-45.

Baudino TA, Cleveland JL (2001). The Max network gone mad. Mol Cell Biol 21:691-702.

Baudino TA, McKay C, Pendeville-Samain H, Nilsson JA, Maclean KH, White EL, Davis AC, Ihle JN, Cleveland JL (2002). c-Myc is essential for vasculogenesis and angiogenesis during development and tumor progression. Genes Dev 16:2530-43.

Baudino, R. and Cleveland, J.L. (2002). The Max Network Gone Mad. Mol Cell Biol. 21, 691-702.

Bello-Fernandez C, Packham G, Cleveland JL (1993). The ornithine decarboxylase gene is a transcriptional target of c-Myc. Proc Natl Acad Sci USA 90:7804-8.

Bellosta P, Hulf T, Balla Diop S, Usseglio F, Pradel J, Aragnol D, Gallant P (2005). Myc interacts genetically with Tip48/Reptin and Tip49/Pontin to control growth and proliferation during Drosophila development. Proc Natl Acad Sci USA 102:11799-804.

Bennecke M, Kriegl L, Bajbouj M, Retzlaff K, Robine S, Jung A, Arkan MC, Kirchner T, Greten FR (2010). Ink4a/Arf and oncogene-induced senescence prevent tumor progression during alternative colorectal tumorigenesis. Cancer Cell 18:135-46.

Berberich S, Hyde-DeRuyscher N, Espenshade P, Cole M (1992). max encodes a sequence-specific DNAbinding protein and is not regulated by serum growth factors. Oncogene 7:775-779.

Berberich SJ, Cole MD (1992). Casein kinase II inhibits the DNA-binding activity of Max homodimers but not Myc/Max heterodimers. Genes dev 6:166-176.

Bernstein PL, Herrick DJ, Prokipcak RD, Ross J (1992). Control of c-myc mRNA half-life in vitro by a protein capable of binding to a coding region stability determinant. Genes Dev 6:642-54.

Bhatia K, Huppi K, Spangler G, Siwarski D, Iyer R, Magrath I (1993). Point mutations in the c-Myc transactivation domain are common in Burkitt's lymphoma and mouse plasmacytomas. Nat Genet 5:56-61.

Blackwell TK, Kretzner L, Blackwood EM, Eisenman RN, Weintraub H (1990). Sequence-specific DNA binding by the c-Myc protein. Science 250:1149-51.

Blackwood EM, Eisenman RN (1991). Max: a helix-loop-helix zipper protein that forms a sequence-specific DNA-binding complex with Myc. Science 251:1211-7.

Blackwood EM, Lugo TG, Kretzner L, King MW, Street AJ, Witte ON, Eisenman RN (1994). Functional analysis of the AUG- and CUG-initiated forms of the c-Myc protein. Mol Biol Cell 5:597-609.

Blackwood EM, Lüscher B, Eisenman RN (1992). Myc and Max associate in vivo. Genes Dev 6:71-80.

Bonfini L, Karlovich CA, Dasgupta C, Banerjee U (1992). The Son of sevenless gene product: a putative activator of Ras. Science 255:603-6.

Bonni A, Brunet A, West AE, Datta SR, Takasu MA, Greenberg ME (1999). Cell survival promoted by the Ras-MAPK signalling pathway by transcription-dependent and –independent mechanism. Science 286:1358-62.

Bos JL, Verlaan-de Vries M, Jansen AM, Veeneman GH, van Boom JH, van der Eb AJ (1984). Three different mutations in codon 61 of the human N-ras gene detected by synthetic oligonucleotide hybridization. Nucleic Acids Res 12:9155-63.

Bouchard C, Dittrich O, Kiermaier A, Dohmann K, Menkel A, Eilers M, Lüscher B (2001). Regulation of cyclin D2 gene expression by the Myc/Max/Mad network: Myc-dependent TRRAP recruitment and histone acetylation at the cyclin D2 promoter. Genes Dev 15:2042-7.

Boulton TG, Nye SH, Robbins DJ, Ip NY, Radziejewska E, Moegenbesser SD, DePinho RA, Pananoyatos N, Cobb MH, Yancopoulos GD (1991). ERKs: a family of protein-serine/threonine kinases that are activated and tyrosine phosphorylated in response to insulin and NGF. Cell 65:663-75.

Boulton TG, Yancopoulos GD, Gregory JS, Slaughter C, Moomaw C, Hsu J, Cobb MH (1990). An insulin-stimulated protein kinase similar to yeast kinases involved in cell cycle control. Science 249:64-7.

Boxer RB, Jang JW, Sintasath L, Chodosh LA (2004). Lack of sustained regression of c-myc-induced mammary adenocarcinomas following brief or prolonged myc inactivation. Cancer Cell 6:577-586.

Braig M, Lee S, Loddenkemper C, Rudolph C, Peters AH, Schlegelberger B, Stein H, Dorken B, Jenuwein T, Schmitt CA (2005). Oncogene-induced senescence as an initial barrier in lymphoma development. Nature 436:660-5.

Brenner C, Deplus R, Didelot C, Loriot A, Viré E, De Smet C, Gutierrez A, Danovi D, Bernard D, Boon T, Pelicci PG, Amati B, Kouzarides T, de Launoit Y, Di Croce L, Fuks F (2005). Myc represses transcription through recruitment of DNA methyltransferase corepressor. EMBO J 24:336-46.

Bretones G, Acosta JC, Caraballo JM, Ferrandiz N, Gomez-Casares MT, Albajar M, Blanco R, Ruiz P, Hung WC, Alberto MP, Leon (2011). SKP2 oncogene is a direct MYC target gene and MYC down-regulates p27(KIP1) through SKP2 in human leukemia cells. J Biol Chem 286:9815-25.

Brightman FA and Fell DA (2000). Differential feedback regulation of the MAPK cascade underlies the quantitative differences in EGF and NGF signalling in PC12 cells. FEBS Lett 482:169-74.

Bull JJ, Muller-Rover S, Patel SV, Chronnell CM, McKay IA, Philpott MP (2001). Contrasting localization of c-Myc with other Myc superfamily transcription factors in the human hair follicle and during the hair growth cycle. J Invest Dermatol 116:617-622.

Burstein DE, Greene LA (1982). Nerve growth factor has both mitogenic and antimitogenic activity. Dev Biol 94:477-482.

Buschbeck M, Ulrich A (2005). The unique C-terminal tail of the mitogen-activated protein kinase ERK5 regulates its activation and nuclear shuttling. J Biol Chem 280:2659-67.

Campisi J (2001). Cellular senescence as a tumor-suppressor mechanism. Trends Cell Biol 11:S27-S31.

Campisi J (2005). Senescent cells, tumor suppression, and organismal aging: good citizens, bad neighbors. Cell 120:513-522.

Campisi J, D'Adda di Fagagna F (2007) Cellular senescence:when bad things happen to good cells. Nature Rev Mol Cell Biol 8:729-740.

Carragher LAS, Snell KR, Giblett SM, Aldridge VSS, Patel B, Cook SJ, Winton DJ, Marais R, Pritchard CA (2010). Braf induces gastrointestinal crypt senescence and promotes tumour progression through enhanced CpG methylation of p16INK4a. EMBO J 2:458-71.

Cartwright P, McLean C, Sheppard A, Rivett D, Jones K, Dalton S (2005). LIF/STAT3 controls ES cell self-renewal and pluripotency by a Myc-dependent mechanism. Development 132:885-96.

Ceballos E, Delgado MD, Gutierrez P, Richard C, Muller D, Ehinger M, Gullberg U, León J (2000). c-Myc antagonizes the effect of p53 on apoptosis and p21WAF1 transactivation in K562 leukemia cells. Oncogene 19:2194-204.

Ceballos E, Munoz-Alonso MJ, Berwanger B, Acosta JC, Hernandez R, Krause M, Hartmann O, Eilers M, Leon J (2005). Inhibitory effect of c-Myc on p53-induced apoptosis in leukemia cells. Microarray analysis reveals defective induction of p53 target genes and upregulation of chaperone genes. Oncogene 24:4559-71.

Chang BD, Swift ME, Shen M, Fang J, Broude EV, Roninson IB (2002). Molecular determinants of terminal growth arrest induced in tumor cells by a chemotherapeutic agent. Proc Natl Acad Sci USA 99:389-94.

Chang DH, Angelin-Duclos C, Calame K (2000). BLIMP-1: trigger for differentiation of myeloid lineage. Nat Immunol, 1, 169-176.

Chen C, Nussenzweig A, Guo M, Kim D, Li GC, Ling CC (1996). Down-regulation of gadd153 by c-myc in rat fibroblasts and its effect on cell growth and radiation-induced apoptosis. Oncogene 13:1659-65.

Chen Z, Trotman LC, Shaffer D, Lin HK, Dotan ZA, Niki M, Koutcher JA, Scher HI, Ludwig T, Gerald W, Cordon-Cardo C, Pandolfi PP (2005). Crucial role of p53-dependent cellular senescence in suppression of Pten deficient tumorigenesis. Nature 436:725-30.

Cheng SW, Davies KP, Yung E, Beltran RJ, Yu J, Kalpana GV (1999). c-MYC interacts with INI1/hSNF5 and requires the SWI/SNF complex for transactivation function. Nat Genet 22:102-5.

Chien Y, Scuoppo C, Wang X, Fang X, Balgley B, Bolden JE, Premsrirut P, Luo W, Chicas A, Lee CS, Kogan SC, Lowe SW (2011). Control of the senescence-associated secretory phenotype by NF-kB promotes senescence and enhances chemosensitivity. Genes Dev 25:2125-36.

Chou TY, Dang CV, Hart GW (1995). Glycosylation of the c-Myc transactivation domain. Proc Natl Acad Sci USA

Chung HJ, Levens D (2005). c-myc expression: keep the noise down! Mol Cells 20:157-66.

Claassen GF, Hann SR (1999). Myc-mediated transformation: the repression connection. Oncogene 18:2925-33.

Collado M, Gil J, Efeyan A, Guerra C, Schuhmacher AJ, Barradas M, Benguria A, Zaballos A, Flores JM, Barbacid M, Beach D, Serrano M, (2005). Tumour biology: senescence in premalignant tumours. Nature 436: 64-2.

Collado M, Blasco MA, Serrano M (2007). Cellular senescence in cancer and aging. Cell 130:223-33.

Coller HA, Grandori C, Tamayo P, Colbert T, Lander ES, Eisenman RN, Golub TR (2000). Expression analysis with oligonucleotide microarrays reveals that MYC regulates genes involved in growth, cell cycle, signaling, and adhesion. Proc Natl Acad Sci USA 97:3260-5.

Conacci-Sorrell M, Eisenman RN (2011). Post-translational control of Myc function during differentiation. Cell Cycle 10, 604-610.

Coppe JP (2008). Senescence-associated secretory phenotypes reveal cell-nonautonomous functions of oncogenic RAS and the p53 tumor suppressor. Plos Biol 6:2853-2868.

Coppe JP. Patil CK, Rodier F, Krtolica A, Beausejour CM, Parrinello S, Hodgson JG, Chin K, Desprez PY, Campisi J (2010). A Human-Like Senescence-Associated Secretory Phenotype Is Conserved in Mouse Cells Dependent on Physiological Oxygen. Plos Biol 5:e9188.

Coppola JA, Cole MD (1986). Constitutive c-myc oncogene expression blocks mouse erythroleukaemia cell differentiation but not commitment. Nature 320:760-763.

Core LJ, Lis J (2008). Transcription Regulation Through Promoter-Proximal Pausing of RNA Polymerase II. Science 319:1791-2.

Courtois-Cox S, Jones SL, Cichowski K (2008). Many roads lead to oncogene-induced senescence. Oncogene 27:2801-9.

Cowley S, Paterson H, Kemp P, Marshall CJ (1994). Activation of MAP kinase kinase is necessary and sufficient for PC12 differentiation and for transformation of NIH 3T3 cells. Cell 77:841-52.

Cowling VH, Chandriani S, Whitfield ML, Cole MD (2006). A conserved Myc protein domain, MBIV, regulates DNA binding, apoptosis, transformation, and G2 arrest. Mol Cell Biol 26:4226-39.

Crespo P, León J (2000). Ras proteins in the control of the cell cycle and cell differentiation. Cell Mol Life Sci 57:1613-36.

Crews S, Barth R, Hood L, Prehn J, Calame K (1982). Mouse c-myc oncogene is located on chromosome 15 and translocated to chromosome 12 in plasmacytomas. Science 218:1319-21.

Dalla-Favera R, Bregni M, Erikson J, Patterson D, Gallo RC, Croce CM (1982a). Human c-myc onc gene is located on the region of chromosome 8 that is translocated in Burkitt lymphoma cells. Proc Natl Acad Sci USA. 79:7824-7.

Dalla-Favera R, Gelmann EP, Martinotti S, Franchini G, Papas TS, Gallo RC, Wong-Staal F (1982b). Cloning and characterization of different human sequences related to the onc gene (v-myc) of avian myelocytomatosis virus (MC29). Proc Natl Acad Sci USA 79:6497-501.

Dang CH, Le A, Gao P (2009). MYC-induced Cancer Cell Energy Metabolism and Therapeutic Opportunities. Clin Cancer Res 15:6479-83

Dang CV (2010). Rethinking the Warburg effect with Myc micromanaging glutamine metabolism. Cancer Res 70:859-62.

Dang CV (2013) MYC, Metabolism, Cell Growth, and Tumorigenesis. Cold Spring Harb Perspect Med 3.

Dang CV, O'Donnell KA, Zeller KI, Nguyen T, Osthus RC, Li F (2006). The c-Myc target gene network. Semin Cancer Biol. 16:253-64.

Dang CV, Resar LM, Emison E, Kim S, Li Q, Prescott JE, Wonsey D, Zeller K (1999). Function of the c-Myc oncogenic transcription factor. Exp Cell Res 253: 63-77.

Dang VD, Benedik MJ, Ekwall K, Choi J, Allshire RC, Levin HL (1999). A new member of the Sin3 family of corepressors is essential for cell viability and required for retroelement propagation in fission yeast. Mol Cell Biol 19:2351-65.

Dang, CV, O'Donnell KA, Zeller KI, Nguyen T, Osthus RC, Li F (2006). The c-Myc target gene network. Semin Cancer Biol 16:253-64.

David G, Grandinetti KB, Finnerty PM, Simpson N, Chu GC, Depinho RA (2008). Specific requirement of the chromatin modifier mSin3B in cell cycle exit and cellular differentiation. Proc Natl Acad Sci USA 105:4168-72.

de Alborán IM, Baena E, Martinez-A C (2004). c-Myc-deficient B lymphocytes are resistant to spontaneous and induced cell death. Cell Death Differ 11:61-8.

de Alboran IM, O'Hagan RC, Gärtner F, Malynn B, Davidson L, Rickert R, Rajewsky K, DePinho RA, Alt FW (2001). Analysis of C-MYC function in normal cells via conditional gene-targeted mutation. Immunity 14:45-55.

De Nadal E, Zapater M, Alepuz PM, Sumoy L, Mas G, Posas F (2004). The MAPK Hog1 recruits Rpd3 histone deacetylase to activate osmoresponsive genes. Nature 427:370-4.

Dean M, Levine RA, Ran W, Kindy MS, Sonenshein GE, Campisi J (1986). Regulation of c-myc transcription and mRNA abundance by serum growth factors and cell contact. J Biol Chem 261:9161-6.

Delgado MD, León J (2010). Myc roles in hematopoiesis and leukemia. Genes & cancer 1:605-16.

Delgado MD, Lerga A, Cañelles M, Gómez-Casares MT, León J (1995). Differential regulation of Max and role of c-Myc during erythroid and rnyelornonocytic differentiation of K562 cells. Oncogene10:1659-65.

DePinho R, Mitsock L, Hatton K, Ferrier P, Zimmerman K, Legouy E, Tesfaye A, Collum R, Yancopoulos G, Nisen P (1987). Myc family of cellular oncogenes. J Cell Biochem 33:257-66.

DePinho RA, Schreiber-Agus N, Alt FW (1991). myc family oncogenes in the development of normal and neoplastic cells. Adv Cancer Res 57:1-46.

Dimri GP, Lee X, Basile G, Acosta M, Scott G, Roskelley C, Medrano EE, Linskens M, Rubelj I, Pereira-Smith O (1995). A biomarker that identifies senescent human cells in culture and in aging skin in vivo. Proc Natl Acad Sci USA 92:9363-7.

Dorland S, Deegenaars ML, Stillman DJ (2000). Roles for the Saccharomyces cerevisiae SDS3, CBK1 and HYM1 genes in transcriptional repression by SIN3. Genetics 154:573-86.

Douglas NC, Jacobs H, Bothwell AL, Hayday AC (2001). Defining the specific physiological requirements for c-Myc in T cell development. Nat Immunol 2:307-315.

Downward J (1992). Regulatory mechanisms for ras proteins. Bioessays 14:177-84.

Dragunow M, Xu R, Walton M, Woodgate A, Lawlor P, MacGibbon GA, Young D, Gibbons H, Lipski J, Muravlev A, Pearson A, During M (2000). c-Jun promotes neurite outgrowth and survival in PC12 cells. Brain Res Mol Brain Res 83:20-33.

Eberhardy SR, Farnham PJ (2001). c-Myc mediates activation of the cad promoter via a post-RNA polymerase II recruitment mechanism. J Biol Chem 276:48562-71.

Eberhardy SR, Farnham PJ (2002). Myc recruits P-TEFb to mediate the final step in the transcriptional activation of the cad promoter. J Biol Chem 277:40156-62.

Ebinu JO, Bottorff DA, Chan EY, Stang SL, Dunn RJ, Stone JC (1998). RasGRP, a Ras guanyl nucleotidereleasing protein with calcium- and diacylglycerol-binding motifs. Science 280:1082-6.

Eccleston JF, Moore KJ, Morgan L, Skinner RH, Lowe PN (1993). Kinetics of interaction between normal and proline 12 Ras and the GTPase-activating proteins, p120-GAP and neurofibromin. The significance of the intrinsic GTPase rate in determining the transforming ability of ras. J Biol Chem 268:27012-9.

Eilers AL, Billin AN, Liu J, Ayer DE (1999). A 13-amino acid amphipathic alpha-helix is required for the functional interaction between the transcriptional repressor Mad1 and mSin3A. J Biol Chem 274:32750-6.

Eischen CM, Woo D, Roussel MF, Cleveland JL (2001). Apoptosis triggered by Myc-induced suppression of Bcl-X(L) or Bcl-2 is bypassed during lymphomagenesis. Mol Cell Biol 21:5063-70.

Eisenman RN (2001). Deconstructing myc. Genes Dev 15:2023-30.

Evan GI, Wyllie AH, Gilbert CS, Littlewood TD, Land H, Brooks M, Waters CM, Penn LZ, Hancock DC (1992). Induction of apoptosis in fibroblasts by c-myc protein. Cell 69:119-28.

Facchini LM, Chen S, Marhin WW, Lear JN, Penn LZ (1997). The Myc negative autoregulation mechanism requires Myc-Max association and involves the c-myc P2 minimal promoter. Mol Cell Biol 17:100-14.

Facchini LM, Penn LZ (1998). The molecular role of Myc in growth and transformation: recent discoveries lead to new insights. FASEB J 12:633-51.

Faiola F, Liu X, Lo S, Pan S, Zhang K, Lymar E, Farina A, Martinez E (2005). Dual regulation of c-Myc by p300 via acetylation-dependent control of Myc protein turnover and coactivation of Myc-induced transcription. Mol Cell Biol 25:10220-34.

Fanidi A, Harrington EA, Evan G (1992). Cooperative interaction between c-myc and bcl2-proto-oncogenes. Nature 359:554-6.

Felsher DW, Bishop JM (1999). Transient excess of MYC activity can elicit genomic instability and tumorigenesis. Proc Natl Acad Sci USA 96:3940-4.

Felton-Edkins ZA, Kenneth NS, Brown TR, Daly NL, Gomez-Roman N, Grandori C, Eisenman RN, White RJ (2003). Direct regulation of RNA polymerase III transcription by RB, p53 and c-Myc. Cell Cycle. 2:181-4.

Feng XH, Liang YY, Liang M, Zhai W, Lin X (2002). Direct interaction of c-Myc with Smad2 and Smad3 to inhibit TGF-beta-mediated induction of the CDK inhibitor p15(Ink4B). Mol Cell 9:133-43.

Fernández PC, Frank SR, Wang L, Schroeder M, Liu S, Greene J, Cocito A, Amati B (2003). Genomic targets of the human c-Myc protein. Genes Dev 17:1115-29.

Finch A, Prescott J, Shchors K, Hunt A, Soucek L, Dansen TB, Swigart LB, Evan GI (2006). Bcl-xL gain of function and p19 ARF loss of function cooperate oncogenically with Myc in vivo by distinct mechanisms. Cancer Cell 10:113-20.

Flores I, Murphy DJ, Swigart LB, Knies U, Evan GI (2004). Defining the temporal requirements for Myc in the progression and maintenance of skin neoplasia. Oncogene 23:5923-30.

Freytag SO (1988). Enforced expression of the c-myc oncogene inhibits cell differentiation by precluding entry into a distinct predifferentiation state in G0/G1. Mol Cell Biol, 8, 1614-1624.

Freytag SO, Dang CV, Lee WM (1990). Definition of the activities and properties of c-myc required to inhibit cell differentiation. Cell Growth Differ 1:339-43.

Frye M, Gardner C, Li ER, Arnold I, Watt FM (2003). Evidence that Myc activation depletes the epidermal stem cell compartment by modulating adhesive interactions with the local microenvironment. Genes Dev 130:2793-2808.

Galaktionov K, Chen X, Beach D (1996). Cdc25 cell-cycle phosphatase as a target of c-myc. Nature 382:511-517.

Gandarillas A, Watt FM (1997). c-Myc promotes differentiation of human epidermal stem cells. Genes Dev 11:2869-82.

Gargano B, Amente S, Majello B, Lania L (2007). P-TEFb is a crucial co-factor for Myc transactivation. Cell Cycle 6:2031-37.

Gartel AL, Shchors K (2003). Mechanisms of c-myc-mediated transcriptional repression of growth arrest genes. Exp Cell Res 283:17-21.

Gavine PR, Neil JC, Crouch DH (1999). Protein stabilization: a common consequence of mutations in independently derived v-Myc alleles. Oncogene 18:7552-8.

Geiger H, Van Zant G (2002). The aging of lympho-hematopoietic stem cells. Nat Immunol 3:329-33.

Ghamari A, van de Corpout MPC, Thongjuea (2013). In vivo live imaging of RNA polymerase II transcription factories in primary cells. Genes Dev 27:767-777.

Gibbons RJ (2005). Histone modifying and chromatin remodelling enzymes in cancer and dysplastic syndromes. Hum Mol Genet 14:R85-92.

Gibbs JB, Sigal IS, Poe M, Scolnick EM (1984). Intrinsic GTPase activity distinguishes normal and oncogenic ras p21 molecules. Proc Natl Acad Sci USA 81:5704-8.

Gil J, Peters G (2006). Regulation of the INK4b-ARF-INK4a tumour suppressor locus: all for one or one for all. Nat Rev Mol Cell Biol 7:667-677.

Giuriato S, Ryeom S, Fan AC, Bachireddy P, Lynch RC, Rioth MJ, Vn Riggelen J, Kopelman Am, Passegue E, Tang F (2006). Sustained regression of tumors upon Myc inactivation requires p53 or thrombospondin-1 to reverse the angiogenic switch. Proc Natl Acad Sci USA 103:16266-71.

Göke J, Chan YS, Yan J, Vingron M, Ng HH (2013). Genome-wide Kinase-Chromatin Interactions Reveal the Regulatory Network of ERK Signaling in Human Embryonic Stem Cells. Mol Cell 50:844-55.

Gonda TJ, Metcalf D (1984). Expression of myb, myc and fos proto-oncogenes during the differentiation of a murine myeloid leukaemia. Nature 310:249-51.

Grandori C, Cowley SM, James LP, Eisenman RN (2000). The Myc/Max/Mad network and the transcriptional control of cell behavior. Annu Rev Cell Dev Biol 16:653-99.

Grandori C, Gomez-Roman N, Felton-Edkins ZA, Ngouenet C, Galloway DA, Eisenman RN, White RJ (2005). c-Myc binds to human ribosomal DNA and stimulates transcription of rRNA genes by RNA polymerase I. Nat Cell Biol 7:311-8.

Greene LA, Rukenstein A (1981). Regulation of acetylcholinesterase activity by nerve growth factor. Role of transcription and dissociation from effects on proliferation and neurite outgrowth. J Biol Chem 256:6363-7.

Greene LA, Tischler AS (1976). Establishment of a noradrenergic clonal line of rat adrenal pheochromocytoma cells which respond to nerve growth factor. Proc Natl Acad Sci USA 73:2424-8.

Grewal SS, Li L, Orian A, Einsenman RN, Edgar BA (2005). Myc-dependent regulation of ribosomal RNA synthesis during Drosophila development. Nat Cell Biol 7:295-302.

Grzenda A, Lomberk G, Zhang JS, Urrutia R (2009). Sin3: master scaffold and transcriptional corepressor. Biochim Biophys Acta 1789:443-50.

Guerrero I, Pellicer A, Burstein DE (1988). Dissociation of c-fos from ODC expression and neuronal differentiation in a PC12 subline stably transfected with an inducible N-ras oncogene. Biochem Biophys Res Commun 150:1185-92.

Guerrero I, Wong H, Pellicer A, Burstein DE (1986). Activated N-ras gene induces neuronal differentiation of PC12 rat pheochromocytoma cells. J Cell Physiol 129:71-6.

Guo QM, Malek RL, Kim S, Chiao C, He M, Ruffy M, Sanka K, Lee NH, Dang CV, Liu ET (2000). Identification of c-myc responsive genes using rat cDNA microarray. Cancer Res 60: 5922-5928.

Gupta S, Campbell D, Derijard B, Davis RJ (1995) Transcription factor ATF2 regulation by the JNK signal transduction pathway. Science 267:389-93.

Gupta S, Seth A, Davis RJ (1993). Transactivation of gene expression by Myc is inhibited by mutation at the phosphorylation sites Thr-58 and Ser-62. Proc Natl Acad Sci USA 90:3216-20.

Habib T, Park H, Tsang M, de Alborán IM, Nicks A, Wilson L, Knoepfler PS, Andrews S, Rawlings DJ, Eisenman RN, Iritani BM (2007). Myc stimulates B lymphocyte differentiation and amplifies calcium signaling. J Cell Biol 179:717-31.

Hanahan D, Weinberg RA (2000). Hallmarks of cancer: the next generation. Cell 144:646-74.

Hancock JF (2003). Ras proteins: different signals from different locations. Nat Rev Mol Cell Biol 4:373-84.

Hancock JF, Cadwallader K, Paterson H, Marshall CJ (1991). A CAAX or a CAAL motif and a second signal are sufficient for plasma membrane targeting of ras proteins. EMBO J. 10:4033-9.

Hancock JF, Paterson H, Marshall CJ (1990). A polybasic domain or palmitoylation is required in addition to the CAAX motif to localize p21ras to the plasma membrane. Cell 63:133-9.

Hann SR (2006). Role of post-translational modifications in regulating c-Myc proteolysis, transcriptional activity and biological function. Semin Cancer Biol 16:288-302.

Hann SR, Dixit M, Sears RC, Sealy L (1994). The alternatively initiated c-Myc proteins differentially regulate transcription through a noncanonical DNA-binding site. Genes Dev 8:2441-52.

Hann SR, King MW, Bentley DL, Anderson CW, Eisenman RN (1988). A non-AUG translational initiation in c-myc exon 1 generates an N-terminally distinct protein whose synthesis is disrupted in Burkitt's lymphomas. Cell 52:185-95.

Hann SR, Thompson CB, Eisenman RN (1985). c-myc oncogene protein synthesis is independent of the cell cycle in human and avian cells. Nature 314:366-9.

Hassig CA, Fleischer TC, Billin AN, Schreiber SL, Ayer DE (1997). Histone deacetylase activity is required for full transcriptional repression by mSin3A. Cell 89:341-7.

Hayflick L, Moorhead PS (1961). The serial cultivation of human diploid cell strains. Exp Cell Res 25:585-621.

Heikkila R, Schwab G, Wickstrom E, Loke SL, Pluznik DH, Watt R, Neckers LM (1987). A c-myc antisense oligodeoxynucleotide inhibits entry into S phase but not progress from G0 to G1. Nature 328:445-9.

Heinzel T, Lavinsky RM, Mullen TM, Söderstrom M, Laherty CD, Torchia J, Yang WM, Brard G, Ngo SD, Davie JR, Seto E, Eisenman RN, Rose DW, Glass CK, Rosenfeld MG (1997). A complex containing NCoR, mSin3 and histone deacetylase mediates transcriptional repression. Nature 387:43-8.

Henriksson M, Bakardjiev A, Klein G, Lüscher B (1993). Phosphorylation sites mapping in the N-terminal domain of c-myc modulate its transforming potential. Oncogene 8:3199-209.

Henriksson M, Lüscher B (1996). Proteins of the Myc network: essential regulators of cell growth and differentiation. Adv Cancer Res 68:109-82.

Herbst A, Hemann MT, Tworkowski KA, Salghetti SE, Lowe SW, Tansey WP (2005). A conserved element in Myc that negatively regulates its proapoptotic activity. EMBO Rep 6:177-83.

Hermeking H, Rago C, Schuhmacher M, Li Q, Barrett JF, Obaya AJ, O'Connell BC, Mateyak MK, Tam W, Kohlhuber F, Dang CV, Sedivy JM, Eick D, Vogelstein B, Kinzler KW (2000). Identification of CDK4 as a target of c-MYC. Proc Natl Acad Sci USA 97:2229-34.

Hochheimer A, Tjian R (2003). Diversified transcription initiation complexes expand promoter selectivity and tissue-specific gene expression. Genes Dev. 17:1309-20.

Hofer F, Fields S, Schneider C, Martin GS (1994). Activated Ras interacts with the Ral guanine nucleotide dissociation stimulator. Proc Natl Acad Sci USA 91:11089-93.

Hoffman B, Liebermann DA (1991). Suppression of c-myc and c-myb is tightly linked to terminal differentiation induced by IL6 or LIF and not growth inhibition in myeloid leukemia cells. Oncogene 6:903-909.

Hoffman B, Liebermann DA, Selvakumaran M, Nguyen HQ (1996). Role of c-myc in myeloid differentiation, growth arrest and apoptosis. Curr Top Microbiol Immunol 211:17-27.

Holt JT, Redner RL, Nienhuis AW (1988). An oligomer complementary to c-myc mRNA inhibits proliferation of HL-60 promyelocytic cells and induces differentiation. Mol Cell Biol 8:963-73.

Hopewell R, Ziff EB (1995). The nerve growth factor-responsive PC12 cell line does not express the Myc dimerization partner Max. Mol Cell Biol 15:3470-8.

Hu S, Xie Z, Onisi A, Yu X, Jiang L, Lin J, Rho HS, Woodard C, Wang H, Jeong JS, Long S, He X, Wade H, Blackshaw S, Qian J, Zhu H (2009). Profiling the human protein-DNA interactome reveals ERK2 as a transcriptional repressor of interferon signalling. Cell 139:610-22.

Hurlin PJ, Huang J (2006). The Max-interacting transcription factor network. Seminar cancer Biol 16:265-274.

Hurlin PJ, Zhou ZQ, Toyo-oka K, Ota S, Walker WL, Hirotsune S, Wynshaw-Boris A (2003). Deletion of Mnt leads to disrupted cell cycle control and tumorogenesis. EMBO J 22:4584-4596.

Iakova P, Awad SS, Timchenko NA (2003). Aging reduces proliferative capacities of liver by switching pathways of C/EBPalpha growth arrest. Cell 113:495-506.

Iritani BM, Eisenman RN (1999). c-Myc enhances protein synthesis and cell size during B lymphocyte development. Proc Natl Acad Sci USA 96:13180-5.

Izumi H, Molander C, Penn LZ, Ishisaki A, Kohno K, Funa K (2001). Mechanism for the transcriptional repression by c-Myc on PDGF beta-receptor. J Cell Sci 114:1533-44.

Jain M, Arvanitis C, Chu K, Dewey W, Leonhardt E, Trinh M, Sundberg CD, Bishop JM, Felsher DW (2002). Sustained loss of a neoplastic phenotype by brief inactivation of Myc. Science 297:102-4.

Jansen-Durr P, Meichle A, Steiner P, Pagano M, Finke K, Botz, J, Wessbecher J, Draetta G, Eilers M (1993). Differential modulation of cyclin gene expression by MYC. Proc Natl Acad Sci USA 90:3685-3689.

Jazayeri A, McAinsh AD, Jackson SP (2004). Saccharomyces cerevisiae Sin3p facilitates DNA doublestrand break repair. Proc Natl Acad Sci USA 101:1644-9.

Jin H, Kase J, Dorr JR (2011) Opposing roles of NFKB in anticancer treatment outcome unveiled by cross-species investigations, Genes Dev 25:2137-46.

Johansen LM, Iwama A, Lodie TA, Sasaki K, Felsher DW, Golub TR, Tenen DG (2001). c-Myc is a critical target for c/EBPalpha in granulopoiesis. Mol Cell Biol 21:3789-3806.

Johnson GL, Lapadat R (2002). Mitogen-activated protein kinase pathways mediated by Erk, JNK and p38 protein kinases. Science 298:1911-2.

Johnson GL, Vaillancourt RR (1994). Sequential protein kinase reactions controlling cell growth and differentiation. Curr Opin Cell Biol 6:230-8.

Johnston LA, Prober DA, Edgar BA, Eisenman RN, Gallant P (1999). Drosophila myc regulates cellular growth during development. Cell 98:779-90.

Jones CJ, Kipling D, Morris M, Hepburn P, SkinnerJ, Bounacer A, Wyllie FS, Ivan M, Bartek J, Wynford-Thomas D, Bond JA (2000). Evidence for a telomere-independent "clock" limiting RAS oncogene-driven proliferation of human thyroid epithelial cells. Mol Cell Biol 20:5690-5699.

Jones TR, Cole MD (1987). Rapid cytoplasmic turnover of c-myc mRNA: requirement of the 3' untranslated sequences. Mol Cell Biol 7:4513-21.

Juin P, Hunt A, Littlewood T, Griffits B, Swigart LB, Korsmeyer S, Evan G (2002). C-Myc functionally cooperates with Bax to induce apoptosis. Mol Cell Biol 22:6158-69.

Junttila MR, Li SP, Westermarck J (2008). Phosphatase-mediated crosstalk between MAPK signaling pathways in the regulation of cell survival. FASE J 22:954-65.

Kamamura S, Moriguchi T, Nishida E (1999). Activation of the protein kinase ERK5/BMK1 by receptor tyrosine kinases. Identification and characterization of a signalling pathway to the nucleus. J Biol Chem 274:26563-71.

Kanazawa S, Soucek L, Evan G, Okamoto T and Peterlin BM (2003). c-Myc recruits P-TEFb for transcription, cellular proliferation and apoptosis. Oncogene 22:5707-5711.

Karn J, Watson JV, Lowe AD, Green SM, Vedeckis W (1989). Regulation of cell cycle duration by c-myc levels. Oncogene 4:773-87.

Kasten MM, Dorland S, Stillman DJ (1997). A large protein complex containing the yeast Sin3p and Rpd3p transcriptional regulators. Mol Cell Biol 17:4852-8.

Kato GJ, Barrett J, Villa-Garcia M, Dang CV (1990). An amino-terminal c-myc domain required for neoplastic transformation activates transcription. Mol Cell Biol 10:5914-20.

Keld R, Guo B, Downey P, Cummins R, Gulmann C, Ang YS, Sharrocks AD (2011). PEA3/ETV4-related transcription factors coupled with active ERK signalling are associated with poor prognosis in gastric adenocarcinoma. Br J Cancer 105:124-30.

Kelly WG, Dahmus ME, Hart GW (1993). RNA polymerase II is a glycoprotein. Modification of the COOHterminal domain by O-GlcNAc. J Biol Chem May 268:10416-24.

Khokhlatchev AV, Canagarajah B, Wilsbacher J, Robinson M, Atkinson M, Goldsmith E, Cobb MH (1998). Phosphorylation of the MAP kinae ERK2 promotes its homodimerization and nuclear translocation. Cell 93:605-15.

Kim J, Chu J, Shen X, Wang J, Orkin SH (2008). An extended transcriptional network for pluripotency of embryonic stem cells. Cell 132:1049-61.

Kim S, Li Q, Dang CV, Lee LA (2000). Induction of ribosomal genes and hepatocyte hypertrophy by adenovirus-mediated expression of c-Myc in vivo. Proc Natl Acad Sci USA 97:11198-202.

Klappacher GW, Lunyak VV, Sykes DB, Sawka-Verhelle D, Sage J, Brard G, Ngo SD, Gangadharan D, Jacks T, Kamps MP, Rose DW, Rosenfeld MG, Glass CK (2002). An induced Ets repressor complex regulates growth arrest during terminal macrophage differentiation. Cell 109:169-80.

Kohl NE, Kanda N, Schreck RR, Bruns G, Latt SA, Gilbert F, Alt FW (1983). Transposition and amplification of oncogene-related sequences in human neuroblastomas. Cell 35:359-67.

Kretzner L, Blackwood EM, Eisenman RN (1992). Myc and Max proteins possess distinct transcriptional activities. Nature 359:426-9.

Krtolika A, Parrinello S, Lockett S, Desprez PY, Campisi J (2001). Senescent fibroblasts promote epithelial cell growth and tumorigenesis: A link between cancer and aging. Proc Natl Acad Sci USA 98:12072-7.

Kuilman T, Michaloglou C, Vredeveld CW, Douma S, van Doorn R, Desmet CJ, Aarden LA, Mooi WJ, Peeper DS (2008). Oncogene-induced senescence relayed by an interleukin-dependent inflammatory network. Cell 133:1019-31.

Kuilman T, Michaloglou C, Mooi WJ, Peeper DS (2010). The essence of senescence. Genes Dev 24:2463-79.

Kuilman T, Peeper DS (2009). Senescence-messaging secretome: SMS-ing cellular stress. Nat rev Cancer 9:81-94.

Kuo MH, Allis CD (1998). Roles of histone acetyltransferases and deacetylases in gene regulation. Bioessays 20:615-26.

Kurland JF, Tansey WP (2008). Myc-mediated transcriptional repression by recruitment of histone deacetylase. Cancer Res 68:3624-9.

Lachman HM, Skoultchi AI (1984). Expression of c-Myc changes during differentiation of mouse erythroleukaemia cells. Nature 310:592-4.

Laherty CD, Yang WM, Sun JM, Davie JR, Seto E, Eisenman RN (1997). Histone deacetylases associated with the mSin3 corepressor mediate mad transcriptional repression. Cell 89:349-56.

Lai CF, Chaudhary L, Fausto A, Halstead LR, Ory DS, Avioli LV, Cheng SL (2001). Erk is essential for growth, differentiation, integrin expression, and cell function in human osteoblastic cells. J Biol Chem 276:14443-50

Landschulz WH, Johnson PF, McKnight SL (1988). The leucine zipper: a hypothetical structure common to a new class of DNA binding proteins. Science 240:1759-64.

Larochelle S, Amat R, Glover-Cutter K, Sanso M, Zhang C, Allen JJ, Shokat KM, Bentley DL, Fisher RP (2012). Cyclin-dependent kinase control of the initiation-to-elongation switch of RNA polymerase II. Nat Struc Molec Biol 19:1108-15.

Larsson LG, Ivhed I, Gidlund M, Pettersson U, Vennstrom B, Nilsson K (1988). Phorbol esterinduced terminal differentiation is inhibited in human U-937 monoblastic cells expressing a v-myc oncogene. Proc Natl Acad Sci USA 852638-2642.

Larsson LG, Pettersson M, Oberg F, Nilsson K, Lüscher B (1994). Expression of mad, mxi1, max and cmyc during induced differentiation of hematopoietic cells: opposite regulation of mad and c-myc. Oncogene 9:1247-52.

Latchman DS (1998). The Brn-3a transcription factor. Int J Biochem Cell Biol 30:1153-7.

Lawlor ER, Soucek L, Brown-Swigart L, Shchors K, Bialucha CU, Evan GI (2006). Reversible kinetic analysis of Myc targets in vivo provides novel insights into Myc-mediated tumorigenesis. Cancer Res 66:4591-4601.

Lazzerini DE, Attwooll C, Pasini D, Helin K (2005). Deregulated E2F activity induces hyperplasia and senescence-like features in the mouse pituitary gland. Mol Cell Biol 25:2660-72.

Lee CH, Leeds P, Ross J (1998). Purification and characterization of a polysome-associated endoribonuclease that degrades c-myc mRNA in vitro. J Biol Chem 273:25261-71.

Lee JD, Ulevitch RJ, Han J (1995). Primary structure of BMK1: a new mammalian map kinase. Biochem Biophys Res Commun 213:715.24.

Lemaitre JM, Buckle RS, Mechali M (1996). c-Myc in the control of cell proliferation and embryonic development. Adv Cancer Res 70:95-144.

León J, Ferrandiz N, Acosta JC, Delgado MD (2009). Inhibition of cell differentiation: a critical mechanism for MYC-mediated carcinogenesis? Cell Cycle 8:1148-57.

Leppä S, Saffrich R, Ansorge W, Bohmann D (1998). Differential regulation of c-Jun by ERK and JNK during PC12 cell differentiation. EMBO J 17:4404-13.

Levens DL (2003). Reconstructing MYC. Genes Dev 17:1071-1077.

Li B, Simon MC (2013). Molecular Pathways: Targeting MYC-induced Metabolic Reprogramming and Oncogenic Stress in Cancer. Clin Cancer Res.

Li C, Wong WH (2001). Model-based analysis of oligonucleotide arrays: Expression index computation and outlier detection. Proc Natl Acad Sci USA 98:31-36.

Li LH, Nerlov C, Prendergast G, MacGregor D, Ziff EB (1994). c-Myc represses transcription in vivo by a novel mechanism dependent on the initiator element and Myc box II. EMBO J 13:4070-9.

Li YJ, Fu XH, Liu DP, Liang CC (2004). Opening the chromatin for transcription. Int J Biochem Cell Biol 36:1411-23.

Li Z, Van Calcar S, Qu C, Cavenee WK, Zhang MQ, Ren B (2003). A global transcriptional regulatory role for c-Myc in Burkitt's lymphoma. Proc Natl Acad Sci USA 100:8164-9.

Lin AW, Lowe SW (2001). Oncogenic ras activates the ARF-p53 pathway to suppress epithelial cell transformation. Proc Natl Acad Sci USA 98:5025-5030.

Lin CY, Loven J, Rahl PB (2012). Transcriptional amplification in tumor cells with elevated c-Myc. Cell 151:56-67.

Lin CY, Loven J, Rahl PB, Paranal RM, Burge CB, Bradner JE, Lee TI, Young RA (2012). Transcriptional Amplification in Tumor Cells with Elevated c-Myc. Cell 151:56-67.

Littlewood TD, Amati B, Land H Evan GI (1992). Max and c-Myc/Max DNA-binding activities in cell extracts. Oncogene 7:1783-1792.

Liu J, Kouzine F, Nie Z, Chung HJ, Elisha-Feil Z, Weber A, Zhao K, Levens D (2006). The FUSE/FBP/FIR/TFIIH system is a molecular machine programming a pulse of c-myc expression. EMBO J 25:2119-30.

Lowe SW, Sherr CJ (2003). Tumor suppression by Ink4a-Arf: progress and puzzles. Curr Opin Genet Dev 13:77-83.

Lowry WE, Richter L, Yachechko R, Pyle AD, Tchieu J, Sridharan R (2008). Generation of human induced pluripotent stem cells from dermal fibroblasts. Proc Natl Acad Sci USA 105:2883-8.

Lowy DR, Willumsen BM (1993). Function and regulation of ras. Annu Rev Biochem 62:851-91.

Luo Q, Li J, Cenkci B, Kretzner L (2004). Autorepression of c-myc requires both initiator and E2F-binding site elements and cooperation with the p107 gene product. Oncogene 23:1088-97.

Lüscher B (2001). Function and regulation of the transcription factors of the Myc/Max/Mad network. Gene 277:1-14.

Lüscher B, Larsson LG (1999). The basic region/helix-loop-helix/leucine zipper domain of Myc protooncoproteins function and regulation. Oncogene 18:2955-66.

Lutterbach B, Hann SR (2004). c-Myc transactivation domain-associated kinases: questionable role for map kinases in c-Myc phosphorylation. J Cell Biochem 72:483-91.

Ma S, Martensson IL (1995). The c-myc protein represses the lambda 5 and TdT initiators. Nucleic Acids Res 23:1-9.

Maclean KH, Keller UB, Rodriguez-Galindo C, Nilsson JA, Cleveland JL (2003). c-Myc augments gamma irradiation-induced apoptosis by suppressing Bcl-XL. Mol Cell Biol 23:7256-70.

Malumbres M, Barbacid M (2003). Ras oncogenes: the first 30 years. Nat Rev Cancer 3:7-13.

Manning G, Whyte DB, Martinez T, Hunter T, Sudarsanam S (2002) The protein kinase complement of the human genome. Science 265:966-70.

Marchetti A, Abril-Marti M, Illi B, Cesareni G, Nasi S (1995). Analysis of the Myc and Max interaction specificity with lambda repressor-HLH domain fusions. J Mol Biol 248:541-50.

Marcu KB, Bossone SA, Patel AJ (1992). Myc function and regulation. Annu Rev Biochem 61, 809-860.

Margaritis T, Holstege FCF (2008). Poised RNA Polymerase II Gives Pause for Thought. Cell 133:581-4.

Marhin WW, Chen S, Facchini LM, Fornace AJ Jr, Penn LZ (1997). Myc represses the growth arrest gene gadd45. Oncogene 14:2825-34.

Marshall CJ (1995). Specificity Of receptor tyrosine kinase signaling: transient versus sustained extracellular signal-regulated kinase activation. Cell 80:179-85.

Marshall NF, Peng J, Xie Z, Price DH (1996). Control of RNA polymerase II elongation potential by a novel carboxyl-terminal domain kinase. J Biol Chem 271:27176-83.

Martin GA, Viskochil D, Bollag G, McCabe PC, Crosier WJ, Haubruck H, Conroy L, Clark R, O'Connell P, Cawthon RM, Innis MA, McCoemick F (1990). The GAP-related domain of the neurofibromatosis type 1 gene product interacts with ras p21. Cell 63:843-9.

Martinon F, Burns K, Tschopp J (2002). The inflammasome: a molecular platform triggering activation of inflammatory caspases and processing of proIL-beta. Mol Cell 10:417-426.

Mason DX, Jackson TJ, Lin AW (2004). Molecular signature of oncogenic rasinduced senescence. Oncogene 23:9238-46.

Mason SA, Cozzi SJ, Pierce CJ, Pavey SJ, Parsons PG, Boyle GM (2009). The induction of senescence-like growth arrest by protein kinase C-activating diterpene esters in solid tumor cells. Invest New Drugs 28:575-86.

Mateyak MK, Obaya AJ, Adachi S, Sedivy JM (1997). Phenotypes of c-Myc-deficient rat fibroblasts isolated by targeted homologous recombination. Cell Growth Differ 8:1039-48.

McGrath JP, Capon DJ, Goeddel DV, Levinson AD (1984). Comparative biochemical properties of normal and activated human ras p21 protein. Nature 310:644-9.

McMahon SB, Van Buskirk HA, Dugan KA, Copeland TD, Cole MD (1998). The novel ATM-related protein TRRAP is an essential cofactor for the c-Myc and E2F oncoproteins. Cell 94:363-74.

McMahon SB, Wood MA, Cole MD (2000). The essential cofactor TRRAP recruits the histone acetyltransferase hGCN5 to c-Myc. Mol Cell Biol 20:556-62.

Menssen A, Hermeking H (2002). Characterization of the c-MYC-regulated transcriptome by SAGE: identification and analysis of c-MYC target genes. Proc Natl Acad Sci USA 99:6274-9.

Menssen A, Hydbring P, Kapelle K, Vervoorts J, Diebold J, Luscher B, Larsson LG, Hermeking H (2012).The c-MYC oncoprotein, the NAMPT enzyme, the SIRT1-inhibitor DBC1, and the SIRT1 deacetylase form a positive feedback loop. Proc Natl Acad Sci USA 109:E187-96.

Meyer N, Kim SS, Penn LZ (2006). The Oscar-worthy role of Myc in apoptosis. Semin Cancer Biol 16:275-87.

Mezquita P, Parghi SS, Brandvold KA, Ruddell A (2005). Myc regulates VEGF production in B cells by stimulating initiation of VEGF mRNA translation. Oncogene 24:889-901.

Michaloglou C, Vredeveld LC, Soengas MS, Denoyelle C, Kuilman T, van der Horst CM, Majoor DM, Shay JW, Mooi WJ, Peeper DS (2005). BRAFE600-associated senescence-like cell cycle arrest of human naevi. Nature 436:720-724.

Miltenberger RJ, Sukow KA, Farnham PJ (1995). An E-box-mediated increase in cad transcription at the G1/S-phase boundary is suppressed by inhibitory c-Myc mutants. Mol Cell Biol 15:2527-35.

Morgenbesser SD, DePinho RA (1994). Use of transgenic mice to study myc family gene function in normal mammalian development and in cancer. Semin Cancer Biol 5:21-36.

Morrish F, Hockenbery D (2003). Myc's mastery of mitochondrial mischief. Cell Cycle 2:11-13.

Muñoz A, Wrighton C, Seliger B, Bernal J, Beug H (1993). Thyroid hormone receptor/c-erbA: control of commitment and differentiation in the neuronal/chromaffin progenitor line PC12. J Cell Biol 121:423-38.

Murre C, McCaw PS, Vaessin H, Caudy M, Jan LY, Jan YN, Cabrera CV, Buskin JN, Hauschka SD, Lassar AB (1989). Interactions between heterologous helix-loop-helix proteins generate complexes that bind specifically to a common DNA sequence. Cell 58:537-44.

Nagy L, Kao HY, Chakravarti D, Lin RJ, Hassig CA, Ayer DE, Schreiber SL, Evans RM (1997). Nuclear receptor repression mediated by a complex containing SMRT, mSin3A, and histone deacetylase. Cell 89:373-80.

Nair SK, Burley SK (2003). X-ray structures of Myc-Max and Mad-Max recognizing DNA. Molecular bases of regulation by proto-oncogenic transcription factors. Cell 112:193-205.

Nair SK, Burley SK (2006). Structural aspects of interactions within the Myc/Max/Mad network. Curr Top Microbiol Immunol 302, 123-43.

Nan X, Ng HH, Johnson CA, Laherty CD, Turner BM, Eisenman RN, Bird A (1998). Transcriptional repression by the methyl-CpG-binding protein MeCP2 involves a histone deacetylase complex. Nature 393:386-9.

Narita M, Nunez S, Heard E, Narita M, Lin AW, Hearn SA, Spector DL, Hannon GJ, Lowe SW (2003). Rb-mediated heterochromatin formation and silencing of E2F target genes during cellular senescence. Cell 113:703-716.

Nascimento EM, Cox CL, MacArthur S, Hussain S, Matthew T, Blanco S, Fryw M (2011). The opposing transcriptional functions of Sin3a and c-Myc are required to maintain tissue homeostasis. Nat Cell Biol 13:1395-1405.

Nau MM, Brooks BJ, Battey J, Sausville E, Gazdar AF, Kirsch IR, McBride OW, Bertness V, Hollis GF, Minna JD (1985). L-myc, a new myc-related gene amplified and expressed in human small cell lung cancer. Nature 318:69-73.

Nesbit CE, Tersak JM, Prochownik EV (1999). MYC oncogenes and human neoplastic disease. Oncogene 18:3004-16.

Nie Z, Hu G, Wei G, Cui K, Yamane A, Resch W, Wang R, Green DR, Tessarollo L, Casellas R (2012). c-Myc Is a Universal Amplifier of Expressed Genes in Lymphocytes and Embryonic Stem Cells. Cell 151:68-79.

Nilsson JA, Maclean KH, Keller UB, Pendeville H, Baudino TA, Cleveland JL (2004). Mnt loss triggers Myc transcription targets, proliferation, apoptosis and transformation. Mol Cell Biol 24:1560-69.

O'Connell BC, Cheung AF, Simkevich CP, Tam W, Ren X, Mateyak MK, Sedivy JM (2003). A large scale genetic analysis of c-Myc-regulated gene expression patterns. J Biol Chem 278:12563-73.

Ogawa H, Ishiguro K, Gaubatz S, Livingston DM, Nakatani Y (2002). A complex with chromatin modifiers that occupies E2F- and Myc-responsive genes in G0 cells. Science 296:1132-6.

O'Hagan RC, Ohh M, David G, de Alboran IM, Alt FW, Kaelin WG Jr, DePinho RA (2000). Mycenhanced expression of Cul1 promotes ubiquitin-dependent proteolysis and cell cycle progression. Genes Dev 14:2185-91.

Okita K, Ichisaka T, Yamanaka S (2007). Generation of germline-competent induced pluripotent stem cells. Nature 448:313-7.

Olsen CL, Gardie B, Yaswen P, Stampfer MR (2002). Raf-1-induced growth arrest in human mammary epithelial cells is p16-independent and is overcome in immortal cells during conversion. Oncogene 21:6328-39.

Orjalo AV, Bhaumik D, Gengler BK, Scott GK, Campisi J (2009). Cell surface-bound IL-1alpha is an upstream regulator of the senescence-associated IL-6/IL-8 cytokine network. Proc Natl Acad Sci USA 106:17031-6.

Oster SK, Ho CS, Soucie EL, Penn LZ (2002). The myc oncogene: MarvelouslY Complex. Adv Cancer Res 84:81-154.

Oster SK, Mao DY, Kennedy J, Penn LZ (2003). Functional analysis of the N-terminal domain of the Myc oncoprotein. Oncogene 22:1998-2010.

Osthus RC, Shim H, Kim S, Li Q, Reddy R, Mukherjee M, Xu Y, Wonsey D, Lee LA, Dang CV (2000). Deregulation of glucose transporter 1 and glycolytic gene expression by c-Myc. J Biol Chem 275: 21797-800.

Palmer TD, Schwartz PH, Taupin P, Kaspar B, Stein SA, Gage FH (2001). Cell culture. Progenitor cells from human brain after death. Nature 411:42-3.

Parada LF, Land H, Weinberg RA, Wolf D, Rotter V (1984). Cooperation between gene encoding p53 tumour antigen and ras in cellular transformation. Nature 312:649-651.

Park DS, Razani B, Lasorella A, Schreiber-Agus N, Pestell RG, Iavarone A, Lisanti MP (2001). Evidence that Myc isoforms transcriptionally repress caveolin-1 gene expression via an INR-dependent mechanism. Biochem 40:3354-62.

Park IH, Zhao R, West JA, Yabuuchi A, Huo H, Ince TA (2008). Reprogramming of human somatic cells to pluripotency with defined factors. Nature 451:141-6.

Patel JH, Du Y, Ard PG, Phillips C, Carella B, Chen CJ, Rakowski C, Chatterjee C, Lieberman PM, Lane WS, Blobel GA, McMahon SB (2004). The c-MYC oncoprotein is a substrate of the acetyltransferases hGCN5/PCAF and TIP60. Mol Cell Biol 24:10826-34.

Patel JH, Loboda AP, Showe MK, Showe LC, McMahon SB (2004). Analysis of genomic targets reveals complex functions of MYC. Nat Rev Cancer 4:562-8.

Pelengaris S, Abouna S, Cheung L, Ifandi V, Zervou S and Khan M (2004). Brief inactivation of c-myc is not sufficient for sustained regression of c-myc-induced tumours of pancreatic islets and skin epidermis. BMC Biol 2:26.

Persson H, Hennighausen L, Taub R, DeGrado W, Leder P (1984). Antibodies to human c-myc oncogene product: evidence of an evolutionarily conserved protein induced during cell proliferation. Science 225:687-93.

Peterlin BM, Price DH (2006). Controlling the elongation phase of transcription with P-TEFb. Mol Cell 23:297-305.

Pham N, Cheglakov I, Koch CA, de Hoog CL, Moran MF, Rotin D (2000). The guanine nucleotide exchange factor CNrasGEF activates ras in response to cAMP and cGMP. Curr Biol 10:555-8.

Popov N, Wahlstrom T, Hurlin PJ, Henriksson M (2005). Mnt transcriptional repressor is functionally regulated during cell cycle progression. Oncogene 24:8326-37.

Prendergast GC and Ziff EB (1989). DNA-binding motif. Nature 341:392.

Prendergast GC, Lawe D, Ziff EB (1991). Association of Myn, the murine homolog of max, with c-Myc stimulates methylation-sensitive DNA binding and ras cotransformation. Cell 65:395-407.

Prendergast GC, Ziff EB (1992). A new bind for Myc. Trends in genetics 8:91-96.

Prior IA, Hancock JF (2001). Compartmentalization of Ras proteins. J Cell Sci 114:1603-8.

Prokipcak RD, Herrick DJ, Ross J (1994). Purification and properties of a protein that binds to the C-terminal coding region of human c-myc mRNA. J Biol Chem 269:9261-9.

Ptashne M, Gann A (1997). Transcriptional activation by recruitment. Nature 386:569-77.

Pylayeva-Gupta, Grabocka E, Bar-sagi D (2011). RAS oncogenes: weaving a tumorigenic web. Nat Rev Cancer 11:761-74.

Quinlan AR, Hall IM (2010). BEDTools: a flexible suite of utilities for comparing genomic features. Bioinformatics 26:841-842.

Rabbitts PH, Watson JV, Lamond A, Forster A, Stinson MA, Evan G, Fisher W, Atherton E, Sheppard R (1985) Metabolism of c-myc gene products: c-myc mRNA and protein expression in the cell cycle. Embo J 4, 2009-15.

Rahl PB, Lin CY, Seila AC, Flynn RA, McCuine S, Burge CB, Sharp PA, Young RA (2010). c-Myc regulates transcriptional pause release. Cell. 141:432-45.

Rao G, Alland L, Guida P, Schreiber-Agus N, Chen K, Chin L, Rochelle JM, Seldin MF, Skoultchi AI, DePinho RA (1996). Mouse Sin3A interacts with and can functionally substitute for the amino-terminal repression of the Myc antagonist Mxi1. Oncogene 12:1165-72.

Rayman JB, Takahashi Y, Indjeian VB, Dannenberg JH, Catchpole S, Watson RJ, te Riele H, Dynlacht BD (2002). E2F mediates cell cycle-dependent transcriptional repression in vivo by recruitment of an HDAC1/mSin3B corepressor complex. Genes Dev 16:933-47.

Ribon V, Leff T, Saltiel AR (1994). c-Myc does not require max for transcriptional activity in PC-12 cells. Mol Cell Neurosci 5:277-82.

Rodríguez J, Calvo F, Gonzalez JM, Casar B, Andrés V, Crespo P (2010). ERK1/2 MAP kinases promote cell cycle entry by rapid, kinase-independent disruption of retinoblastoma–lamin A complexes. J Cel Biol 191:967-979.

Rodriguez-Viciana P, Warne PH, Khwaja A, Marte BM, Pappin D, Das P, Waterfield MD, Ridley A, Downward J (1997). Role of phosphoinositide 3-OH kinase in cell transformation and control of the actin cytoskeleton by Ras. Cell 89:457-67.

Rosenwald IB, Rhoads DB, Callanan LD, Isselbacher KJ, Schmidt EV (1993). Increased expression of eukaryotic translation initiation factors eIF-4E and eIF-2 alpha in response to growth induction by c-myc. Proc Natl Acad Sci USA 90:6175-78.

Roussel MF, Cleveland JL, Shurtleff SA, Sherr CJ (1991). Myc rescue of a mutant CSF-1 receptor impaired in mitogenic signalling. Nature 353:361-3.

Roy AL, Carruthers C, Gutjahr T, Roeder RG (1993). Direct role for Myc in transcription initiation mediated by interactions with TFII-I. Nature 365:359-61.

Sakamuro D, Eviner V, Elliott KJ, Showe L, White E, Prendergast GC (1995). c-Myc induces apoptosis in epithelial cells by both p53-dependent and p53-independent mechanisms. Oncogene 11:2411-8.

Sakamuro D, Prendergast GC (1999). New Myc-interacting proteins: a second Myc network emerges. Oncogene 18:2942-54.

Salghetti SE, Kim SY, Tansey WP (1999). Destruction of Myc by ubiquitin-mediated proteolysis: cancer associated and transforming mutations stabilize Myc. EMBO J 18:717-26.

Sarkisian CJ, Keister BA, Stairs DB, Boxer RB, Moody SE, Chodosh LA (2007). Dose-dependent oncogene-induced senescence in vivo and its evasion during mammary tumorigenesis. Nat Cell Biol 9:493-505.

Schlosser I, Hölzel M, Mürnseer M, Burtscher H, Weidle UH, Eick D (2003). A role for c-Myc in the regulation of ribosomal RNA processing. Nucleic Acids Res 31:6148-56.

Schreiber-Agus N, Chin L, Chen K, Torres R, Rao G, Guida P, Skoultchi AI, DePinho RA (1995). An amino-terminal domain of Mxi1 mediates anti-Myc oncogenic activity and interacts with a homolog of the yeast transcriptional repressor SIN3. Cell 80:777-86.

Schroder K, Tschopp J (2010). The inflammasomes. Cell 140:821-32.

Schuhmacher M, Kohlhuber F, Holzel M, Kaiser C, Burtscher H, Jarsch M, Bornkamm GW, Laux G, Polack A, Weidle UH, Eick D (2001). The transcriptional program of a human B cell line in response to Myc. Nucleic Acids Res 29:397-406.

Sears R, Nuckolls F, Haura E, Taya Y, Tamai K, Nevins JR (2000). Multiple Ras-dependent phosphorylation pathways regulate Myc protein stability. Genes Dev 14:2501-14.

Sears RC (2004). The life cycle of C-myc: from synthesis to degradation. Cell Cycle 3:1133-7.

Seoane J, Le HV, Massague J (2002). Myc suppression of the p21(Cip1) Cdk inhibitor influences the outcome of the p53 response to DNA damage. Nature 419:729-34.

Seoane J, Pouponnot C, Staller P, Schader M, Eilers M, Massagué J (2001). TGFbeta influences Myc, Miz-1 and Smad to control the CDK inhibitor p15INK4b. Nat Cell Biol 3:400-8.

Serrano M, Lin AW, McCurrach ME, Beach D, Lowe SW (1997). Oncogenic ras provokes premature cell senescence associated with accumulation of p53 and p16INK4a. Cell 88:593-602.

Serrano M, Blasco MA (2001).Putting the stress on senescence. Curr Opin Cell Biol. 14:123.

Shachaf CM, Kopelman AM, Arvanitis C, Karlsson A, Beer S, Mandl S, Bachmann MH, Borowsky AD, Ruebner B, Cardiff RD (2004). Myc inactivation uncovers pluripotent differentiation and tumour dormancy in hepatocellular cancer. Nature 431:1112-7.

Shay JW, Roninson IB (2004). Hallmarks of senescence in carcinogenesis and cancer therapy. Oncogene 23:2919-33.

Sheiness D, Bishop JM (1979). DNA and RNA from uninfected vertebrate cells contain nucleotide sequences related to the putative transforming gene of avian myelocytomatosis virus. J Virol 31: 514-21.

Shelton DN, Chang E, Whittier PS, Choi D, Funk WD (1999). Microarray analysis of replicative senescence. Curr Biol 9:939-45.

Shi Y, Glynn JM, Guilbert LJ, Cotter TG, Bissonnette RP, Green DR (1992). Role for c-myc in activationinduced apoptotic cell death in T cell hybridomas. Science 257:212-4.

Shields JM, Pruitt K, McFall A, Shaub A, Der CJ (2000). Understanding Ras: 'it ain't over 'til it's over'. Trends Cell Biol 10:147-54.

Shrivastava A, Saleque S, Kalpana GV, Artandi S, Goff SP, Calame K (1993). Inhibition of transcriptional regulator Yin-Yang-1 by association with c-Myc. Science 262:1889-92.

Silverstein RA, Ekwall K (2005). Sin3: a flexible regulator of global gene expression and genome stability. Curr Genet 47:1-17.

Soucie EL, Annis MG, Sedivy J, Filmus J, Leber B, Andrews DW, Penn LZ (2001). Myc potentiates apoptosis by stimulating Bax activity at the mitochondria. Mol Cell Biol 21:4725-36.

Spencer CA, Groudine M (1991). Control of c-myc regulation in normal and neoplastic cells. Adv Cancer Res 56:1-48.

Spotts GD, Patel SV, Xiao Q, Hann SR (1997). Identification of downstream-initiated c-Myc proteins which are dominant-negative inhibitors of transactivation by full-length c-Myc proteins. Mol Cell Biol 17:1459-68.

Staller P, Peukert K, Kiermaier A, Seoane J, Lukas J, Karsunky H, Möröy T, Bartek J, Massagué J, Hänel F, Eilers M (2001). Repression of p15INK4b expression by Myc through association with Miz-1. Nat Cell Biol 3:392-9.

Steiner P, Philipp A, Lukas J, Godden-Kent D, Pagano M, Mittnacht S, Bartek J, Eilers M (1995). Identification of a Myc-dependent step during the formation of active G1 cyclin-cdk complexes. EMBO J 14:4814-26.

Stone J, de Lange T, Ramsay G, Jakobovits E, Bishop JM, Varmus H, Lee W (1987). Definition of regions in human c-myc that are involved in transformation and nuclear localization. Mol Cell Biol 7:1697-709.

Strasser A, Harris AW, Bath ML, Cory S (1990). Novel primitivr lymphoid tumours induced in transgenic mice by cooperation between myc and bcl-2. Nature 348:331-3.

Sudo T, Yagasaki Y, Hama H, Watanable N, Osada H (2002). Exip, a new alternative splicing variant of p38 alpha, can induce an earlier onset of apoptosis in HeLa cells. Biochem Biophys Res Commun 291:838-43.

Sun Y, Xu Y, Roy K, Price BD (2007). DNA damage induced acetylation of lysine 3016 of ATM activates ATM kinase activity. Molec Cell Biol 27:8502-8509.

Suojun Z, Feng W, Dongsheng G, Ting L (2012). Targeting Raf/MEK/ERK pathway in pituitary adenomas. Eur J Cancer 48:389-95.

Sweet RW, Yokoyama S, Kamata T, Feramisco JR, Rosenberg M, Gross M (1984). The product of ras is a GTPase and the T24 oncogenic mutant is deficient in this activity. Nature 311:273-5.

Tabin CJ, Bradley SM, Bargmann CI, Weinberg RA, Papageorge AG, Scolnick EM, Dhar R, Lowy DR, Chang EH (1982). Mechanism of activation of a human oncogene. Nature 300:143-9.

Takahashi K, Tanabe K, Ohnuki M, Narita M, Ichisaka T, Tomoda K, Yamanaka S (2007). Induction of pluripotent stem cells from adult human fibroblasts by defined factors. Cell 131:861-72.

Tao H, Umek RM (1999). Reciprocal regulation of gadd45 by C/EBP alpha and c-Myc. DNA Cell Biol 18:75-84.

Taub R, Kirsch I, Morton C, Lenoir G, Swan D, Tronick S, Aaronson S, Leder P (1982). Translocation of the c-myc gene into the immunoglobulin heavy chain locus in human Burkitt lymphoma and murine plasmacytoma cells. Proc Natl Acad Sci USA 79:7837-41.

Thompson CB, Challoner PB, Neiman PE, Groudine M (1985). Levels of c-myc oncogene mRNA are invariant throughout the cell cycle. Nature 314:363-6.

Thomson TM, Green SH, Trotta RJ, Burstein DE, Pellicer A (1990). Oncogene N-ras mediates selective inhibition of c-fos induction by nerve growth factor and basic fibroblast growth factor in a PC12 cell line. Mol Cell Biol 10:1556-63.

Toyo-oka, Bowen TJ, Hirotsune S, Li Z, Jain S, Ota S, Escoubet-Lozach L, Garcia-Bassets I, Lozach J, Rosenfeld MG (2006). Mnt-deficient mammary glands exihibit impaired involution and tumors with caracteristics of myc overexpression. Cancer research 66:5565-73.

Trapnell C (2009). TopHat: discovering splice junctions with RNA-Seq. Bioinformatics 25:1105-11.

Trougakos IP, Saridaki A, Panayotou G, Gonos ES (2006). Identification of differentially expressed proteins in senescent human embryonic fibroblasts. Mech Ageing Dev 127:88-92

Vafa O, Wade M, Kern S, Beeche M, Pandita TK, Hampton GM, Wahl GM (2002). c-Myc can induce DNA damage, increase reactive oxygen species, and mitigate p53 function: a mechanism for oncogene-induced genetic instability. Mol Cell 9:1031-44.

van Ingen H, Baltussen MA, Aelen J, Vuister GW (2006). Role of structural and dynamical plasticity in Sin3: the free PAH2 domain is a folded module in mSin3B. J Mol Biol 358:485-97.

van Ingen H, Lasonder E, Jansen JF, Kaan AM, Spronk CA, Stunnenberg HG, Vuister GW (2004). Extension of the binding motif of the Sin3 interacting domain of the Mad family proteins. Biochemistry 43:46-54.

Vannier D, Balderes D, Shore D (1996). Evidence that the transcriptional regulators SIN3 and RPD3, and a novel gene (SDS3) with similar functions, are involved in transcriptional silencing in S. cerevisiae. Genetics 144:1343-53.

Vaqué JP, Fernández-García B, García-Sanz P, Ferrandiz N, Bretones G, Calvo F, Crespo P, Marín MC, León J (2008). c-Myc inhibits Ras-mediated differentiation of pheochromocytoma cells by blocking c-Jun up-regulation. Mol Cancer Res 6:325-39.

Vaqué JP, Navascues J, Shiio Y, Laiho M, Ajenjo N, Mauleón I, Matallanas D, Crespo P, León J (2005). Myc antagonizes Ras-mediated growth arrest in leukemia cells through the inhibition of the Ras-ERK-p21Cip1 pathway. J Biol Chem 280:1112-22.

Vaux DL, Cory S, Adams JM (1988). Bcl2 gene promoters haemopoietic cell survival and cooperates with c-myc to immortalize pre-B cells. Nature 335:440-2.

Vavvas D, Li X, Avruch J, Zhang XF (1998). Identification of Nore1 as a potential Ras effector. J Biol Chem 273:5439-42.

Vennström B, Bishop JM (1982). Isolation and characterization of chicken DNA homologous to the two putative oncogenes of avian erythroblastosis virus. Cell 28:135-43.

Vennström B, Sheiness D, Zabielski J, Bishop JM (1982). Isolation and characterization of c-myc, a cellular homolog of the oncogene (v-myc) of avian myelocytomatosis virus strain 29. J Virol 42:773-9.

Vervoorts J, Luscher-Firzlaff JM, Rottmann S, Lilischkis R, Walsemann G, Dohmann K, Austen M, Luscher B (2003).Stimulation of c-MYC transcriptional activity and acetylation by recruitment of the cofactor CBP. EMBO Rep 4:484-90.

Vidal M, Strich R, Esposito RE, Gaber RF (1991). RPD1 (SIN3/UME4) is required for maximal activation and repression of diverse yeast genes. Mol Cell Biol 11:6306-16.

Vita M, Henriksson M (2006). The myc oncoprotein as a therapeutic target for human cancer. Semin Cancer Biol 16:318-30.

Von Kriegsheim A, Baiocchi D, Birtwistle M, Sumpton D, Bienvenut W, Morrice N, Yamada K, Lamond A, Kalna G, Ortonv R, Gilbert D and Kolch W (2009). Cell fate decisions are specified by the dynamic ERK interactome. Nat Cell Biol 11:1458-64.

Wagner AJ, Small MB, Hay N (1993). Myc-mediated apoptosis is blocked by ectopic expression of Bcl-2. Mol Cell Biol 13:2432-40.

Wang H, Clark I, Nicholson PR, Herskowitz I, Stillman DJ (1990). The Saccharomyces cerevisiae SIN3 gene, a negative regulator of HO, contains four paired amphipathic helix motifs. Mol Cell Biol 10:5927-36.

Wang X, Peters MA, Utama FE, Wang Y, Taparowsky EJ (1999). The Adrenomedullin gene is a target for negative regulation by the Myc transcription complex. Mol Endocrinol 13:254-67.

Wanzel M, Herold S, Eilers M (2003). Transcriptional repression by Myc. Trends Cell Biol 13:146-50.

Watnick RS, Cheng YN, Rangarajan A, Ince TA, Weinberg RA (2003). Ras modulates Myc activity to repress thrombospondin-1 expression and increase tumor angiogenesis. Cancer Cell 3:219-31.

Wei W, Sedivy JM (1999). Differentiation between senescence (M1) and crisis (M2) in human fibroblast cultures. Exp Cell Res 253:519-22.

Welcker M, Orian A, Jin J, Grim JE, Harper JW, Eisenman RN, Clurman BE (2004). The Fbw7 tumor suppressor regulates glycogen synthase kinase 3 phosphorylation-dependent c-Myc protein degradation. Proc Natl Acad Sci USA 101:9085-90.

Welstead GG, Schorderet P, Boyer LA (2008). The reprogramming language of pluripotency. Curr Op Genet Dev 18:123-9.

Wennerberg K, Rossman KL, Der CJ (2005). The Ras superfamily at a glance. J Cell Sci 118:843-6.

Wenzel A, Cziepluch C, Hamann U, Schürmann J, Schwab M (1991). The N-Myc oncoprotein is associated in vivo with the phosphoprotein Max(p20/22) in human neuroblastoma cells. EMBO J 10:3703-12.

Wernig M, Meissner A, Foreman R, Brambrink T, Ku M, Hochedlinger K (2007). In vitro reprogramming of fibroblasts into a pluripotent ES-cell-like state. Nature 448:318-24.

Wierstra I, Alves J (2008). The c-myc promoter: still Mystery and Challenge. Adv Cancer Res 99:113-333.

Wilda M, Busch K, Klose I, Keller T, Woessmann W, Kreuder J, Harbott J, Borkhardt A (2004). Level of MYC overexpression in pediatric Burkitt's lymphoma is strongly dependent on genomic breakpoint location within the MYC locus. Genes Chromos Cancer 41:178-82.

Willumsen BM, Christensen A, Hubbert NL, Papageorge AG, Lowy DR (1984). The p21 ras C-terminus is required for transformation and membrane association. Nature 310:583-6.

Wilson A, Murphy MJ, Oskarsson T, Kaloulis K, Bettess MD, Oser GM, Pasche AC, Knabenhans C, Macdonald HR, Trumpp A (2004). c-Myc controls the balance between hematopoietic stem cell selfrenewal and differentiation. Genes Dev 18:2747-63.

Wolfman A, Macara IG (1990). A cytosolic protein catalyzes the release of GDP from p21ras. Science 248:67-9.

Wood MA, McMahon SB, Cole MD (2000). An ATPase/helicase complex is an essential cofactor for oncogenic transformation by c-Myc. Mol Cell 5:321-30.

Wu CH, van Riggelen J, Yetil A, Fan AC, Bachireddy P, Felsher DW (2007). Cellular senescence is a important mechanism of tumor regression upon c-myc inactivation. Proc Natl Acad Sci USA 104:13028-33.

Wu KJ, Polack A, Dalla-Favera R (1999). Coordinated regulation of iron-controlling genes, H-ferritin and IRP2, by c-MYC. Science 283:676-9.

Wu S, Cetinkaya C, Munoz-Alonso MJ, von der Lehr N, Bahram F, Beuger V, Eilers M, Leon J, Larsson LG (2003). Myc represses differentiation-induced p21CIP1 expression via Miz-1-dependent interaction with the p21 core promoter. Oncogene 22:351-60.

Xiao J, Pradhan A, Liu Y (2005). Functional role of JNK in neuritogenesis of PC12-N1 cells. Neurosci Lett 392:231-4.

Xu Y, Sengupta PK, Seto E, Smith BD (2006). Regulatory factor for X-box family proteins differentially interact with histone deacetylases to repress collagen alpha2(I) gene (COL1A2) expression. J Biol Chem 281:9260-70.

Yada M, Hatakeyama S, Kamura T, Nishiyama M, Tsunematsu R, Imaki H, Ishida N, Okumura F, Nakayama K, Nakayama KI (2004). Phosphorylation-dependent degradation of c-Myc is mediated by the F-box protein Fbw7. EMBO J 23:2116-25.

Yamada T, Yamaguchi Y, Inukai N, Okamoto S, Mura T, Handa H (2006). P-TEFb-mediated phosphorylation of hSpt5 C-terminal repeats is critical for processive transcription elongation. Mol Cell 21:227-37.

Yamamoto T, Ebisuya M, Ashida F, Okamoto K, Yonehara S, Nishida E (2006). Continuous ERK activation downregulates antiproliferative genes throughout G1 phase to allow cell-cycle progression. Curr Biol 16:1171-82.

Yang BS, Geddes TJ, Pogulis RJ, de Crombrugghe B, Freytag SO (1991). Transcriptional suppression of cellular gene expression by c-Myc. Mol Cell Biol 11:2291-5.

Yang W, Shen J, Wu M, Arsura M, FitzGerald M, Suldan Z, Kim DW, Hofmann CS, Pianetti S, Romieu-Mourez R (2001). Repression of transcription of the p27(Kip1) cyclin-dependent kinase inhibitor gene by c-Myc. Oncogene 20:1688-702.

Yang X, Zhang F, Kudlow JE (2002). Recruitment of O-GlcNAc transferase to promoters by corepressor mSin3A: coupling protein O-GlcNAcylation to transcriptional repression. Cell 110:69-80.

Yin X, Grove L, Prochownik EV (1998). Lack of transcriptional repression by max homodimers. Oncogene 16:2629-37.

Zeller KI, Jegga AG, Aronow BJ, O'Donnell KA, Dang CV (2003). An integrated database of genes responsive to the Myc oncogenic transcription factor: identification of direct genomic targets. Genome Biol 4:R69.

Zeller KI, Zhao X, Lee CW, Chiu KP, Yao F, Yustein JT, Ooi HS, Orlov YL, Shahab A, Yong HC, Fu Y, Weng Z, Kuznetsov VA, Sung WK, Ruan Y, Dang CV, Wei CL (2006). Global mapping of c-Myc binding sites and target gene networks in human B cells. Proc Natl Acad Sci USA 103:17834-9.

Zervos AS, Faccio L, Gatto JP, Kyriakis JM, Brent R (1995). Mxi2, a mitogen-activated protein kinase that recognizes and phosphorylates Max protein. Proc Natl Acad Sci USA 92:10531-4.

Zhang H, Pan KH, Cohen SN (2003). Senescence-specific gene expression fingerprints reveal cell-type-dependent physical clustering of upregulated chromosomal loci. Proc Natl Acad Sci USA 100:3251-6.

Zhang HM, Li L, Papadopoulou N, Hodgson G, Evans E, Galbraith M, Dear M, Vougier S, Saxton J, Shaw PE (2008). Mitogen-induced recruitment of ERK and MSK to SRE promoter complexes by ternary complex factor Elk-1. Nucleic Acids Res 36: 2594-607.

Zhang XF, Settleman J, Kyriakis JM, Takeuchi-Suzuki E, Elledge SJ, Marshall MS, Bruder JT, Rapp UR, Avruch J (1993). Normal and oncogenic p21ras proteins bind to the amino-terminal regulatory domain of c-Raf-1. Nature 364:308-13.

Zhang Y, Iratni R, Erdjument-Bromage H, Tempst P, Reinberg D (1997). Histone deacetylases and SAP18, a novel polypeptide, are components of a human Sin3 complex. Cell 89:357-64.

Zhang Y, Ng HH, Erdjument-Bromage H, Tempst P, Bird A, Reinberg D (1999). Analysis of the NuRD subunits reveals a histone deacetylase core complex and a connection with DNA methylation. Genes Dev 13:1924-35.

Zhang Y, Sun ZW, Iratni R, Erdjument-Bromage H, Tempst P, Hampsey M, Reinberg D (1998). SAP30, a novel protein conserved between human and yeast, is a component of a histone deacetylase complex. Mol Cell 1:1021-31.

Zhang Y, Wang Z, Li X, Magnuson NS (2008). Pim kinase-dependent inhibition of c-Myc degradation. Oncogene 27:4809-19.

Zhang Y, Liu T, Meyer C, Eeckhoute J, Johnson DS, Bernstein BD, Nusbaum C, Myers RM, Brown M, Li W, Liu XS (2008). Model-based Analysis of ChIP-Seq (MACS). Genome Biology 9:R137.

Zhang W, Liu HT (2002). MAPK signal pathways in the regulation of cell proliferation in mammalian cells. Cell Res 12:9-18.

Zhou Y, Santoro R, Grummt I (2002). The chromatin remodeling complex NoRC targets HDAC1 to the ribosomal gene promoter and represses RNA polymerase I transcription. EMBO J 21:4632-40.

Zhou ZQ, Hurlin PJ (2001). The interplay between Mad and Myc in proliferation and differentiation. Trends Cell Biol 11:S10-4.

Zindy F, Eischen CM, Randle DH, Kamijo T, Cleveland JL, Sherr CJ, Roussel MF (1998). Myc signalling via the ARF tumor suppressor regulates p53-dependent apoptosis and immortalization. Genes Dev 12:2424-33.